ÉTUDE CINÉTIQUE DE LA PRODUCTION DE BIOGAZ À PARTIR DE FUMIER DE POULET

Abdulhalim Musa Abubakar

KINETIC STUDY OF BIOGAS PRODUCTION FROM CHICKEN MANURE

BY

ABDULHALIM MUSA ABUBAKAR

PGA/19/05/02/08806

DISSERTATION SUBMITTED TO THE SCHOOL OF POSTGRADUATE STUDIES, UNIVERSITY OF MAIDUGURI, IN PARTIAL FULFILLMENT OF THE REQUIREMENTS FOR THE AWARD OF MASTER OF ENGINEERING (M.ENG) DEGREE IN CHEMICAL ENGINEERING

FEBRUARY, 2023

ABSTRACT

The use of biogas as fuel for transportation, electricity generation, heating and in cooking stoves, justify its production as alternative fuel to natural gas. Waste, posing serious danger to the environment, especially chicken manures (CM) containing disease-causing microorganisms, if utilized via anaerobic digestion to generate biogas will go a long way in mitigating its effect. This work hence, desires to turn the detrimental health challenges that these microbes could cause humans and animals to generate useful by-products. Therefore, this work aims at studying the kinetics of biogas production using CM. The objectives entail utilizing a bench-scale digester to produce biogas; studying the growth kinetics of microorganisms acting on the feedstock; profile the gas generated and using POLYMATH regression tool to study comparatively, the modified Gompertz, Cone, Transfert and Logarithmic biogas yield kinetic models. Method followed involves feeding the digester with 7 kg of CM after proximate analysis, determining the biomass concentration and daily gas production over a 40 days retention period using the biogas and cell growth data in models to describe the conditions inside the digesting system and the biogas potential of the CM substrate and lastly, analyzing the raw gas produced to know its constituent gases. CM with 24:1 carbon-to-nitrogen ratio, 47% moisture, 13.21% volatile solid and 17.06% protein content resulted in 0.883m^3 of biogas containing 63% methane and 29% carbon dioxide. CM containing an initial average of 3.67×10^9 *mg/L cell concentration grew over time giving* μ_{max} *and* K_s *parameters in the basic Monod model equivalent to 0.076 hr^{-1} and* 3.838×10^8 *mg/L respectively; satisfying further, the Han and Levenspiel, Loung, Wayman and Tseng, Monod with decay rates and Moser growth models. Estimates from Logistic, Cone, modified Gompertz and Transfert models, were proven to be the best in that order utilizing several statistical data. Information from the models would help scale up gas production if all conditions were satisfied. Possibility of achieving the same fit with other feedstock should be experimented.*

CERTIFICATION

We certify that this dissertation entitled "**KINETIC STUDY OF BIOGAS PRODUCTION FROM CHICKEN MANURE**'' has been duly presented by PGA/19/05/02/08806 of the Department of Chemical Engineering, Faculty of Engineering, University of Maiduguri. Copies of the dissertation are submitted for evaluation by the Panel of Examiners and subsequent oral defense by the candidate.

Supervisor:

Signature: …….

Name: ……...

Date: …….

Head of Department

Signature: ……

Name: …….

Date: ……

Co-Supervisor:

Signature: ……

Name: ……..

Date: ……

Having met the stipulated requirements, the dissertation has been accepted by the school of Postgraduate Studies.

Signature: ……

Name: ……..

for Dean of Postgraduate Studies

……..

Date

DECLARATION

I hereby declare that this research work was written by me for the award of Master of Engineering (M.Eng.) in Chemical Engineering. I solemnly declare that to the best of my knowledge; no part of this report has been submitted here or elsewhere in a previous application for award of a degree. All sources of knowledge used have been duly acknowledged.

---------- ----------

Abdulhalim Musa Abubakar Date

DEDICATION

This work is dedicated to Almighty Allah for His support.

ACKNOWLEDGEMENTS

I wish to acknowledge the support rendered in the course of this project by my parents, Alhaji Musa Abubakar and Hajiya Madinatu Musa Abubakar; your support is highly appreciated. Friends, relatives and colleagues who in one way or the other are involved in successes recorded so far are also acknowledged. My supervisors, Engr. Dr. Kiman Silas and Engr. Dr. Mohammed Modu Aji are highly appreciated for time and dedication in ensuring that this project meet required standard. The HOD, Engr. Dr. Alhaji Shehu Grema, the Post Graduate Coordinator, Chemical Engineering Department, Dr. Abdu Zubairu and Engr. Dr. Usman A. Ibrahim are appreciated for their mentorship, leadership and guidance. Also, the External Examiner, Dr, Nuruddeen Salahuddeen of Bayero University Kano (BUK) is appreciated for his useful criticisms and recommendations. May Allah Almighty bless you all. I thank Allah, the Most Gracious, the Merciful for His infinite blessings and guide.

TABLE OF CONTENTS

LIST OF TABLES

LIST OF FIGURES

Figure Page

ABBREVIATIONS AND NOMENCLATURE

AD	Anaerobic Digestion
PVC	Polyvinyl Chloride
LDPE	Low-Density Polyethylene
HDPE	High-Density Polyethylene
CM	Chicken Manure
C/N	Carbon-to-Nitrogen Ratio
RT	Retention Time
TAN	Total Ammonia Nitrogen
VS	Volatile Solids
VFA	Volatile Fatty Acid
TS	Total Solids
EMB	Eosin Methylene Blue
SKM	Structured Kinetic Model
UKM	Unstructured Kinetic Model
X	Cell concentration
S	Substrate concentration
CFU	Colony-forming unit
K_s	Half Saturation Constant
μ_{max}	Maximum Specific Growth Rate
μ	Specific Growth Rate
Y or $Y_{X/S}$	Biomass-to-substrate Yield
K_h	First Order Hydrolysis Constant
S_0	Initial Substrate Concentration
X_0	Initial Biomass Concentration
N	Number of Cells at time t
N_0	Initial Number of Cell
K_d	Kinetic Constant of Death Occurrences
N_{st}	Number of cells (conc.) in the medium at the end of stationary phase
r_x	Rate of Cell Generation
r_s	Rate of Substrate Consumption
t_d, G	Doubling/Generation Time
b	Death Constant
S_m	Terminal or Maximum Substrate Inhibitory Concentration
m	Curve Parameter
S_θ	Threshold Substrate Concentration
SF	Shape Factor
k	Specific (maximum) Biogas Production Rate
BP	Biogas Potential
LP	Lag Phase
e	Logarithmic Constant
CBY	Cumulative Biogas Yield
SMA	Specific Methanogenic Activity
R^2	Coefficient of Determination
BF	Bias Factor
AF	Accuracy Factor
RMSE	Root Mean Square Error
NRMSE	Normalized Root Mean Square Error
BIC	Bayesian Information Criterion
AIC	Akaike Information Criterion
RSS	Residual Sum of Squares
RMS	Residual Mean Square
MAPE	Mean Absolute Percentage Error
MSPE	Mean Square Percentage Error
MC	Moisture Content
AC	Ash Content
OM	Organic Matter
PD	Particle Density
FS	Fixed Solid
EDXRF	Energy-Dispersive X-Ray Flurescene
APHA	American Public Health Association
SDE	Serial Dilution Experiment
X_D	Number of cells at time t into the death phase
$X_{D,0}$	Number of cell (conc.) in the medium at the end of the stationary phase
q	Mass of substrate to mass of cells at time t

K_i, K_1, K_2	Inhibition Constant	$X_{Expt.}$	Cell concentration from SDE
n	Shape Factor	$S_{Expt.}$	Substrate concentration from SDE
X_m	Maximal Cell Concentration	F	Flowrate
α, a, b_b	Constants	P	Production
NA	Nutrient Agar	X_{calc}	X from Regression
U	Volume	S_{calc}	S from Regression
X_∞	Cell concentration achievable	TDF	Total Dilution Factor
TNTC	Too Numerous to Count	TFTC	Too Few to Count

CHAPTER ONE

INTRODUCTION

1.1 Background of the Study

Suitability of kinetic models to determine the importance of relationship between variables to guide empirical design, assess the experimental results and define the specific parameters of the system performance is regarded as kinetic study (Lim *et al.*, 2021). Essentially, kinetics of biogas production deals specifically with production variation with time (Sukhesh & Rao, 2018). The variation could be growth of microorganisms during feedstock decomposition, concentration of pretreatment chemicals, substrate depletion and biogas generation with time. The anaerobic digestion utilizes organic waste feedstock such as municipal, agricultural and industrial waste in a bioreactor which results into the generation of biogas. Chicken manure (CM) is basically an agricultural waste obtained from households and poultry farms and is a good feedstock for biogas production (Ulusoy *et al.*, 2018). The kinetic characteristics of microbes involved in the degradation of the feedstock provides information on how to optimize the process for high yield of biogas (Pecar *et al.*, 2020). Other factors affecting a successful anaerobic digestion are pH, Chemical Oxygen Demand (COD), Retention Time (RT), temperature, Organic Loading Rate (OLR), pressure, inoculation ratio, nutrients and mixing technology (Bhatt and Tao, 2020; Fahriansyah and Sriharti, 2019). The resulting biogas contains methane, carbon dioxide, hydrogen, ammonia and moisture and can be upgraded to serve as an alternative fuel to natural gas for use in generating electricity, heat generation, fuel for transportation and in cooking stoves (Fuchs *et al.*, 2018; Granado *et al.*, 2017).

Modeling of anaerobic digestion system is required to reduce time and extent resources utilization in the system, to transform laboratory to industrial scale and, designing of system for optimum operational parameters (Kainthola *et al.*, 2019). For scale-up purposes, kinetics of the anaerobic digestion (AD) process is a critical factor to study (Almomani, 2020). To assess the performance of AD systems, numerous kinetic models have been used by researchers, namely, Transference Function model, Modified First Order model, Chen and Hashimoto model, Monod model, First Order model, Substrate Mass Balance model, Cone Model, Modified Gompertz model, Monod equation, Contois model, Moser model, Andrew model, and Tessier models (Rajput &

Visvanathan, 2018; Velazquez-Marti *et al.*, 2018). Some of this models were used during kinetic study of biogas production from CM codigested with multiple biodegradable feedstock, previously (Jiang *et al.*, 2021; Duan *et al.*, 2018; Li *et al.*, 2016). However, scholarly papers consulted in this study shows that Liu *et al.* (2018), Ma *et al.* (2021) and Selvaraj *et al.* (2018) digest CM and studied its kinetics utilizing only the modified Gompertz model, where they obtained varying results as a result of differences in conditions set up in their experiments. As for growth models, only cow manure kinetic data was analyzed using Contois model by Alqahtani (2013). Dependent variables, in most cases, cumulative biogas yield (CBY) and specific growth rates are generated using diverse methods and approaches. For instance, daily biogas yield can be measured using weighing devices or the liquid displacement method during complete or partial digestion of the CM feedstock. While researchers prefer to analyse kinetic results obtained from chemical nutrients (e.g. phenol) and wastewaters using growth models instead of organic matters such as manures and other biodegradable wastes. Obviously, there is no straight and clearly defined approach of obtaining kinetic data for growth model analysis as there are numerous feedstock to handle, millions of microorganisms to consider and several factors influencing the process. Hence, this study, coupled methods utilized at different stages of studies in literature on different samples to model procedure that takes into considerations factors affecting the production of biogas from CM from beginning to the end, as novelty of this work. Thus, using a clearly stated objectives, a comprehensive methodology from previous work studied with other substrates can be replicated for CM ass feedstock.

1.2 Aim and Objectives of the Study

The aim is to study the kinetics of biogas production using chicken manure. The specific objectives are to:

i. produce biogas from chicken manure using a bench-scale anaerobic digester
ii. study the growth kinetics of microbes aiding the degradation of the feedstock
iii. profile the biogas produced and carry out a comparative kinetic study with existing model including the modified Gompertz, Cone, Transfert and Logarithmic models by POLYMATH regression software

1.3 Statement of the Problem

Due to nutrient insufficiency often recorded in biogas production from chicken manure, it is mostly codigested with other feedstock thereby preventing its exploitation as sole biogas feedstock. Microorganisms responsible for biogas production are sensitive to conditions in their environment and may die when these conditions are unfavorable. Also, previous kinetic studies analysed biogas production from chicken manure for only few selected models developed by researchers.

1.4 Significance of the Study

Previous study has indicated the potential of chicken manure for biogas. Therefore, kinetics of biogas production from chicken manure feedstock critically aid control of anaerobic digestion for the purpose of optimizing its production. This study would help in knowing concentration of microorganism and substrate which will either accelerates or retards the yield of biogas.

1.5 Scope of the Study

The work is limited to the production of biogas using a bench-scale anaerobic digester, the study of kinetics of microbes and the use of regression software to compare different biogas yield kinetic models.

CHAPTER TWO

LITERATURE REVIEW

2.1 Chicken Manure (CM) Utilization

A good raw material capable of generating biogas is CM, due to its high nitrogen content and low carbon-nitrogen ratio (Ulusoy *et al.*, 2018; Wang *et al.*, 2019; Eronmosele *et al.*, 2020). They are obtained generally from poultry farms and chicken processing industries as chicken processing waste (CPW) in form of legs, blood, heads, skin, bones, feathers, viscera, besides the whole carcasses if the bird is dead (Li *et al.*, 2016). These contents makes CM an organic matter that is highly biodegradable (Keskin *et al.*, 2018; Yilmaz and Sahan, 2020) and an important bioenergy source to derive improved fuel (Tanczuk *et al.*, 2019; Hakimi *et al.*, 2021; Zahedi *et al.*, 2020). Other significance could be poultry waste minimization when used as substrate for anaerobic digestion to manufacture biofertilizer, a co-product of the fermentation process (Ksheem, 2015; Li *et al.*, 2016; Singh *et al.*, 2018; Hakimi *et al.*, 2021).

CM is a promising feedstock for slow pyrolysis (Tanczuk *et al.*, 2019). Certain nutrient sources such as sulphur, N_2, potassium, phosphorus, fat, amino acids and protein can as well be recovered from the manure (Yilmaz and Sahan, 2020; Oosterkamp and Oosterbeek, 2018; Selvaraj *et al.*, 2018; Li *et al.*, 2016; Ksheem, 2015). Ammonia and/or ammonium can also be recovered from CM by hydrothermal conversion of the high N_2 content in it (Matsumura *et al.*, 2021). A recent study carried out by Cheong *et al.* (2019), demonstrated the generation of electricity from the fluidized bed combustion of CM. Generally, utilization of CM fundamentally solves the environmental pollution problems (Wang *et al.*, 2019).

2.1.1 Environmental Impacts of Chicken Manure

Amongst all agricultural activities, the poultry sector is one capable of generating huge amount of organic waste (Keskin *et al.*, 2018). Livestock farmers, especially those handling poultry birds like geese, ducks, turkey, chicken, guinea fowl, quail, ostrich and pigeon in poultry houses disposes off the waste generated from these animals on the environment. Chicken waste are often applied on agricultural land as manure or compost as a traditional treatment approaches, dumped at landfill, or incinerated, contaminating the environment in the process (Ksheem, 2015; Cao *et al.*, 2016). For instance, too much of nitrogen and phosphorus in CM results in eutrophication during

landfill and composting (Cao *et al.*, 2016). In addition, chicken waste provides a breeding environment for flies and parasites, pathogen release, eutrophication of surface waters, threat to local air quality when used as fertilizer, pollution to soil, health risks and groundwater contamination (Cao *et al.*, 2016; Cayci *et al.*, 2017; Hassan *et al.*, 2017; Keskin *et al.*, 2018).

Its effect on soil properties is classified into three, and includes physical, chemical, and biological effects. CM in solid or liquid phases used on irrigated soils risks increased soil and groundwater salinity, excessive nitrate leaching to ground water as chemical effect. Biologically, problems arising are; introduction of pathogens, deterioration of soil carbon, and decreasing populations of desirable microbes (Ksheem, 2015; Hassan *et al.*, 2017; Cheong *et al.*, 2019). The soil physical property like structure/texture may also be affected (Hassan *et al.*, 2017). Improper disposal of CM waste must be addressed to mitigate its effect on the ecosystem. CM should be pre-process or pretreated by thermo-chemical and/or physical processing technologies like torrefaction, ozone treatment, re-feeding to animals, composting, steam treatment, drying, ozone treatment, pyrolysis, esterification, gasification, co-gasification, fermentation or digestion, combustion and co-combustion (Cheong *et al.*, 2019; Tanczuk *et al.*, 2019). Cheong *et al.* (2019) affirms that, combustion can be a viable and dependable way to treat CM, principally when coupled with energy recovery.

2.1.2 Availability of Chicken Manure Feedstock

In Turkey, Onay (2020), reported that 30 kilo tons of CM is produced daily, with potential for renewable energy recovery. Deqingyuan chicken farm, reckons as the chief egg farm plant in Asia and reap chicken manures from the farm for biogas production (Yilmaz and Sahan, 2020). Annually, China alone outputs about 15 million tons of chicken manure (Wang *et al.*, 2021). Estimates of chicken manure global production stood at 457 million tonnes per year (Ksheem, 2015; Zahedi *et al.*, 2020). Number of poultry birds in a certain location could also signal its potential for manure recovery and subsequent utilization for anaerobic digestion. Relevant studies shows that a chicken farm with about 100,000 chickens is capable of producing up to 10t of chicken manure daily (Wang *et al.*, 2021). In Indonesia for instance, Yusof *et al.* (2019), has it that, there are 523 million birds in that country. Brazil sat on the top global ranking of chicken exports (Barreto *et al.*, 2019) and occupies the second position in chicken production in the world (Silva *et al.*, 2021). In Europe, $\cong 1.886 \times 10^9$ poultry heads produced 10^7 tonnes of poultry manure according to Rubežius *et al.* (2020). Chicken population in Nigeria is 150.682 million (second in

Africa) of which 15% are semi-commercially farmed, 25% commercially and 68% in backyards, based on a report by Francis *et al.* (2016). One year after, a higher population of 180 million chicken are estimated to exist in Nigeria, of which only 21% are intensively reared. Specifically, 83 million chickens are raised in extensive systems and 60 million in semi-intensive systems, most of which are indigenous chickens, contributing substantially to the nation's gross domestic product (GDP) (Lasagna *et al.*, 2017). In the North Eastern part of Nigeria, specifically Yobe State, it was reported that, there are 3.4 million chicken reared domestically (Annuar *et al.*, 2008). Currently, the populations are sure to surpassed the previously reported figures by Annuar *et al.* (2008), Francis *et al.* (2016) and Lasagna *et al.* (2017). Maiduguri, an area in the same location, employed mostly, the deep litter rearing system, although facing challenges including, bad housing, poor management practices, inadequate vaccination, and diseases resulting in high mortality rate. Common diseases identified by Francis *et al.*, (2016) faced by poultry farmers in Maiduguri metropolis are newcastle, fowl pox, gumboro, fowl typhoid, fowl cholera, chronic respiratory disease, helminthiasis, ectoparasitism and, coccidiosis.

2.2 Biodigester for Biogas Production

Bioreactors could be termed digesters (Nong *et al.*, 2020). It is an airproof reactor tank or vessel (Jyothilakshmi and Prakash, 2016) that is simple, cheap, robust, easy to operate and maintained (Khayal, 2019). Biogas digesters or simply biodigesters are considered small-scale if subjected to domestic use and large-scale as in industrial digesters (IRENA, 2016). They are flexible because they can be made from plastics such as Polyvinyl Chloride (PVC), Low-Density Polyethylene (LDPE) or High-Density Polyethylene (HDPE) (Fahriansyah and Sriharti, 2019). Microorganisms such as fungi, microorganism and protozoa can survive in an oxygen free environment, degrading the feedstock to produce biogas and digestate. The process is identical to what happens in a cow's stomach where stomach microorganism convert food into dungs and biogas (Lenkiewicz and Webster, 2017).

Biogas is composed of methane (CH_4), carbon dioxide (CO_2), hydrogen (H_2), hydrogen sulphide (H_2S), ammonia (NH_3), nitrogen (N_2), oxygen (O_2) and water vapor (H_2O) in varying amount. The more the waste is degraded, the more the gas is produced (Jaffar and Rehman, 2020). The decomposed substrate is the residue called the digestate which is rich in macro- and micro nutrients, and used as biofertilizer (Jyothilakshmi and Prakash, 2016; Elalami *et al.*, 2019;

Chowdhury *et al.*, 2020). The digestate will have little or no smell if the digester is working perfectly (Lenkiewicz and Webster, 2017).

Despite the multitude of compounds present in biogas, it is still 20% lighter than air, where its yield and composition depends on digestion condition, feedstock and co-substrate type (Neshat *et al.*, 2017; Raja and Wazir, 2017; Bharathiraja *et al.*, 2018). Biogas is a colorless and odorless gas whereas biomethane are upgraded biogas where composition of more than 40% methane will be responsible for characteristic flammability of gas (Lenkiewicz and Webster, 2017; Parsaee *et al.*, 2019; HomeBioGas, 2021). This flame is hotter than fire (Bharathiraja *et al.*, 2018) and clear blue (Raja and Wazir, 2017; Aziz *et al.*, 2019; HomeBioGas, 2021), similar to Liquefied Petroleum Gas (LPG). Biogas are characterized with low energy density, slow flame speed and partial combustion; a property that is considered negative (Bharathiraja *et al.*, 2018). In addition, ignition temperature is in the range of 50-750^{0}C (Raja and Wazir, 2017). Compounds including NH_3, H_2S and CO_2 in biogas are poisonous, the main reason why biogas can suffocate one if exposed to in an enclosed area (Lenkiewicz and Webster, 2017). Though CO_2 content could be brought to desirable level during upgrading process by scrubbing. Energy units of biogas is megajoules (MJ) (IRENA, 2016) and 1 m^3 of raw biogas at STP containing 60% CH_4 will give a heating value of 21.5 MJ or 5.97 kW h (Bharathiraja *et al.*, 2018).

2.3 Anaerobic Digestion of Chicken Manure

CM is an alkaline, semi-solid organic material that is made up of diverse composition of other organic materials (Ali *et al.*, 2017; Lohani *et al.*, 2020). Ali *et al.* (2017), reported that daily chicken excretion ranges from 80-125g (wet)/chicken. Dry matter content or total solid (TS) content of CM is 20-25% of the excreta which is rich in nitrogen, with high amount of biodegradable fraction and volatile solid (VS) content of 55-65% (Dalk and Ugurlu, 2015; Ali *et al.*, 2017; Duan *et al.*, 2018). Percentage water content of more than 70% in CM is considered unattractive for utilization (Cao *et al.*, 2016). It also contain pathogens (methanogenic microorganism), high phosphorus, low C-N ratio, and high salinity level (Ksheem, 2015; Noori and Ismail, 2019). Lohani *et al.* (2020) reported a chicken manure with TS = 47.3%, pH = 8.1, VS = 68% and C-N ratio of 18. To prevent chicken manure from decomposing, prior to anaerobic digestion, they are often kept at a very low temperature of -20°C or higher (up to 4℃) (Li *et al.*, 2013). Dry fermentation has the merits of high biogas production rates, low water consumption and low cost (Li *et al.*, 2020).

The agricultural sector where CM is derived, is the main source of total ammonia emission into the atmosphere (Cayci *et al.*, 2017; Baltrėnas *et al.*, 2019). It has been stated clearly, that the high nitrogen content of CM makes it a suitable material for anaerobic digestion. However, nitrogen, together with sulphur inhibits the digestion process (Oosterkamp and Oosterbeek, 2018). The level of nitrogen in CM is attributed to the conversion of uric acid and undigested proteins into total ammonia nitrogen (TAN) during digestion (Dalk and Ugurlu, 2015). For a successful AD process, the inhibitory effect of NH_3 (threshold value of 200 mg/L) as well as the low C-N ratio of CM must be overcome (Li *et al.*, 2016; Cheong *et al.*, 2019; Yilmaz and Sahan, 2020) as it may cause volatile fatty acid (VFA) to accumulate and inhibit microbial activities (Dalk and Ugurlu, 2015). Air stripping is a pretreatment technique to get rid of NH_3 from CM wastewater (Fakkaew and Polprasert, 2021). TAN inhibition can be reduced by feeding the system with feedstock containing low TS (Dalk and Ugurlu, 2015). For a stable AD performance and a balanced nutrient, mono-digestion of CM is often frown at. Anaerobic co-digestion of CM with other feedstock is mostly carried out by researchers as alternative method of solving the ammonia problem (Onay, 2020). Example is co-digestion of FW, goat manure and CM (Lohani *et al.*, 2020) and co-digestion of ethanol plant effluent with CM among others (Cheong *et al.*, 2019).

2.3.1 Stages of Degradation and Factors Affecting Gas Production

AD process consist of four stages (Rajput and Visvanathan, 2018; Parsaee *et al.*, 2019; Sawyerr *et al.*, 2019; Uche *et al.*, 2020): namely hydrolysis, acidogenesis, acetogenesis and methanogenesis via various set of microbes (Raja and Wazir, 2017; Brémond *et al.*, 2018; Kainthola *et al.*, 2019). The acidogenesis and acetogenesis stages are sometimes coupled together as the acidification step making it a three stage process of: hydrolysis, acidification and methanogenesis (Uche *et al.*, 2020). Microorganisms acting in those stages are different and forms the constituent gases in biogas.

Biogas yield is simply the resulting biogas output per unit mass of substrate or volatile solid (Wu *et al.*, 2016). Factors influencing the production of biogas are feedstock type, pH, volatile fatty acids (VFA), nutrients, tank volume, retention time, pressure, organic loading rate (OLR), chemical oxygen demand (COD), temperature, trace elements, carbon to nitrogen (C/N) ratio, alkalinity and particle size (IRENA, 2016; Neshat *et al.*, 2017; Raja and Wazir, 2017; Fahriansyah and Sriharti, 2019; Kainthola *et al.*, 2019; Sawyerr *et al.*, 2019; Zhang *et al.*, 2019; Bakraoui *et*

al., 2020; Bhatt and Tao, 2020). How these parameters are carefully chosen is crucial to optimizing AD for biogas production (Sarker *et al.*, 2019).

2.3.2 Kinetic Study

How speed of a reaction will change under certain reaction conditions together with clarified information about the mechanism of such reaction is often regarded as kinetic study. More precisely, it is the study of rates of chemical reactions. Several factors have been highlighted to influence the anaerobic digestion of organic feedstock such as chicken manure for the production of biogas. However, these factors are mildly incorporated into kinetic models to explain the activities resulting in biogas production. Presently, there are three models that have been used consistently to describe the kinetics of the anaerobic decomposition of substrate. They are growth kinetics, kinetics of biogas production, and kinetics of substrate degradation models, among which kinetics of biogas production is the most important (Rea, 2014; Van *et al.*, 2018; Momodu & Adepoju, 2021).

2.4 Microbial Growth Kinetics

In CM, there are mostly three types of micro-organisms, namely, *Salmonella* spp., *Escherichia coli* (E. coli), and *Cryptosporidium*. During anaerobic batch fermentation of CM, these microorganisms grow under a variety of physical, chemical, and nutritional conditions. They do so, by extracting nutrients from the medium (CM slurry) and converting them into biological compounds. This changes is accomplished through a cell's use of a number of dissimilar enzymes in a strings of reactions to produce metabolic products, which either remain in the cell (intracellular), providing the cell with energy or be secreted from the cells (extracellular) as bioproducts (Liu, 2017). Growth therefore, is believed to mean, both replication of cells and change in cell size. The growth and multiplication of microorganism in controlled environments, thus arouse the interest of microbiologists, biochemical engineers and, cell-growth experts, as they instigate bioprocess simulation and control scheme design (González-figueredo *et al.*, 2018). Generally, according to UlukardeŞler and Atalay (2018), kinetics of microorganisms growth can be investigated in two ways. One, is to measure the substrate concentrations during experiment, a procedure that is tiring and consumes a lot of time and a second, faster and easier methods that entails measuring the gas production rates in the course of the synthesis. Clearly, microbial growth

and substrate consumption rates are two parameters anaerobic digestion kinetics models focuses on (Tena *et al.*, 2021).

For bioreactors operating in batch mode, kinetics of biogas production is proportional to specific growth rate of methanogenic microorganism inside the digester (Noori and Ismail, 2019; Venkateshkumar *et al.*, 2020). Two types of microbial growth models can be distinguished (González-figueredo *et al.*, 2018): Structured Kinetic Models (SKMs) describing changes in cell population and classified into chemically structured models, morphologically structured models and, genetically structured models and, Unstructured Kinetic Models (UKMs) representing the metabolic behavior of the biomass cell production. The significance of these growth models are to estimate the growth of microorganisms under environmental conditions (Hawkins *et al.*, 2019), predict the behavior of biochemical reactions (González-figueredo *et al.*, 2018), assist engineers to design and control biological processes (Muloiwa *et al.*, 2020) and, to determine the performance parameters influencing the product yield (Gallipoli *et al.*, 2020).

2.4.1 Determination of Cell Numbers by Serial Dilution

Data of cell numbers or concentration (X) together with substrate concentration (S) over a specified time interval are parameters usually plugged into microbial growth kinetic models to estimate other performance constants. It is a usual practice for Microbiologists to estimate the number of cells in a sample, a procedure called microorganism count, which involves two major approaches. Cell numbers are measured via direct methods, where cells are counted or indirect method which depends on cell presence/activity measurement without necessarily counting individual cells (Datta, 2021).

In direct cell counting, cells in a liquid culture or colonies on a plate are counted and is divided into pour plate and spread plate method. Prior to either of the two methods, serial dilution of culture is carried out. A dilution is created by measuring a known volume (usually, 1 ml) or weight of a sample containing microbes and adding it to a tube containing a known volume of sterile water, thus making the resulting solution less concentrated than the original. Initially, more of these tubes containing sterile water are arranged on a rack (O'Toole, 2016). When this process is repeated, as seen in Figure 2.2a, for each new tube, thus making a series of more and more dilute samples, it is called a serial dilution.

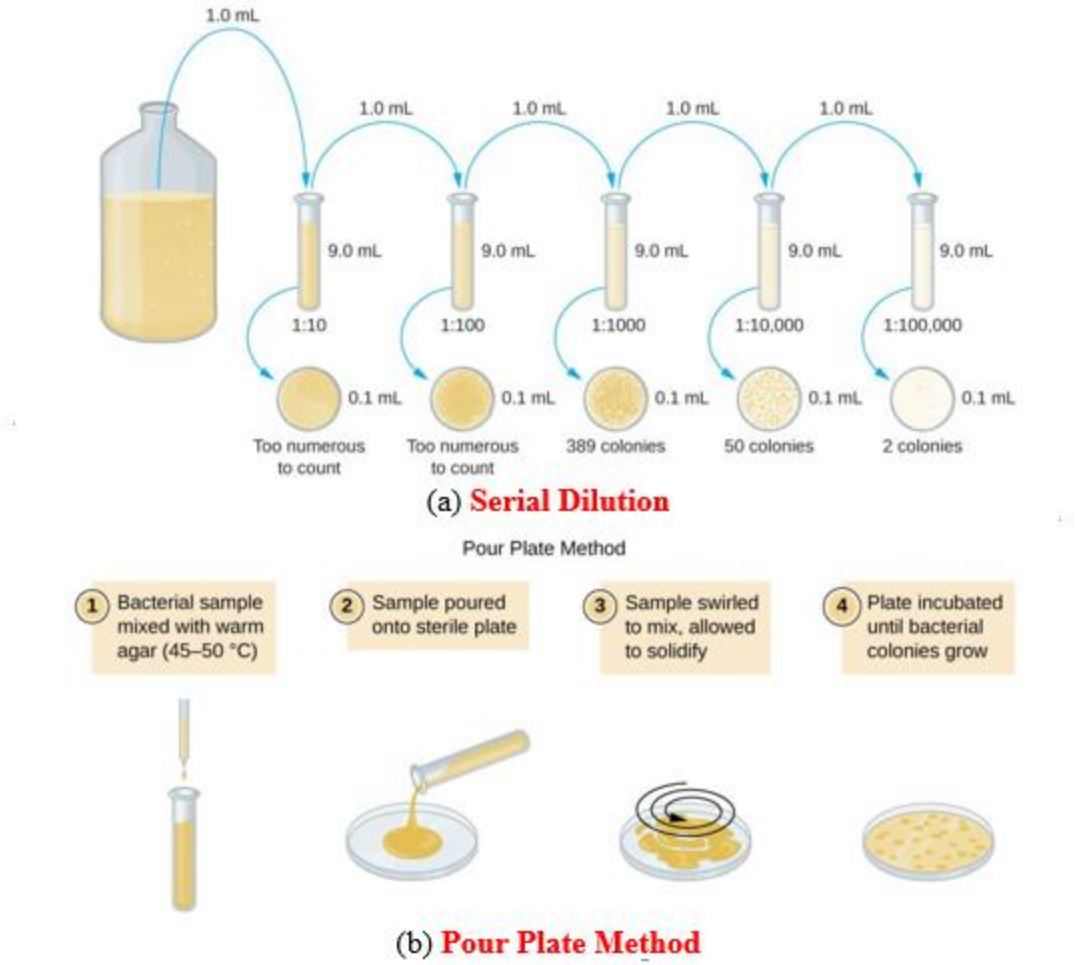

Figure 2.1: Depicting the Serial Dilution and Pour Plating Technique

The number of serial dilution is selected based on an initial estimate of the culture density. After serial dilution, culture media, a mixture of nutrient and agar is prepared by mixing with appropriate amount of water, stirred and autoclaved to sterilize it at 121^0C for some time before cooling to a temperature of 45^oC. The liquid nutrient agar is poured on a petri dish and the diluted culture is poured on it (see Figure 2.1b) and incubated in order to form visible colonies. The choice of media influences the formation of colonies by some cells, as they may not form colonies in a wrong media (O'Toole, 2016; Um-e-Habiba *et al.*, 2021).

Colonies are counted on the agar surface following the incubation period of around 24 hours. The viable plate count is a count of viable or live cells and is based on the principle that viable cells replicate and give rise to visible colonies when incubated under suitable conditions for the specimen (Liu, 2017). Total viable count was according to procedure explained by Hossain *et al.*

(2017). If the numbers of visible colonies after plating is low, it is indirectly pointing to the fact that the community is dominated by slow-growing microorganism (Salvesen and Vadstein, 2000). Two to three plates are normally taken from each dilution and the mean of the number of colonies counted on each plate is recorded. Overall, rigorous mixing of samples with the dilution medium is essential to getting reliable results. The viable plate count requires precision and skill if accurate results are to be obtained, though seen as a low estimate of the actual number of cells (Datta, 2021). One limitation of the plate count method is that, large sizes of unculturable cells are often present (Salvesen and Vadstein, 2000). The units of the microbial count are usually expressed as colony-forming unit per millilitre (CFU/ml) in liquid product or colony-forming unit per milligram (CFU/mg) in solid product (Marwan *et al.*, 2018; Datta, 2021). Using the dilution factor, as shown in Equation 2.6, used to compute the number of cells in the actual cell culture, microbial concentration (X) or CFU/ml can then be calculated following Equation 2.7 (Um-e-Habiba *et al.*, 2021).

$$\text{Dilution factor (DF)} = \frac{\text{(Diluent volume)+(Stock solution)}}{\text{Volume of stock transfered}} \tag{2.6}$$

$$\text{CFU/mL} = \frac{\text{(No. of colonies)}\times\text{(Total dilution factor, TDF)}}{\text{Volume of culture in mL}} \tag{2.7}$$

2.4.2 Microbial Growth Curve

Microorganisms grown in batch culture or closed culture, where no nutrients are added and majority of the waste is not removed, follow a reproducible growth pattern referred to as the growth curve. Lots of mathematical models have been proposed for microorganism growth curve in a batch culture of the AD (Selvaraj *et al.*, 2018). Growth curve, as used in biology, chemistry and medical sciences, often displays a phase in which the specific growth rate, μ begins at a value of zero in a certain period (resulting in a lag time) and then increases to a maximal value (μ_m) (Kyurkchiev *et al.*, 2016; Dinh *et al.*, 2018). A plot of $\log X$ with time is known as growth curve. When a batch system containing CM slurry is fed with known initial substrate concentration, S_0, and known initial concentration of microbial cells or inoculum, X_0, it will be observed that, overtime, the substrate concentration decreases with time (i.e. $\frac{dS}{dt}$ is negative) as the cell concentration increases with time (i.e. $\frac{dX}{dt}$ is positive). Kandasamy *et al.* (2020) had used CM to culture *Cladocerans*, *Diaphanasoma sarsi* and *Ceriodaphnia cornuta* and determine their

population. As clearly demonstrated in Figure 2.2, microorganism growth can be represented in four phases, namely, the lag phase, exponential phase, stationary phase, and death phase (Liu, 2017; Marwan *et al.*, 2018; Muloiwa *et al.*, 2020).

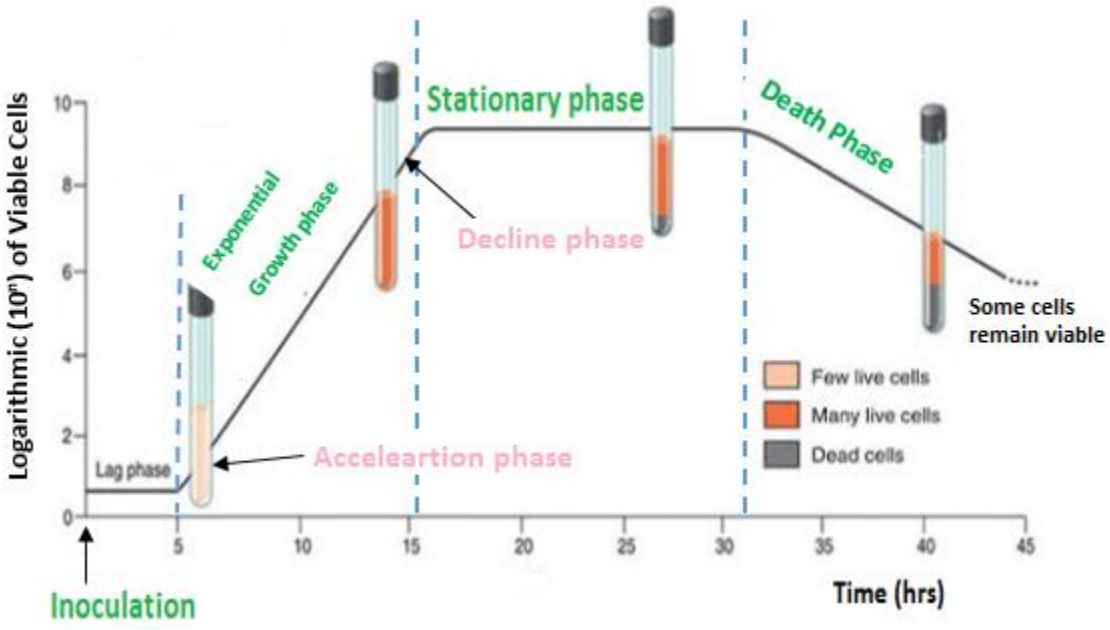

Figure 2.2: Typical Growth Curve for a Batch System (Perni *et al.*, 2005)

Immediately after inoculation, the lag phase occurs. It is a period illustrating the adaptation of cells to a new environment $\left(\frac{dX}{dt} = \frac{dS}{dt} = 0\right)$. In this phase, new enzyme systems are activated, cells are not replicating themselves and the length of this phase is influenced by the physiological state of the inoculum. The diauxic growth or multiple lag phases occurs when more than one medium is present, usually as a result of a shift in metabolic pathways in the middle of a growth cycle (Liu, 2017). The next phase where cells have adapted to the new environment is known as the maximum growth phase/exponential growth phase or logarithmic growth phase ($\frac{dX}{dt}$ and $\frac{dS}{dt}$ are changing). It is represented by a straight line, a period of balanced growth, in which all of the cell components are growing at the same rate (pseudo-steady state), which follows the Malthus relation, $\mu = \frac{1}{X}\frac{dX}{dt}$.

The stationary phase is the stage where the total growth rate is zero or cell division rate equals to cell death rate. There is no longer an upsurge in viable microorganism cell numbers and cellular metabolic activity is reduced (Marwan *et al.*, 2018). The death phase comes after the stationary phase. Here cells loose their viability or are destroyed by harsh environment, lysis, depletion of

nutrient or toxic by-product. Equation (2.8) (Ge *et al.*, 2019) through (2.9) gives the relationship between temperature (T), specific growth rate, μ and kinetic constant of the death occurences, k_d (h^{-1}),

Cell death rate: $$\frac{dN}{dt} = -k_d N \quad (2.8)$$

$$N = N_{st} e^{-k_d \tau} \quad (2.9)$$

where N_{st} = number of cells (conc.) in the medium at the end of the stationary phase, N = number of cells at time t, into the death phase.

Again, substrate balance can be carried out, assuming first order hydrolysis model represents the overall process (Gallipoli *et al.*, 2020). Substrate-to-biomass yield or yield coefficient, Y, is the ratio of mass of new cells (dX) and the mass of substrate consumed (dS) (Abraham, 2018). Literature studies affirmed that, several simplified models have been applied for estimating performance parameters (such as μ_{max} and K_s) (Gallipoli *et al.*, 2020; Tena *et al.*, 2021).

2.4.3 Substrate Utilization Model

The notion that organisms consume substrate in 3 ways can be used to formulate relationships for the rate of substrate utilization, $\left(-\frac{dS}{dt}\right)$ as follows:

(1) Maintenance – substrate could be converted by the microbes into energy to maintain its standard of living (Bodegom, 2007). Rate of substrate consumed in order to maintain the cells is proportional to the number of cells as seen in Equation 2.10 (Mazaheri and Shojaosadati, 2013), where m_s = maintenance coefficient (g substrate/g cell.h).

$$-\frac{\mathrm{dS}}{\mathrm{dt}}\Big|_{\mathrm{maintenance}} = \mathrm{m_s X} \quad (2.10)$$

The higher m_s is, the more the substrate is depleted and this is used to describe multiple substrates. For convenience, m_s was assumed as zero in this work.

(2) Cell mass – substrate may be depleted to produce new cellular components leading to the formation of new cells. Rate of substrate consumed to produce more cells is proportional to the rate of new cells produced, where the cell yield coefficient, $Y_{X/S}$ is placed in front of $-\frac{dS}{dt}$ to give Equation 2.11.

$$-\frac{\mathrm{dS}}{\mathrm{dt}}\Big|_{\mathrm{cells}} = \frac{1}{\mathrm{Y_{X/S}}} \frac{\mathrm{dX}}{\mathrm{dt}} \quad (2.11)$$

(3) Products – substrate could also be used to synthesize chemical products. Here, the product-to-substrate yield, $Y_{P/S}$ is the constant of proportionality. It was therefore assumed here that, no chemical product was formed, hence $-\frac{dS}{dt}\Big|_{product}$ in Equation 2.12 (Sakthiselvan *et al.*, 2019) is zero.

$$-\frac{\mathrm{dS}}{\mathrm{dt}}\Big|_{\mathrm{product}} = \frac{1}{\mathrm{Y_{P/S}}}\frac{\mathrm{dP}}{\mathrm{dt}} \qquad (2.12)$$

Total sum of all these change in substrate consumption was carried out as shown in Equation 2.13 to give Equation 2.14 (Yang *et al.*, 2021), assuming substrate assimilated into energy for growth is negative.

$$-\Delta\mathrm{S} = \left(-\frac{\mathrm{dS}}{\mathrm{dt}}\Big|_{\mathrm{maintenance}}\right) + \left(-\frac{\mathrm{dS}}{\mathrm{dt}}\Big|_{\mathrm{cells}}\right) + \left(-\frac{\mathrm{dS}}{\mathrm{dt}}\Big|_{\mathrm{product}}\right) \qquad (2.13)$$

Specific substrate utilization rate, q ($m_{substrate}/m_{cells}$.time), as well as the first order hydrolysis constant, K_h was estimated by combining equations in Equation 2.14 (Lin *et al.*, 2008; Syaichurrozi & Rusdi, 2020).

$$-\frac{\mathrm{dS}}{\mathrm{dt}} = \frac{1}{\mathrm{Y_{X/S}}}\frac{\mathrm{dX}}{\mathrm{dt}} = \frac{\mu\mathrm{X}}{\mathrm{Y_{X/S}}} = \mathrm{qX} = \mathrm{K_h S} \qquad (2.14)$$

Making S subject in Equation 2.16, substrate concentration data was generated via Equation 2.15 and is termed S-experimented or $S_{Expt.}$.

$$\mathrm{Y_{X/S}} = \frac{\text{g cell mass produced}}{\text{g substrate consumed}} = -\frac{\Delta\mathrm{X}}{\Delta\mathrm{S}} = \frac{\mathrm{X}-\mathrm{X_o}}{\mathrm{S}-\mathrm{S_0}} \qquad (2.15)$$

$$\mathrm{S_{Expt.}} = \mathrm{S_o} - \frac{\mathrm{X_{Expt.}}-\mathrm{X_o}}{\mathrm{Y_{X/S}}} \qquad (2.16)$$

2.5 Existing Growth Kinetic Models

Over the years, several microbial growth kinetic models had been proposed. Table 2.1, depicts 23 models developed to analyze growth characteristics in batch bioreactors.

Table 2.1: Specific Growth Rate Models

S/No.	Model Name	Expression	Reference
1	Monod	$\mu = \frac{\mu_{max} S}{K_s + S}$	(Dlangamandla *et al.*, 2019)
2	Monod with Decay rate	$\mu = \frac{\mu_{max} S}{K_s + S} - b$	(UlukardeŞler and Atalay, 2018b)
3	Contois	$\mu = \frac{\mu_{max}\, S}{K_s\, X + S}$	(Ardestani, 2012)
4	Contois with Decay rate	$\mu = \frac{\mu_{max}\, S}{K_s\, X + S} - b$	(UlukardeŞler and Atalay, 2018b)
5	Andrew	$\mu = \frac{\mu_{max}}{1 + \frac{K_s}{S} + \frac{S}{K_i}}$	(González-figueredo *et al.*, 2018; Xu *et al.*, 2018)
6	Andrew with Decay rate	$\mu = \frac{\mu_{max}}{1 + \frac{K_s}{S} + \frac{S}{K_i}} - b$	(UlukardeŞler and Atalay, 2018b)
7	Moser Model	$\mu = \frac{\mu_{max} S^n}{K_s + S^n}$	(Lv *et al.*, 2022)
8	Tessier	$\mu = \mu_{max}\left(1 - e^{-S/K_s}\right)$	(Wang & Witarsa, 2016; Halmi *et al.*, 2014)
9	Halden	$\mu = \frac{\mu_{max}\, S}{K_s + S + \frac{S^2}{K_i}}$	(Bayen *et al.*, 2018)

S/No.	**Model Name**	**Expression**	**Reference**
10	Haldane	$\mu = \frac{\mu_{max}\, S}{(K_s + S)\left(1 + \frac{S}{K_i}\right)}$	(Xu *et al.*, 2018; Halmi *et al.*, 2014)
11	Verhulst	$\mu = \mu_{max}\left(1 - \frac{X}{X_m}\right)$	(Muloiwa *et al.*, 2020; Annuar *et al.*, 2008)
12	Powell	$\mu = \mu_{max}\ \frac{1 + \frac{S}{K_s} + \propto}{2 \propto}\left[1 - \left\{1 - \frac{4\ \propto \frac{S}{K_s}}{\left(1 + \frac{S}{K_s} + \propto\right)^2}\right\}^{1/2}\right]$	(Muloiwa *et al.*, 2020; Annuar *et al.*, 2008)
13	Dabes	$\mu = \mu_{max}\ \frac{1 + \frac{S}{K_s} + \propto}{4 \propto}\left[1 - \left\{1 - \frac{8\ \propto \frac{S}{K_s}}{\left(1 + \frac{S}{K_s} + \propto\right)^2}\right\}^{1/2}\right]$	(Annuar *et al.*, 2008)
14	Heijnen and Romein	$\mu = \mu_{max}\left[\frac{\frac{S}{K_s}}{\frac{S}{K_s} - 1 + 2^{1/n}}\right]^n$	(Annuar *et al.*, 2008)
15	Aiba-Edwards	$\mu = \mu_{max}\frac{S}{K_s + S}e^{-S/K_i}$	(Tazdait *et al.*, 2013; González-figueredo *et al.*, 2018; Xu *et al.*, 2018)
16	Webb	$\mu = \frac{\mu_{max}\, S\left(1 + \frac{S}{K_i}\right)}{S + K_s + \frac{S^2}{K_i}}$	(Muloiwa *et al.*, 2020)
17	Luong	$\mu = \frac{\mu_{max} S}{K_s + S}\left[1 - \frac{S}{S_m}\right]^n$	(Hamitouche *et al.*, 2012; Xu *et al.*, 2018)

S/No.	Model Name	Expression	Reference
18	Yano and Koga	$\mu = \mu_{max}\left(\frac{S}{K_s + S + \frac{S^2}{K_1} + \frac{S^3}{K_2^2}}\right)$	(Tazdait *et al.*, 2013)
19	Han and Levenspiel	$\mu = \mu_{max} S\left[\frac{\left(1 - \frac{S}{S_m}\right)^n}{S + K_s\left(1 - \frac{S}{S_m}\right)^m}\right]$	(Halmi *et al.*, 2014)
20	Wayman and Tseng	$\mu = \frac{\mu_{max} S}{K_s + S} - i(S - S_\theta)$	(Zhenlin *et al.*, 2019)
21	Alagappan and Cowan	$\mu = \frac{\mu_{max} S}{K_s + S + \frac{S^2}{K_i}} - i(S - S_\theta)$	(Choi *et al.*, 2008)
22	Double exponential	$\mu = \mu_{max}\left[e^{-S/K_i} - e^{-S/K_s}\right]$	(Gummadi and Santhosh, 2010)
23	Logarithmic	$\mu = a + b\ln(S)$	(Muloiwa *et al.*, 2020)

Broadly, growth models are divided into kinetic models with inhibition (e.g. Tseng and Wayman, Andrews, Webb, Aiba-Edwards and Tessier/Double Exponential) and kinetic models without inhibition (e.g. Tessier, Moser and Contois model) (Velazquez-Marti *et al.*, 2018). According to Wang & Witarsa (2016), the feasibility of applying separate kinetics for substrate decomposition would lead to better simulations and needs to be addressed comprehensively.

2.5.1 Monod Equation

The simplest among them is the Monod equation (Jijai and Siripatana, 2017). The classical equation describes the proportional link between the μ and low S, in turn explaining the microbial growth, physiology, and biochemistry using a hyperbolic function of extracellular resource concentration (Amirian *et al.*, 2022; González-figueredo *et al.*, 2018). Monod equation for acidogenic microorganism kinetics is given by Equation (2.17) (Delgadillo-Mirquez *et al.*, 2018),

$$\mu = \frac{\mu_{max}\, S}{K_s + S} \qquad (2.17)$$

where, μ_{max} = maximum specific growth rate (hr^{-1}), K_s = saturation constant (mg/L), S = substrate concentration (mg/L) and μ = specific growth rate (hr^{-1}). From there, knowing that $D = \mu$ and making S the subject, Equation (2.18) for estimating substrate concentration knowing both K_s and μ_{max} can be formed;

$$S = \frac{DK_s}{\mu_{max} - D} = \frac{\mu K_s}{\mu_{max} - \mu} \qquad (2.18)$$

where, D = dilution (hr^{-1}), μ_{max} = maximum specific growth rate (hr^{-1}), K_s = saturation constant (mg/L), S = substrate concentration (mg/L) and μ = specific growth rate (hr^{-1}). The Monod model assumes that the digesting culture media has only one limiting substrate (Muloiwa *et al.*, 2020; González-figueredo *et al.*, 2018). Two special cases for the Monod growth formulae exist. At high substrate concentration (i.e. $S \gg K_s$ with zero order), growth will occur at the maximal growth rate, μ_{max}, making Equation (2.17) simplified to Equation (2.19) and (2.20):

$$\frac{dX}{dt} = \mu_{max} X \qquad (2.19)$$

$$\mu_{max} = \frac{\ln\left(\frac{X}{X_0}\right)}{t} \qquad (2.20)$$

where, X_0 = initial cell concentration (CFU/ml), t = fermentation time (day), μ_{max} = maximum specific growth rate (hr^{-1}) and X = cell concentration at time, t. The integrated form of equation (2.19) gave rise to Equation (2.20) (Salvesen and Vadstein, 2000; Grow, 2017). And at low substrate concentration (i.e. $S \ll K_s$), growth will have a first order dependence on substrate concentration, as μ is highly sensitive to S and the Monod equation simplifies to Equation (2.21).

$$\frac{dX}{dt} = \frac{\mu_{max}\, SX}{K_s} \qquad (2.21)$$

To determine the Monod constant parameters, μ_{max} and K_s, a plot of μ againsts S obtained from experiments is done. From Figure 2.7a, the substrate-affinity constant, K_s, is the value of S at $\mu_{max}/2$ and μ_{max} is the tangent to the inflection point (Arifan *et al.*, 2021). Alternatively, when the reciprocal of the Monod equation is taken, it allows the equation to be transformed into an equation of a straight line with known slope and intercept, to help determine μ_{max} and K_s. A plot

of $\frac{1}{\mu}$ againsts $\frac{1}{S}$ is known as the Lineweaver-Burke plot (Equation 2.22 and Figure 2.3b) (Germec & Turhan, 2021).

$$\frac{1}{\mu} = \frac{K_S}{\mu_{max}}\left(\frac{1}{S}\right) + \frac{1}{\mu_{max}} \qquad (2.22)$$

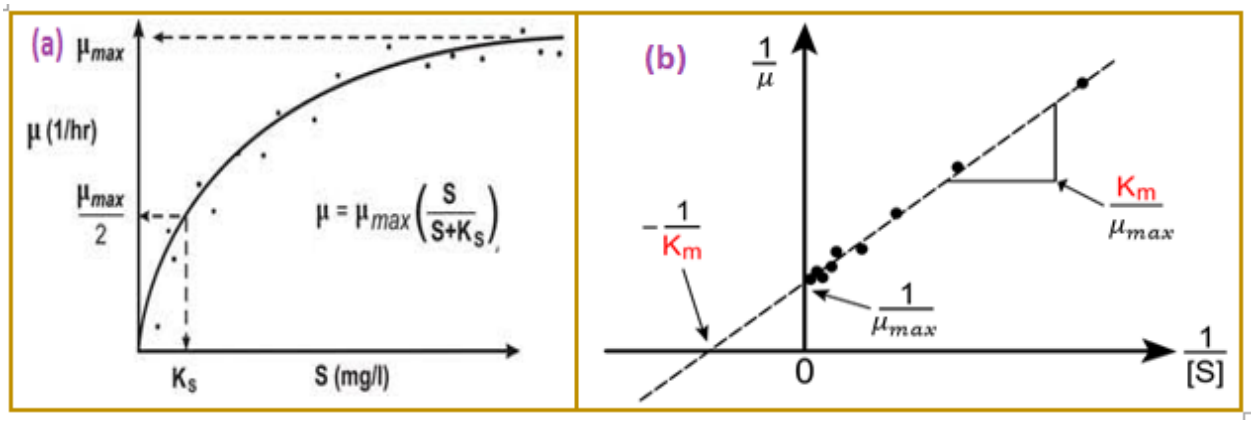

Figure 2.3: (a) Monod Equation fit to Observed Data (b) Lineweaver-Burke Plot

Alternative plots to the Lineweaver-Burke plot is shown in Figure 2.4.

Name	Equation	Plot
Hanes-Woolf Plot	$\frac{S}{\mu} = \frac{k_m}{\mu_{max}} + \frac{1}{\mu_{max}} S$	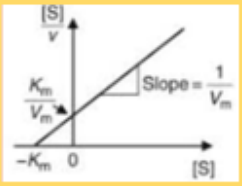
Eadie-Hofstee Plot	$\mu = \mu_{max} - k_m \frac{\mu}{S}$	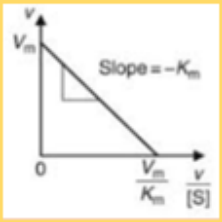
Integration Method	$\frac{\ln\left(\frac{S_0}{S}\right)}{t} = -\frac{1}{k_m}\frac{(S_0 - S)}{t} + \frac{\mu_{max}}{k_m}$	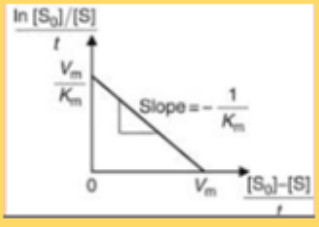

Figure 2.4: Alternative Plots to Determine Monod Parameters (Paar *et al.*, 2019; Germec & Turhan, 2021)

Globally, it is agreed that the Monod model suffers some drawbacks. These limitations are (González-figueredo *et al.*, 2018; Muloiwa *et al.*, 2020): (a) Monod model not being able to describe specific growth rate in the presence of toxic substrate concentration or substrate inhibition effect, (b) separate entity, regulatory complex, adaptive sensitivity to environmental changes, and ability of cell organelles to produce various products in inherent metabolism cannot be considered, (c) at high S, the μ_{max} is independent of the substrate concentration, (d) at low S, growth is dependent on substrate concentration, (e) Monod model does not account for the fact that cells may require substrate for maintenance during the death phase and, (f) model does not account for the lag and death phase during the growth phase. To alleviate these disadvantages, other models incorporating several other parameters have been developed.

2.5.2 Substrate Inhibition Model

The Andrews' equation for substrate inhibition is simple and widely accepted for describing growth inhibition kinetics of microorganisms (Tazdait *et al.*, 2013; Velazquez-Marti *et al.*, 2018). The same author went on to explain the inhibition constant. The inhibition constant, K_i in Andrews' model describes the degree of toxicity of the substrate towards the microorganisms population. Low K_i, shows the high sensitivity the microorganisms had to substrate inhibition. Therefore, K_i is the S at which microorganisms' growth or substrate degradation reduced to 50% of μ_m or maximum specific degradation rate of the substrate as a result of substrate inhibition. Halden model (Hamitouche *et al.*, 2012) is an extended form of the Monod model by introducing the inhibition constant, K_i at low and high substrate concentration, making the model being able to handle both toxic and non-toxic substrate (Delgadillo-Mirquez *et al.*, 2018). It is also called the methanogenic microorganism kinetics used to emphasize the VFA accumulation causing inhibition in AD process (Delgadillo-Mirquez *et al.*, 2018).

Haldane model has been affirmed as good in describing some experimental data involving inhibition of enzymes and microbial growth. In the model, μ rises to an optimum value and then drops as S increases, where the curve shape is dependent upon the values of K_i and K_s (Alqahtani, 2013). Webb model is a modified version of the Haldane model, describing μ as a function of S only. Though, Webb's model intended to improve upon the Haldane model, an endeavor that wasn't successful (Velazquez-Marti *et al.*, 2018; Muloiwa *et al.*, 2020). Another extension of the Monod equation is the unstructured and inhibitory model called Aiba-Edwards model. Aiba-

Edwards model introduces an exponential to the ratio of S and inhibitory constant, K_i, a parameter that takes care of the presence of toxic S in the bioreactor. The model is capable of describing the lag and death phase but struggles when describing critical values of inhibitory substrate (González-figueredo *et al.*, 2018; Muloiwa *et al.*, 2020). Heijnen and Romein in 1995 both came up with a universal microbial growth and substrate uptake model by simplifying cellular procedures to a coupled scheme of anabolic and catabolic reactions (Annuar *et al.*, 2008). Luong model (Xu *et al.*, 2018) can also be used to describe the kinetics of substrate inhibition. It allows the description of substrate limitation observed at a low concentration and also allow substrate inhibition observe at high concentration to be accounted for through the parameter S_m, the maximum substrate concentration above which growth ceases (Hamitouche *et al.*, 2012). Yano and Koga suggested a model after a theoretical study on the dynamic performance of single-vessel continuous digestion subject to growth inhibition at high concentrations of rate-limiting substrates (Tazdait *et al.*, 2013). Using phenol, Han and Levenspiel tabled a general expression used previously to describe substrate inhibition (Alqahtani, 2013).

2.5.3 Kinetic Model Without Inhibition

One important feature about the Contois model is that, cell mass growth rate depends on both substrate and cell concentrations with growth being inhibited at high concentration of microbes (Bayen *et al.*, 2018). The assumption here is that X is inversely proportional to μ (Yunardi *et al.*, 2015). It further explains the changes in population density that is of effect to the net specific growth rate through insertion of the biomass concentration, X, into the existing Monod structure (Annuar *et al.*, 2008). The model had been used to examine the hydrolysis rate of extracellular enzymes in the course of production of a biochemical reaction by hydrolytic microorganism (Hassan *et al.*, 2017). Just like the Monod model, Blackman model, and Tessier model, the Contois model cannot describe the lag and death phase and does not capture substrate inhibition (Muloiwa *et al.*, 2020). In the analysis carried out by UlukardeŞler and Atalay (2018b), application of Contois equation with decay rate for CM gave $\mu_{max} = 0.3$, B = 15 and b = 0.5 for CM having dry solid (%) of 26.975. Also, Contois model has been used to simulate the cleaning of wastewater by microorganisms, model aerobic degradation of wastewater originating from black olive industrial treatment and aerobic biodegradation of solid municipal organic waste, model anaerobic treatment of textile wastewater, anaerobic digestion of ice-cream wastewater, anaerobic reduction of sulphate by sulphate-reducing microorganism and anaerobic treatment of dairy manure, and to

carryout hydrolytic kinetics of swine waste, cellulose, sewage sludge and cattle manure (Alqahtani, 2013; Wang and Li, 2014; Lv *et al.*, 2022).

Tessier model simply labels μ as an exponential function of the S, μ_{max}, and K_S. It takes maintenance energy for cell activity into account, which means the maximum growth rate will be reduced when the S is lower and the microorganisms are competing for resources (Wang and Witarsa, 2016). Wang & Witarsa (2016) employed Contois and Tessier model to connote the biochemical rates of decomposing materials. Moser model integrated a tunable parameter 'n' into the Monod framework, so as to account for potential interactions between binding sites on the enzyme molecule (Velazquez-Marti *et al.*, 2018; Muloiwa *et al.*, 2020). Blackman model had similar assumptions as the Monod model. At low S, growth is dependent on substrate and at high S, when nutrients is limiting, growth is independent of substrate concentration (Muloiwa *et al.*, 2020). There is a first order relationship between μ and S at low S and a zero order relationship at higher S (Annuar *et al.*, 2008). Powell looks at the influence of passive diffusion of a particular substrate as the key limiting step affecting microorganisms growth, without considering substrate inhibition, hence struggles to describe the lag and death phase (Annuar *et al.*, 2008; Muloiwa *et al.*, 2020).

The worst model due to its weakness in describing the lag, stationary, and death phase is agreed to be the Logarithmic model. Logarithmic model is well known for overestimating cell growth, and if the S is low, it can produce negative growth rate (Muloiwa *et al.*, 2020). As clearly seen in Table 2.6, the model describes μ as a function of logarithm of S. Dabes derived a "3-parameter" model describing microorganisms growth on a single limiting substrate by considering that only 2 of the long series of catalyzed, reversible enzyme-substrate reactions involved in substrate metabolism had slow reaction rates (Annuar *et al.*, 2008). Verhulst model gained prominent utilization in industrial and environmental microbiology, and was used to investigate the kinetics of filamentous fungi by Ardestani (2012).

2.6 Kinetics of Biogas Production

Kinetics of biogas production essentially targets the variation of the production as a function of time (Ali *et al.*, 2018). Microorganisms are necessary to enable anaerobic digestion of feedstock to product as most kinetic models assumes that biogas produced are function of microbial growth (Selvaraj et al., 2018; Sukhesh & Rao, 2018). AD is regarded as a dynamic process affected by different other parameters including inoculum source, heating, mixing, addition or non-addition of

nutrients, pretreatment and storage condition (Li *et al.*, 2016). Thus, caution should be taken while carrying out the batch analysis test using the fermentation process, as this is key to evaluating the kinetics of biogas production (Zeb *et al.*, 2019). Empirical observations obtained from experimental data are sources for most kinetic growth models (González-figueredo *et al.*, 2018). Kinetic studies helps in knowing the suitability of kinetic models to determine the significance of relationship between variables to guide the experimental design, assess the experimental results, and to define the specific parameters of the system performance (Lim *et al.*, 2021). With real kinetic parameters, performing different simulations to explore the effect of changing experimental conditions is conceivable (Pecar *et al.*, 2020). In addition, these parameters, which are maximum biogas production rate, biogas yield potential and duration of the lag phase of the reaction, will facilitate the design and scale-up of laboratory experiment into industrial size application, after obtaining them by fitting experimental values with the models (Selvaraj *et al.*, 2018; Ulukardesler, 2021). It is pertinent to emphasize the significance of kinetic study of biogas production using chicken manure as feedstock as shown in Table 2.2:

Table 2.2: Merits of Biogas Kinetic Study

S/No.	Importance	Reference
1.	Regulate and maximize the flow of gas generated	(Delgadillo-Mirquez *et al.*, 2018)
2.	Plant sizing/capacity and formulate relationship between dissimilar parameters affecting the AD process	(Hassan *et al.*, 2017)
3.	Evaluate empirical results, check initial hypothesis, control and predict the process performance, aid plant design optimization	(Zhao *et al.*, 2016; Parralejo *et al.*, 2019)
4.	Scale up analysis and estimation of treatment efficiencies of full-scale bioreactors	(Lim *et al.*, 2021)
5.	Empirical kinetic studies results can be used for simulating the digester behavior and predicting biogas production	(Lim *et al.*, 2021)
6.	Construction and application of chemical and/or biochemical processes	(Pecar *et al.*, 2020)
7.	Gain insight on characteristics of the process for further optimization	(Pecar *et al.*, 2020)
8.	Understanding basic mechanism of complex AD process involving different microorganisms for process design and control	(Sukhesh and Rao, 2018)
9.	Analyze the metabolic pathways and mechanisms involve during the AD	(Opurum *et al.*, 2021)
10.	Predict bioreactor efficiency	(Opurum *et al.*, 2021)
11.	Evaluate the hydrolytic process and make comparison among diverse lignocellulosic components.	(Yang *et al.*, 2021)

2.6.1 Modified Gompertz Model

Modified Gompertz model is among the best, popular, most adequate and comprehensive biogas kinetic models for simulating batch organic waste anaerobic decomposition (Jijai and Siripatana, 2017; Syaichurrozi *et al.*, 2018; Zeb *et al.*, 2019). The semi-empirical model (Jijai and Siripatana, 2017), is a modified form of the Gompertz equation that assumes cumulative biogas production is a function of hydraulic retention time (Ghatak and Mahanta, 2014; Latinwo and Agarry, 2015; Van *et al.*, 2018; Alfa *et al.*, 2020; Arifan *et al.*, 2021). It is important in analyzing product

formation rate or cell growth rate because of the direct relationship between microbes and biogas yield (Syaichurrozi *et al.*, 2018; Abid *et al.*, 2021). For this reason, the modified Gompertz model is the most reliable model for defining microorganisms' growth (Selvaraj *et al.*, 2018).

The model can describe cell density in the light of lag phase duration and exponential growth rates during microorganisms' growth in anaerobic digestion processes (Alfa *et al.*, 2020; Gallipoli *et al.*, 2020; Ma *et al.*, 2021). It fails to describe the beginning of the process, and no-sense of lag phase constant has been considered (Van *et al.*, 2018). It is common to estimate kinetic constants from the modified Gompertz models data obtained from experimental study and checked for fitness of the model (Ali *et al.*, 2018; Kainthola *et al.*, 2019; Gallipoli *et al.*, 2020). The growth rate of the modified Gompertz equation curve is positive, and the curve shape is directly linked to the equation parameters, assuming growth is inhibited by substrate level logarithmically (Van *et al.*, 2018; Hongguang *et al.*, 2019). Table 2.3 presents different models on biogas kinetics together with their parameters.

Table 2.3: Biogas Kinetic Models

Models Name	Equations	Parameters	Reference
Modified Gompertz	$\mathrm{CBY} = \mathrm{BP}e^{-e^{\left[\frac{k.e}{BP}(LP-t)+1\right]}}$	BP, k, LP	(Haryanto *et al.*, 2018; Keskin *et al.*, 2018; Van *et al.*, 2018)
Logistic	$\mathrm{CBY} = \frac{\mathrm{BP}}{1+e^{\left[\frac{4.k(LP-t)}{BP}+2\right]}}$	BP, LP, k	(Gallipoli *et al.*, 2020; Lim *et al.*, 2021; Opurum, 2021)
Transfert	$\mathrm{CBY} = \mathrm{BP}e^{-e^{\left[1-\frac{k.e}{BP}(LP-t)\right]}}$	BP, k, LP	(Ali *et al.*, 2018)
Cone	$\mathrm{CBY} = \frac{\mathrm{BP}}{1+(kt)^{-SF}}$	BP, k, SF	(Shen *et al.*, 2018; Jiang *et al.*, 2021)

where, CBY = cumulative biogas yield at digestion time t days (mL/g VS); BP = maximum biogas potential of the substrate (mL/g VS); β = non-degradable fraction of the substrate; k = specific (maximum) biogas production rate (day^{-1}); LP = lag phase (day); e = logarithmic constant (=

2.718282); t = incubation or retention time (day) and; SF = shape factor or shape coefficient of the curve. Apart from CBY and t, all other parameters are referred to as kinetic parameters. Kinetic parameters are essential for biodigester design and optimal operation of large-scale anaerobic plants (Paritosh *et al.*, 2017). They can be used to examine the effect of the substrate ratios on biogas production (Abdelhay *et al.*, 2021) to see whether values of kinetic constants depended on substrates and degree of fragmentation (Szlachta *et al.*, 2018).

The lag phase, LP (Zeb *et al.*, 2019), is the minimum time needed by anaerobic microorganism to adapt in the substrates before the microorganism produced biogas (Ghatak and Mahanta, 2014; Zhao *et al.*, 2017; Syaichurrozi *et al.*, 2018) or the time needed for active methanogenesis to occur (Iqbal *et al.* 2011). Though not specifically methanogenesis, it could mean, the initial duration required for hydrolysis, acidogenesis, and acetogenesis in producing acids, alcohols, and H_2/CO_2 from organic matter (Sukhesh and Rao, 2018). More precisely, is the delay period (Sukhesh and Rao, 2018) or minimum time between inoculation and biogas appearance (Szlachta *et al.*, 2018). When LP is less than zero (or negative), it implies that the system needs no lag time to produce biogas and LP can be taken as 0 day (Faraz, 2020). Ideally, LP is often longer than 1 day (Van *et al.*, 2018). The parameter, k, is the rate at which biogas is generated at exponential phase of the digestion (Sukhesh and Rao, 2018). Specific Methanogenic Activity (SMA) is the ratio of k and the amount of volatile solid or inoculum used (Cheong *et al.*, 2019). It is obvious from Table 2.8 that not all model captured the same kinetic parameters, others had included shape factor and β.

2.6.2 Cone, Transfert and Logistic Model

Cone model is less popular in the literature in terms of its application to simulate biogas formation (Syaichurrozi *et al.*, 2018). It is one of the models that points to digestion efficiency and substrate biodegradability (Jiang *et al.*, 2021). The Transfert and the modified Gompertz model takes similar parameters and are opposite as seen in the inner exponential term of their equation. Logistic kinetic model is among the complex models specifically developed to study the LP (Opurum, 2021). It is a sigmoid curve used to explain a time-dependent procedure in which at the starting stage, the exponential growth is witnessed and upon saturation, the growth slows down and achieve plateau at the end (Lim *et al.*, 2021). Logistic function model finds application in biomethane potential tests and solid waste fermentation/methanation in landfills, taking into account that the rate of biogas production is directly proportional to the amount of gas already generated, k and BP (Gallipoli *et al.*, 2020). The model describes CBY from batch digesters, assuming that the gas

generation is a function of microorganism growth (Deepanraj *et al.*, 2015). An extension of the Logistic model is the Bi-logistic model (Opurum *et al.*, 2021). It tried to include the diauxic growth effect in biogas production (Liu, 2017).

2.6.3 Less Common Biogas Kinetic Model

To predict the rate-limiting or hydrolysis step in anaerobic digestion for accurate representation of the extent of biodegradation, CBY, and the BP results, the classical First-Order kinetic model might be a model of choice to simulate dissimilar substrates (Li *et al.*, 2013; Li *et al.*, 2019; Abid *et al.*, 2021). In complex substrate such as the lignocellulosic material, there are fluctuations in the non-degradable fraction, canceling out the reliability of the first order model to simulate the entire process. Hence, in 2013, a modified First-Order model to improve the simulation precision by encompassing the effect of biodegradability of substrate was proposed (Li *et al.*, 2013).

Just like the Fitzhugh and Richards model, they are the only model that incorporates the shape factor (n), a parameter that signals the presence or absence of lag phase (Zhao *et al.*, 2016; Parralejo *et al.*, 2019). Essentially, it allows the determination of k and the behavior of biogas production which is based on 'n'. Also, the Fitzhugh model try to explore the hydrolytic and methanogenic performances of different digesters (Yang *et al.*, 2021). The transference function is applied traditionally to measure the efficacy of conventional pretreatments, used to fit inputs and outputs mathematically in reaction curve-type model or black box model (Li *et al.*, 2013). The model predicts maximum biogas production uniquely based on methane production using a sigmoid curve following the principle that a process could be analyzed as a system receiving inputs and generating output; what is called control (Gallipoli *et al.*, 2020).

Venkateshkumar *et al.* (2020) proposed a new model he called the 'Proposed model' that relates CBY which depends on input parameters like individual substrates and its combinations and inoculation time. Chen and Hashimoto model (Pererva *et al.*, 2020) has been applied satisfactorily for both batch and continuous AD processes for the evaluation of anaerobic fermentation reactions (Li *et al.*, 2019). Lots of other models developed are not common in field applications. Table 2.4 gives the results of regression to determine the unknown kinetic parameters of single or combinations of some of these models for mono-digestion and co-digestion of chicken manure and other feedstock.

Table 2.4: Estimates of Biogas Kinetic Parameters of Chicken Manure

Author	Model Kinetic	Feedstock	Outcome/Conclusion
(Li *et al.*, 2016)	First-Order Kinetic Model & Gompertz Model	Chicken manure, chicken processing waste (CPW), miscanthus and seagrass	Methane yield of CM = 400 ml g^{-1} VS
(Ma *et al.*, 2021)	Modified Gompertz Model	Chicken manure	BP = 13.8 L/gVS, k = 0.69 L/gVS/day, LP =5.20 days and RT = 80 days
(Liu *et al.*, 2018)	Modified Gompertz Model	Chicken manure	LP = 343.5 h, BP = 345.2 ml, maximum CH_4 yield rate = 0.948 ml/h and RT=930 hr
(Selvaraj *et al.*, 2018)	Modified Gompertz Model	Raw poultry litter	BP = 18.77 l/kg VS, k = 1.08 (l/kg.day) and LP = 1.5 days
(Jiang *et al.*, 2021)	Cone & Modified Gompertz Model	Chicken manure and corn straw	Cone model: k = 10.8850±0.2109 mL/(gVS·day), LP =7.0328±0.1241 day, R^2 = 0.9987, and AIC = 43.48. Modified Gompertz: k = 0.0688±0.0000 day^{-1}, SF =3.7073±0.0985, R^2 = 0.9989, and AIC = 39.41
(Duan *et al.*, 2018)	Logistic & Modified Gompertz Model	Chicken manure + algal digestate	Modified Gompertz: k =7.71-12.07 mL/(gVS.day), LP = 11.37-15.73 day, and R^2 =0.9924-0.9984. Logistic model: k =5.90-11.56 mL/(gVS.day), LP =11.48-15.80 day, and R^2 =0.9908-0.9966

2.6.4 Cumulative Biogas Measurement

Gas is generated continuously during AD and is collected using a tube or balloon. Measuring the amount of gas generated at specified interval is important in calculating the CBY. In some studies, especially the liquid displacement technique explained by Syaichurrozi *et al.* (2018) and Uche *et al.*, (2020), gas is measured but is lost at the same time as the method doesn't favour the recovery of the gas generated. Less stressful, but fairly accurate measurement technique is to weigh the gas collector at every interval by opening a non-return valve. The weight of the collector measured is subtracted from previous measurement obtained to get the weight of the gas. Taking biogas density of 1.2 kg/m^3, based on range reported by Teferra and Wubu (2018), the volume of biogas produced can be calculated by dividing biogas mass by density. Summing successively, the biogas weight at a certain time with the next, gives the CBY. Biogas composition is most often characterized using GC-MS as indicated by Tetteh and Rathilal (2020) for the constituents compositions of the gas.

2.7 POLYMATH and Regression Parameters

POLYMATH is an educational software recommended for mathematicians, engineers and financial analysts. POLYMATH solves four types of numerical problems arising in those subjects, namely, system of nonlinear equations, system of ordinary differential equations (ODEs), data regression and system of linear equations. POLYMATH can solve up to 300 set of nonlinear\ equations with 300 explicit equations using four types of solution approaches, including 'safenewt', 'fastnewt', 'safebroydn' and constrained nonlinear equations. Both the microorganisms growth kinetic model and the biogas kinetic model can be run in regression software to determine their respective kinetic parameters. The most extensively used statistical technique is regression analysis, which involves detecting, evaluating, and analyzing the connection between the dependent and variables. The regression window in POLYMATH is divided into 3 tabs, namely, 'Regression', 'Analysis' and the 'Graph' tab. Parameters of nonlinear growth kinetics and those of biogas models can hence be estimated (Selvaraj *et al.*, 2018; Syaichurrozi *et al.*, 2018). Also, Origin Pro (an alternative software) as well as POLYMATH uses Levenberg-Marquardt method to estimate the unknown parameters of a non-linear model. Origin Pro provides the same regression capability seen in POLYMATH but has more advantage in its ability to compare models.

In the regression software, there are certain parameters used to describe the goodness of the fit (Venkateshkumar *et al.*, 2020). To know if there is substantial difference between models with different number of parameters, in terms of the quality of fit to the same experimental data, various models such as coefficient of determination (R^2), Normalized Root Mean Square Error (NRMSE), Bias Factor (BF), Root-Mean-Square Error (RMSE) and adjusted R^2 (Barreto *et al.*, 2019), Accuracy Factor (AF), Akaike Information Criterion (AIC) and F-test (Halmi *et al.*, 2014). A regression parameter useful in estimating R^2, AIC, BIC and in F-test is called the Residual sum of squares (RSS) given by Equation 2.23,

$$\mathrm{RSS} = \sum(|\text{Measured biogas}| - |\text{Predicted biogas}|)^2 \qquad (2.23)$$

where, RSS = Residual Sum of Squares. Most often, the coefficient of determination, R^2, a magnitude of strength of relationship between experimental and predicted values of the biogas yield (Lim *et al.*, 2021) in Equation (2.24) is applied (Pererva *et al.*, 2020).

$$\mathrm{R^2} = 1 - \frac{\sum(|\text{Measured biogas}| - |\text{Predicted biogas}|)^2}{\sum(\mathrm{y_i} - \bar{\mathrm{y}})^2} \qquad (2.24)$$

It is applied when assessing the quality of fit of a model, but in nonlinear regression, where difference in the number of parameters between one model to another is normal, the adoption of the method does not readily provides comparable analysis (Pererva *et al.*, 2020). In this case, an adjusted R^2 is used to compute the quality of nonlinear models based on Equation (2.25):

$$\text{Adjusted } \mathrm{R^2} = 1 - \frac{\mathrm{RMS}}{\mathrm{S_Y^2}} = 1 - \frac{(1-\mathrm{R^2})(\mathrm{n}-1)}{\mathrm{n}-\mathrm{p}-1} \qquad (2.25)$$

where, RMS = Residual Mean Square, s_y^2 is the total variance of the y-variable, p = number of independent variables in the model, excluding the constant, and n is the number of measurements. Similar to R^2, the root mean square error (RMSE) explains the standard deviation value between measured and estimated biogas yield by measuring the difference between predicted and target values and shows also, the degree of linearity of predicted and target values (Najafi *et al.*, 2019; Venkateshkumar *et al.*, 2020). Specifically, it is the sum of squares of differences between the predicted and experimental values and of biogas yield (Sukhesh and Rao, 2018; Lim *et al.*, 2021). RMSE are also called Root-Mean-Square Deviation (RMSD), Root Mean Square Prediction Error (RMSPE), or Standard Error of Estimate. RMSE value are very low (Venkateshkumar *et al.*, 2020) and is given by Equation (2.26) (Kang *et al.*, 2021),

$$\mathrm{RMSE} = \sqrt{\frac{1}{\mathrm{n}}\sum(\mathrm{predicted} - \mathrm{observed})^2} \qquad (2.26)$$

where, n = number of measurements. It is expected that the model with the smaller number of parameters will give a smaller RMSE values (Halmi *et al.*, 2014). Mean Absolute Percentage Error (MAPE) as presented in Equation (2.27) can be calculated to find which model is best to fit the measured biogas yield during AD by assuming that at MAPE < 20%, the model could be said to be a good model (Syaichurrozi *et al.*, 2018).

$$\mathrm{MAPE} = \frac{1}{\mathrm{n}}\sum\left(\frac{|\mathrm{Measured\ biogas} - \mathrm{Predicted\ biogas}|}{|\mathrm{Measured\ biogas}|}\right) \times 100\% \qquad (2.27)$$

This is followed by Equation (2.28) given the mean square percentage error:

$$\mathrm{MSPE} = \frac{1}{\mathrm{n}}\sum\left(\frac{|\mathrm{Measured\ biogas} - \mathrm{Predicted\ biogas}|}{|\mathrm{Measured\ biogas}|}\right)^2 \qquad (2.28)$$

where, n stands for number of measurements. Akaike's Information Criterion (AIC) (Aragón-noriega *et al.*, 2015), serves the purpose of estimate the probability of a model to predict future values (Hawkins *et al.*, 2019), determine a correct model by comparing kinetic models (Lim *et al.*, 2021), provides a relative approximation of the data lost from empirical sources, helps in model selection by determining the relative quality of specific statistical model for the experimental data available, and encourages non-use of complicated model for fitting empirical values (Halmi *et al.*, 2014). A negative AIC is preferred for a set of predicted model (i.e. a value of -12 is more preferred than -5), because a lower AIC value indicates a better fit (Halmi *et al.*, 2014; Hawkins *et al.*, 2019). The AIC expression is shown in Equation (2.29-2.31) (Pererva *et al.*, 2020),

$$\mathrm{AIC} = \mathrm{N}.\ln\left(\frac{\mathrm{RSS}}{\mathrm{N}}\right) + 2\mathrm{M} + \frac{2\mathrm{M}(\mathrm{M}+1)}{\mathrm{N}-\mathrm{M}-1} \quad \text{when } \frac{N}{M} < 40 \qquad (2.29)$$

$$\mathrm{AIC} = \mathrm{N}.\ln\left(\frac{\mathrm{RSS}}{\mathrm{N}}\right) + 2\mathrm{M} \quad \text{when } \frac{N}{M} \geq 40 \qquad (2.30)$$

$$\mathrm{BIC} = \ln\left(\frac{\mathrm{RSS}}{\mathrm{N}}\right) + \mathrm{M}.\ln(\mathrm{N}) \qquad (2.31)$$

where N is the number of data points or observations, RSS is the residual sum of square of the vertical distances for the points from curve and M is the number of parameters fit by the model. Much similar statistical analysis model is the Bayesian Information Criterion (BIC) given by Equation (2.31). Another important regression parameter applied in testing the goodness of fit of

kinetic models are the bias factor (BF) and the accuracy factor (AF). BF formulae is as shown in Equation (2.32) and its value equal to 1 is a demonstration of perfect match between observed and predicted values.

$$\mathrm{BF} = 10^{\frac{\sum \log\left(\mathrm{Observed}/\mathrm{Predicted}\right)}{\mathrm{n}}} \qquad (2.32)$$

This means, for degradation studies or microbial growth curves, BF > 1 is a fail-safe model while a model given BF < 1 indicates a fail-dangerous model (Halmi *et al.*, 2014). Halmi *et al.* (2014) also pointed out that AF is often ≥ 1, further stating that higher values points to a less precise prediction, as shown in Equation (2.33). Though, when the predicted and observed values match perfectly, BF = AF = 1 (Kang *et al.*, 2021).

$$\mathrm{AF} = 10^{\frac{\sum \left|\log\left(\mathrm{Predicted}/\mathrm{Observed}\right)\right|}{\mathrm{n}}} \qquad (2.33)$$

CHAPTER THREE

METHODOLOGY

3.1 Materials and Equipment Used

Equipment used are digital colony counter, 5 mL syringe, culture plates, pH/Temperature meter (PH-2601), electric furnace-20141, laboratory incubator (NL9052-1), YX-280A portable autoclave, drying oven-nouvelle 6111 plus, car tyre tube, EDXRF analyzer, laboratory clamp, GC-MS 6800, test-tube, test-tube rack, white translucent sample bottle, 500mL glass media storage bottle, 1601 (500mL) plastic measuring cylinder, digital weighing balance and spirit lamp. Materials used are chicken manure, distilled water, sterilized bottle water and nutrient agar was used in various stages of the research.

3.2 Bioreactor Setup

A fabricated cylindrical laboratory-scale anaerobic digester of height, 55.3cm, diameter, 27.5cm, thickness, 0.4cm and volume of 32850 cm^3 as shown in Figure 3.1 was used as a batch reactor.

Figure 3.1: Bioreactor for Biogas Production

The top consists of an inlet that takes in feed for digestion, bottom outlet opening to collect mixed slurry or digestate for microbial count, and a gas outlet in which a pipe was connected to the gas holder. The pipe attached to the narrow tube gas outlet at the top is 3.81 cm and the circular rubber gas holding tube has 70 cm outer diameter, 24cm inner radius and 10cm width. A means of stopping the outflow of the gas generated within the digester (specifically a clamp) was attached at the top of the gas outlet. A manual stirrer of length equal to 49.53 cm that goes deep into the digester for intermittent stirring of liquid slurry is provided. At the end of it are two metal

horizontal blades for stirring aids attached to a long metal shaft and an L-shape handle which is seen outside the batch tank. The digester tank is made of iron and painted black to regulate heat transfer between the tank and the environment.

3.3 Feedstock Preparation and Characterization

Semi-solid CM with detectable amount of moisture containing chicken dung, blood, urine, feather, and poultry feeds was collected from the Faculty of Agriculture poultry farm of the University of Maiduguri was collected. The manure was then characterized for ash content, moisture content, volatile matter content, C/N ratio, nutrient content and elemental compositions via the stated empirical steps. Moisture content (MC) was calculated according to equation given by Matheri *et al.* (2017) while total solids (TS), carbon-to-nitrogen (C/N) ratio and ash content (AC) on wet basis were according to Najafi *et al.* (2019), Noori & Ismail (2019) and the American Society for Testing and Materials (ASTM) standard test method for ash content respectively. Organic matter (OM) content and particle density (PD) were based on Ksheem and volatile solid (VS) content was determined based on the American Public Health Association (APHA) standard method. Also, VS/TS value, a ratio that tells whether the substrate contains more organics suitable for biogas production was determined. Equation 3.1 reported by Li *et al.* (2013) and Noori and Ismail (2019) was then used to calculate the % crude protein content.

$$\%Nitrogen = \frac{\%Protein}{6.25} \tag{3.1}$$

Elemental composition of the CM substrate was determined using EDXRF analyzer.

3.4 Digester Start-Up

3.4.1 Process Start-Up

Using a digital weighing balance, 7.2 kg of dried CM was measured and mixed thoroughly with 7.05 kg of water (H_2O) to keep the substrate-to-H_2O ratio at 1:1.05; approximately equal to 1:1 agreed upon in majority of researches, to form a slurry in large container including Eronmosele *et al.* (2020) who used the ratio 1:1:1 of water, poultry droppings and waterleaf and poultry droppings, water and elephant grass. Substrate concentration, S, is the amount of substrate present that can be converted to product. With known mass of CM and known volume of H_2O (i.e.

0.00756m^3 taking 1000 kg/m^3 as density of H_2O), the initial substrate concentration, S_o, was calculated based on Equation 3.2.

$$S_o = \frac{\text{amount of sample}}{\text{amount of } H_2O} \qquad (3.2)$$

S_o was used to estimate the biomass-to-substrate yield, $Y_{X/S}$, of the digestion process as it is an important constant parameter. After this step, the mixture pH and initial temperature was measured using a pH/temperature meter before injecting into the batch digester via the top inlet using a funnel and closed tightly. The bottom outlet of the digester was kept closed and the gas pipe and gas holder was connected to hold the generated gas. A clamp was put mid-way close to the top of the narrow gas outlet pipe to prevent the generated biogas from entering the gas holder. The biodigester was then kept at the surrounding temperature.

3.4.2 Temperature and pH Measurement

Using a pH-temperature meter 2601, both the pH and temperature inside the digester were read daily for 40 days. There wasn't any heating of sought of the biodigester. The process relied on the ambient temperature of the environment to digest the CM feedstock. Some amounts of acid and base was added to neutralize the CM substrate for the microbial survival.

3.5. Microbial Count

3.5.1. Determination of Microbial Concentration

To determine the initial cell or biomass concentration, X_o, 5ml of mixed sample was collected before it was charged into the reactor in a small bottle and closed tightly. X_o was used together with S_o when computing $Y_{X/S}$ and procedures taken to obtain X_o at t = 0 is based on the serial dilution prior to the pour plate method of cell concentration (X) measurement, according to Equation 3.3 (Shariful Islam *et al.*, 2021; Okpokwasili and Nweke, 2005).

$$Y_{X/S} = \frac{\text{g cell mass produced}}{\text{g substrate consumed}} = -\frac{\Delta X}{\Delta S} = \frac{X - X_o}{S - S_o} \qquad (3.3)$$

The microbial concentration was observed to decrease and subsequent values were determined repeating the same step. It has also been reported by Haleem *et al.* (2013) that a number of microbes are present in poultry meats and procedures followed to determine these microbial contents was similar to one explained here.

3.5.2 Serial Dilution

Nine test-tubes arranged in a rack was used to run the serial dilution experiment (SDE). The experiment was conducted in triplicate (i.e. SDE1, SDE2 and SDE3). The dilution factors (DF) in all the SDEs was calculated using Equation 3.4 given by Reynolds (2016).

$$\text{Dilution Factor(DF)} = \frac{\text{Final volume } (V_f)}{\text{Initial volume } (V_i)} = \frac{(\text{Amount transfered}) + (\text{Diluent volume})}{\text{Amount transfered}} \quad (3.4)$$

The total dilution factor (TDF) in all SDEs was calculated.

3.5.3 Preparation of Culture Media

Following the method described in the Swe Biotech Nutrient Agar (NA) manual, the nutrient agar was prepared. In order to ensure proper dissolution of agar in H_2O and also sterilize the media, the nutrient agar bottle was put inside an autoclave. Thus, sterile H_2O was first poured in an autoclave to the level of the indicator line and the NA bottle was placed inside and lid covered tightly. The autoclave was set to temperature of 121℃ and heated until the pressure gauge reads a 0 psi after which the bottle was removed. The melted agar was allowed to cool to about 45℃ in a water bath. Normally, if the liquid agar is too hot, certain microorganism are killed automatically, and if very cold, it will solidify in the bottle or as it is poured into petri dishes or plates. Hence, serial dilution was carried out prior to media preparation so that the agar is used immediately it cools to 45℃.

3.5.4 Pour Plate Technique

After the dilutions, 1 ml of inoculum was transferred to the empty sterile dishes from the ninth tube of each run using a labelled syringe. The pour plate method using serial dilution is a method used for quantifying microorganism in a sample. The procedure was carried out by pouring the prepared media into 3 plates (for the SDEs) by first flaming the mouth of the vessel, making sure it covers the entire bottom surface of the plate and lastly covering the plates. The poured plates were gently swirled for about 30 seconds, not allowing them to splash onto the lid or over the edge. The media (or liquid agar) was observed to solidify after cooling and is more opaque than the yellowish liquid media prepared. After solidification, the plates were inverted to prevent moisture from condensing on the surface. The 3 plates of solidified agar were then incubated at 37℃ for 24 hours to form visible cell colony. The test tubes were washed and allowed to dry to be used the next day.

3.5.5 Colonic Counting

On day 2, the plates were removed from the incubator and colonies counted using the colonic counter and results recorded for SDE1, SDE2 & SDE3. CFU/ml was then calculated using Equation 3.5 (Um-e-Habiba *et al.*, 2021; Arana *et al.*, 2013).

$$\text{CFU/ml} = \frac{(\text{No. of colonies})(\text{Total dilution factor, TDF})}{\text{Volume of culture plated in mL}} \qquad (3.5)$$

Using TDF = 10^9 for 1ml of inoculum plated, CFU/ml of the triplicate step were recorded. The average of these data were then computed as initial microbial concentration of day 1 (X_0) of the CM feedstock. The used plates were then discarded. The method was carried out according to explanations given by Brugger *et al.* (2012).

To ensure homogeneous composition of substrate, expedite cell growth and break possible agglutination of microial cells in the digester, the mixed CM slurry was stirred using the manual stirrer before taking the 5ml sample for microbial count. For subsequent days, microbial concentration, X, was determined repeating the serial dilution, pour plating and colonic counting procedures. Specifically, out of the 500ml of NA prepared, 3×20ml = 60ml was used a day and 480 ml in 8 days before another culture media is prepared. When X starts to decrease, the death phase of the microorganism is therefore reached and cell counts stops. The microorganism concentrations recorded over this period was recorded as $X_{Expt.}$ implying cell concentration gotten from the SDEs for the triplicate run of experiment.

3.6 Cumulative Biogas Measurement

Flow of biogas out of the digester as well as into the gas holder was restricted using two clamps. At time t = 0 day or the instances after the CM was fed into the batch fermenter and gas holder is connected, clamp 1 was used to clip the gas pipe (which is 1 ½ yards) at the top of the digester to prevent outflow of any gas generated inside the tank space to the gas collector. Initially, the weight of the empty gas holder was measured, and equals to 0.705 kg. With biogas generation, the size and weight of the gas collector was observed to increase following the removal of clamp 1. To measure the weight of the gas holder, so as to determine the amount of biogas generated, clamp 2 was used to tighten the mouth of the tube close to the gas holder. The top clamp or clamp 1 was then removed for about 5 seconds to allow the generated gas flow out of the digester and is placed back immediately. Clamp 2 was then removed and weight of the gas holder was measured and left

freely. The difference in weight of gas plus gas holder was computed to determine the weight of gas generated daily and results were recorded.

Taking biogas density of 1.2 kg/m^3, based on range reported by Teferra and Wubu (2018), the volume of biogas produced was calculated by dividing biogas mass by density. CBY produced was computed and the biogas composition was characterized using GC-MS as indicated by Tetteh and Rathilal (2020).

3.7 Growth Kinetics

In cell growth kinetics, growth infer cell replication plus a change in cell size. To keep growing, cells need to take nutrients from the CM slurry and change them to cellular matter (biomass) and energy. It is an autocatalytic process described by Equation 3.6 and 3.7.

$$\text{Substrate/nutrient} + \text{cells/biomass} \rightarrow \text{extracellular products} + \text{more cells} \quad (3.6)$$

$$\sum_i S_i + X \rightarrow \sum_j P_j + nX, \quad n > 1 \quad (3.7)$$

Relationship between S, X, product (P) and associated models was used to study the kinetics of biogas production from CM.

3.7.1 Growth Curve Plot

To depict the microbial growth curve for the CM slurry containing microbes, the logarithm of the average cell concentration ($X_{avg.}$) from the 3 SDEs was taken. A plot of this logarithm versus time always gives the growth curve and was used to explain the different phases of the microbial growth and the resulting biogas output.

3.7.2 Finding Generation Time and Decay Constant

At the exponential phase, the population growth is caused by continuous binary fission or cell division into two new cells from an initial number of cells. The number of generation, n of these new cells was estimated using Equation 3.9 during the period of the exponential growth phase after linearizing Equation (3.8) (Um-e-Habiba *et al.*, 2021).

$$N = N_0 2^n \quad (3.8)$$

$$n = \frac{\log N - \log N_0}{\log 2} \quad (3.9)$$

where, N_0 = initial number of cells counted, N = number of cells at time, t. The doubling time, t_d or generation time, G, are same and was computed using Equation (3.10), where k = maximum specific utilization rate (g substrate/g of microorganisms/day) and t = time interval.

$$G = \frac{t}{n} = \frac{1}{k} \tag{3.10}$$

Similarly, the first order model ($\frac{dX}{dt} = \mu X$) for a closed batch system was linearized so as to derive a new expression (from Equation 3.11 and Equation 3.12) for t_d.

$$\mu = \frac{\ln\left(\frac{X}{X_0}\right)}{t}; \qquad X = (\%\ \text{increase})X_0 \tag{3.11}$$

$$t_d = \frac{\ln 2}{\mu} \tag{3.12}$$

The simplest procedure of finding G is through the use of Equation 3.10, by generating k data from the slope $\left(= \frac{\log 2}{G}\right)$ of the plot of log N against time (hr), looking at Equation 3.13.

$$\log N = \log N_0 + \frac{t}{G}\log 2 \tag{3.13}$$

In essence, G was found using Equation 3.10 and 3.12. At the death phase, the rate of cell death is given by Equation (3.14) (Ge *et al.*, 2019),

$$\frac{dX}{dt} = -bX \tag{3.14}$$

where, X = cell concentration (mg/L), b = decay constant (hr^{-1}) and t = retention time (hr). Equation 3.14 was integrated over the initial ($X_{D,0}$) and final cell concentration (X_D) within the period (Equation 3.15) and linearized (Equation 3.16) to estimate the first-order decay coefficient or kinetic constant of the death occurrences, b.

$$X_D = X_{D,0}e^{-bt} \tag{3.15}$$

$$\ln(X_D) = \ln\left(X_{D,0}\right) - bt \tag{3.16}$$

Appropriately, $X_{D,0}$ = number of cells (concentration) in the medium at the end of the stationary phase while X_D = number of cells at time t into the death phase. Using Equation (3.16), a plot of $\ln(X_D)$ versus time was made and 'b' was calculated from the slope of the graph.

3.7.3 Substrate Concentration Determination

Using the values of S_0, X_0, and $Y_{X/S}$ (obtained in from Equation 3.3), the experimental S (or $S_{Expt.}$) in mg/L was determined using Equation 3.17 for every experimental X (or $X_{Expt.}$) (CFU/mL)

$$S_{Expt.} = S_o - \frac{X_{Expt.} - X_o}{Y_{X/S}} \qquad (3.17)$$

3.7.4 Material Balance

For the well-mixed unsteady state batch biological system (Figure 3.2) where all nutrients are fed initially into the culture and cells produced in the culture grow until one or more nutrient is exhausted, material balance over this process was formed, and it follows Equation 3.18 through 3.22.

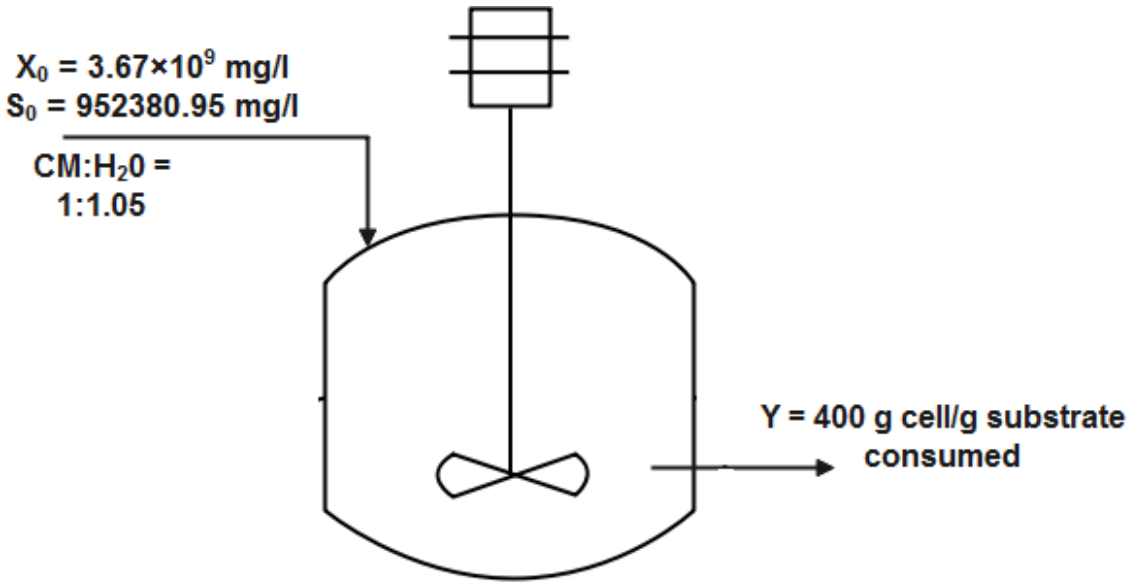

Figure 3.2: Flow Diagram of the Batch System

Overall balance: Accumulation = Input – Output + Generation (3.18)

Cells: $$\frac{d(VX)}{dt} = F_{in}X_{in} - F_{out}X_{out} + r_xV \qquad (3.19)$$

Limiting substrate: $$\frac{d(VS)}{dt} = F_{in}S_{in} - F_{out}S_{out} + r_sV \qquad (3.20)$$

Product: $$\frac{d(VP)}{dt} = F_{in}P_{in} - F_{out}P_{out} + r_pV \qquad (3.21)$$

Water: $$\frac{d(VW)}{dt} = F_{in}W_{in} - F_{out}W_{out} + r_w V \quad (3.22)$$

Subscript 'in' and 'out' implies input and output respectively, where F = flow rate, r = rate, S = substrate, X = cell, W = water and P = product. A batch process is a closed culture occurring when $F_{in} = F_{out} = 0$ and volume, V is constant. The ideology was implemented for other possible assumptions which are (a) concentration of H_2O remains the same ($W_{in} = W_{out}$) and insignificant water was generated (r_w), (b) reactor was well-mixed ($P_{out} = P_{in}; S_{out} = S_{in}; X_{out} = X_{in}$), (c) no product in feed ($P_{in} = 0$) and (d) cell growth was greater than cell death rate ($r_x = \mu X$) to give Equations 3.23 through 3.24.

Cells: $$\frac{dX}{dt} = \mu X = r_x \quad (3.23)$$

Substrate: $$\frac{dS}{dt} = r_s \quad (3.24)$$

3.7.5 Generating Appropriate Data for Monod Plot

Monod Equation given in Equation 3.25 (Um-e-Habiba *et al.*, 2021; Sakthiselvan *et al.*, 2019) was used to prove the fact that a relationship exists between S and μ.

$$\mu = \frac{\mu_{max} S}{K_s + S} \quad (3.25)$$

Specific growth rate, μ, can be positive (growth) or negative (death) and is a function of pH, temperature, osmotic pressure and concentration of inhibitors, product and substrate. Most importantly, calculated values of new X and S data, X_{calc} and S_{calc} was gotten by regression through estimation of two parameters, K_s and μ_{max} necessary for optimization of the process via the listed steps.

Step 1 – the carrying capacity of the environment or maximal biomass concentration, X_∞ was calculated using Equation 3.26.

$$X_\infty = X_0 + YS_0 \quad (3.26)$$

Equation 3.27, used independently for estimating μ without Monod was combined with Equation 3.23 and integrated to give Equation 3.30, following the steps shown in Equation 3.28 to 3.29.

$$\mu = k\left(1 - \frac{X}{X_\infty}\right) \quad (3.27)$$

$$\frac{dX}{dt} = \mu X = k\left(1 - \frac{X}{X_\infty}\right)X \qquad (3.28)$$

$$\int_{X_0}^{X} \frac{dX}{\left(1-\frac{X}{X_\infty}\right)X} = \int_0^t k dt \qquad (3.29)$$

$$X_{calc} = \frac{X_0 e^{kt}}{1-\frac{X_0}{X_\infty}[1-e^{kt}]} \qquad (3.30)$$

Regression was performed using POLYMATH to find new data that fits $X_{Expt.}$ versus time (hr) called X_{calc}, thereby estimating k. S_{calc} was thus, computed using Equation 3.31.

$$S_{calc} = S_o - \frac{X_{calc}-X_o}{Y_{X/S}} \qquad (3.31)$$

Step 2 – By combining Monod (Equation 3.25) and Equation 3.27, as Equation 3.32, X_{calc} data was used to determine K_s by finding new set of S data (or S_{reg}) that fits S_{calc} data using POLYMATH.

$$\mu = \frac{\mu_{max} S}{K_s+S} = k\left(1 - \frac{X}{X_\infty}\right) \qquad (3.32)$$

K_s, was guessed repeatedly to give K_s and used together with $Y_{X/S}$ and X_∞ mg/L to find S_{reg} in Equation 3.33 taking $Y_{X/S} = \frac{\mu_{max}}{k}$ as given by Talaiekhozani *et al.* (2015).

$$S_{reg} = \frac{K_s\left(\frac{X_\infty - X_{calc}}{X_\infty}\right)}{\frac{\mu_{max}}{k} - \left(\frac{X_\infty - X_{calc}}{X_\infty}\right)} = \frac{K_s\left(\frac{X_\infty - X_{calc}}{X_\infty}\right)}{Y_{X/S} - \left(\frac{X_\infty - X_{calc}}{X_\infty}\right)} \qquad (3.33)$$

Both X_{calc} and S_{calc} as well as $X_{Expt.}$ and $S_{Expt.}$ were plotted against time and graphs were compared.

Step 3 – Rate of biomass growth, $\frac{dX}{dt}$, was estimated using X_{calc} by substituting into Equation 3.28 with known k. From the same equation, μ can be estimated using either Equation 3.34 or Equation 3.27.

$$\mu = \frac{1}{X_{calc}} \frac{dX}{dt} \qquad (3.34)$$

Step 4 – Equation 3.25 and 3.27 was compared and concluded that $\mu_{max} = k$. This enable S to be customized from Equation 3.32 to compute S_{Monod} given by Equation 3.35.

$$S_{Monod} = \frac{K_S}{X_{calc}}(X_\infty - X_{calc}) = \frac{\mu K_S}{\mu_{max} - \mu} \qquad (3.35)$$

Step 5 - μ in step 3 and S_{Monod} in step 4 was plotted to give the Monod plot, selecting only values from the growth phase, as the Monod equation is only valid at the exponential phase. From the Monod plot, μ_{max} and K_s was further confirmed. Rate of substrate utilization, r_s or $(\frac{dS}{dt})$ as well as that of cell production, r_x or $(\frac{dX}{dt})$ was determined using Equation 3.24 and 3.28 respectively and plotted against time.

μ_{max} and K_s values was validated using Lineweaver-Burke plot, Hanes-Woolf pot or Eadie-Hofstee plot. Ram *et al.* (2019) and Perni *et al.* (2005) explained vividly how the two optimization parameters can be estimated from growth curve data.

3.8 Kinetic Parameter Estimation

CBY data with retention period recorded was then entered in the datasheet of the nonlinear regression section of the POLYMATH 6.10 Educational Release. One of the user-defined functions such as the Gompertz model, was entered into the model box and initial estimates of the unknown parameters (BP, LP, SF, k) were guessed and entered. POLYMATH then re-estimate these kinetic parameters using the Levenberg-Marquardt method, together with predicted values of CBY and the regression parameters, namely, R^2, RMSE and adjusted R^2. The guess was continuously adjusted until R^2 values estimated is very much closer to unity. POLYMATH was then set to plot the measured CBY entered initially and predicted CBY estimated on the same axis together with time to display the fit. Selvaraj *et al.* (2018) and Syaichurrozi *et al.* (2018) were observed to use the same software to determine those regression parameters in their kinetic study. The same procedure was repeated for the remaining models as well as the growth kinetic models in order to determine the values of μ_{max}, b, K_i, S_θ, S_m, i, a, b_b and K_s. Other regression parameters determined was MAPE, RSS, AF and BF. RSS, MAPE, BF and AF were calculated based on formulas given by Selvaraj *et al.* (2018) and Syaichurrozi *et al.* (2018), Halmi *et al.* (2014) and Kang *et al.* (2021).

The biogas models were saved in Origin 2018 software as user-defined functions initially, to produce the CBY observed and predicted fitted plots, similar to POLYMATH. Next, in the Origin window, 'Compare Models' was entered under 'Analysis' in the Menu Bar to estimate the

Akaike's Information Criterion (AIC), F-test and Bayesian Information Criterion (BIC), all used to state which model is most correct.

CHAPTER FOUR

RESULT AND DISCUSSION

4.1 Manure Properties on Anaerobic Digestion

4.1.1 Presence of Metallic Nutrient

Figure 4.1 shows the concentrations (in mg/Kg or ppm) of CM characterized for metallic ions using EDXRF, as described in Horf et al. (2021).

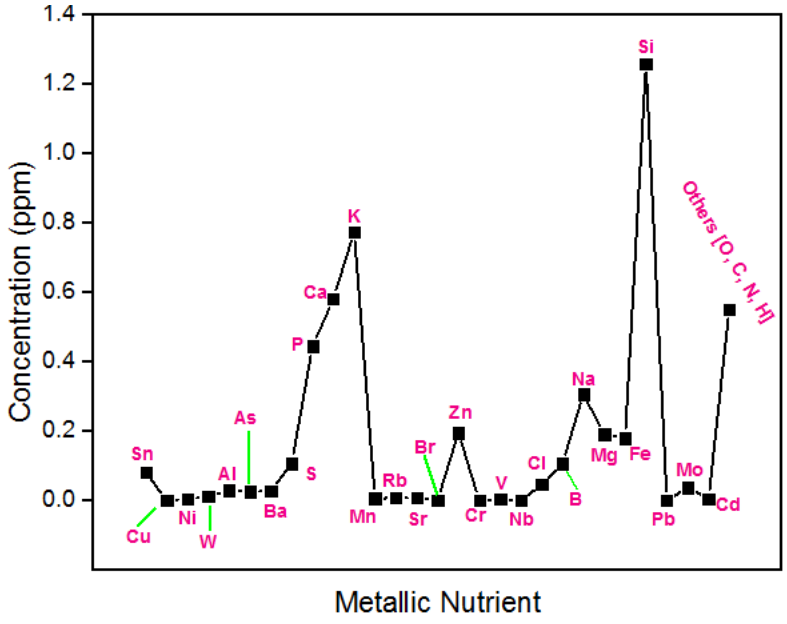

Figure 4.1: Metallic Nutrient Concentration in Chicken Manure

Twenty-four metals have been identified in the CM and were divided into heavy metals (macro-nutrient) and light metals (micro-nutrients). Heavy metals present are Fe, Ni, Mo, V, W, Cr, Cu, Zn, As, Sr, Ba, Pb, Cd and Sn in low concentrations ranging from 0-0.1956ppm. Mancini *et al.* (2018), reveals that heavy metals pose some danger to microbial activity; however, low concentrations obtained in this work had far less potential of inhibiting the growth of microorganism during AD. The concentrations of the heavy metals in poultry manure, according to Zhang *et al.* (2012) are 65.6mg/kg dm of Cu, 3.3 mg/kg dm of As and 1.6 mg/kg dm of Cd. Microbes need preferably, light metals such as Ca, Fe, Mg, K, Na, Al and P for growth according to Sawyerr *et al.* (2019) and Nsair *et al.* (2020). Moreover, most poultry manure contain 13 nutrients including S, Cl, B, N, P, K, Ca, Mg, Mn, Cu, Zn, Fe and Mo. The presence of these

micro-nutrient in the chicken manure substrates, especially Na (0.3071ppm), P (0.44494ppm), K (0.7742ppm), Fe (0.18ppm) and Mg (0.191ppm) makes the chicken manure sample a suitable feedstock for AD as microorganisms present utilizes these nutrients for metabolism and growth. High Si (1.26ppm) content obtained was due the presence of bone, feather and soil particles in the chicken manure. Non-metallic elements such as C, O, S, H and N were included in the plot, though oxygen was expected to be very less as the microorganism requires no oxygen. Because these elements are also part of moisture, protein, carbohydrate and lipid content of the CM, they tend to be cumulatively high.

4.1.2 Influence of Proximate Analysis Data of Chicken Manure

In this study, the 47% moisture content seen in fresh CM (Table 4.1) will provide a good environment for metabolism. The reason of making the feed ratio 1:1 was because TS:MC ratio (53%:47%) was closer to that ratio. Thus, bringing the CM-to-water ratio to 1: –thick slurry moisture type as described by Piekutin *et al.* (2021) before charging into the reactor, makes it a semi-dry AD process, mostly employed for agricultural waste like CM. When water content is low (dry fermentation/high solid), mixing to ensure uniform composition inside the digester was difficult. Because, the CM will be too heavy for the mixer blades to push so as to evenly distribute the pH, nutrients and microbes within the CM slurry, resulting in dead zones or stagnant regions. Singh *et al.* (2018) and Dede and Ozer (2018) reported %MC of 39.73% and 25.23% respectively. Organic matter is basically the store house for the nutrient content as shown previously. Therefore, OM content in this work implies nutrient content of the feedstock including those in 12% ash (containing Mg, K, P, Ca and C) value of the CM. Dede and Ozer (2018) obtained a value of 76.92% for broiler poultry manure that is closer to 88% reported in this work. An environment with such amount would invariably be a suitable environment for microrganism and is in consonance with VS/TS ratio of 0.25 shown in Table 4.1.

Table 4.1: Chicken Manure Characterization

Property	Amount	Property	Amount
Moisture content	47%	Volatile solid content	13.21%
Total Solids	53%	Fixed solid content	86.79%
Ash content (dry basis)	22.6%	VS/TS	0.25
Ash content (wet basis)	12%	Carbon content	66.17%
Organic matter content	88%	Nitrogen content	2.73%
Particle density	0.0163 g/cm^3	Crude Protein	17.06%
C/N Ratio	24:1		

The weight of individual solid particle that make up the CM per unit volume, otherwise called particle density (PD) is a determinant of the porosity and how easy microorganism breakdown the CM substrate. PD below 1.0 g/cm^3 usually indicates high OM content. Additionally, the PD value of 0.0163g/cm^3 obtained in this study and 543.8kg/m^3 (0.5438g/cm^3) reported by Brunerová *et al.* (2020) are both within the expected range. Though, the 53% TS seen is lower than the 74.77% reported by Dede and Ozer (2018); which means lower organic matter/nutrients for micro-organisms to feed on which in turn imply, low microbial population.

Adeyemo *et al.* (2019), Dede and Ozer (2018), and Singh *et al.* (2018) reported a nitrogen content of 3.87%, 5.13% and 3.83% in their CM sample. This, together with other literature works consulted shows that, nitrogen content in CM ranges from 2.6-5.7%, of which the 2.73% obtained in this study is within the boundaries of the percent range. Carbon content in this work is 66.17% which is higher compared to 21.12-34.93% obtained by the same authors. A much higher C/N ratio of 24:1 against those reported by Abubakar and Yunus (2021) and the mentioned authors is favorable because Dalk and Ugurlu (2015) affirms that low C/N ratio causes VFA accumulation and lowers the pH. Since the protein content (another source of nitrogen) is low (17.06%)

compared to 34.5% reported by Singh *et al.* (2018), chances of C/N ratio going to much over acceptable limit is reduced.

4.2 Effect of Biodigester Condition

4.2.1 pH and Temperature Effect

Figure 4.2 shows daily record of mesophilic temperature and pH of the AD process over the 40 days retention period.

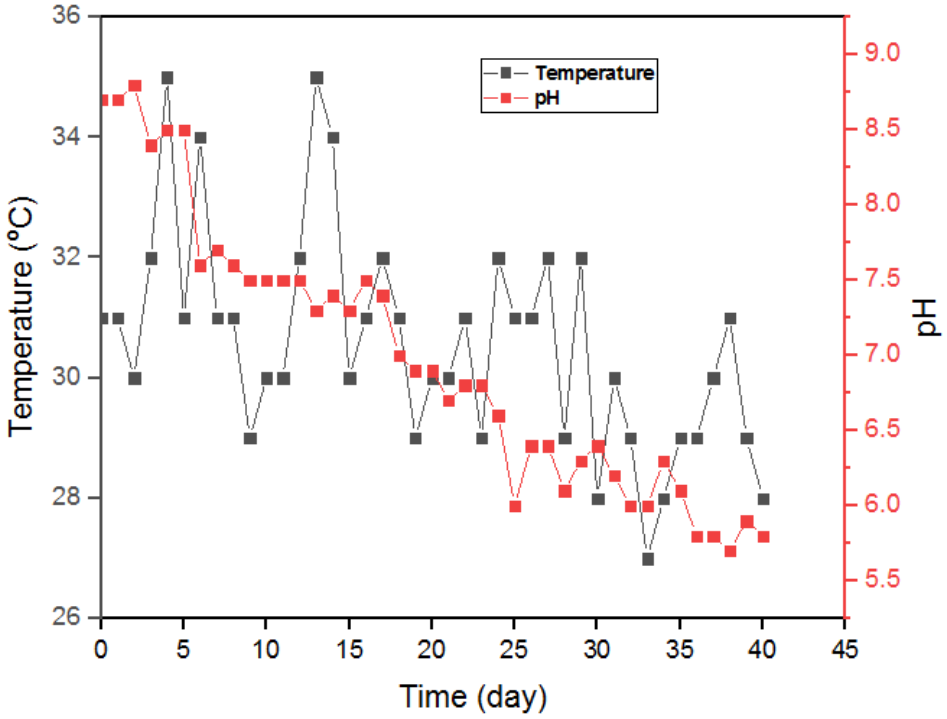

Figure 4.2: Daily pH and Temperature Record during Digestion Process

Shapovalov *et al.* (2019) tabulated %TS content (15-30%) and temperature in respect to CH_4 yield from CM, where it was seen that at high temperature (55-65℃), methane yield was negligible. This was attributed to the non-existence of thermophilic microorganism that are capable of adapting to such temperature. The temperature reported here was not constant but, it was within the mesophilic range – perfect for enzyme function and balanced free NH_3 content and is in accordance with what Eronmosele *et al.* (2020) obtained by co-digesting poultry droppings and elephant grass. Based on Raja and Wazir (2017), the choice of temperature is based on the climate condition, biogas yield based on temperature in the range of 27-35℃ measured between October and December in Maiduguri would not be same if temperature is lower or higher.

Entire pH range (5.7-8.8) of the CM slurry during AD was a little bit out of the survival range of micro-organism reported by Elalami *et al.*, (2019) (i.e. 6.0-8.0). The initial pH = 8.7 at t = 0 day for the CM agreed with Lohani *et al.* (2020), that CM was alkaline in nature. So, no growth was expected at this pH as microorganism fight to adapt to their environment. Again, further fall in pH was caused by microbial activity inside the digester. Fluctuations in pH affected CBY as shown in Figure 4.3. A positive microbial concentration was not expected when pH < 6, due to deaths.

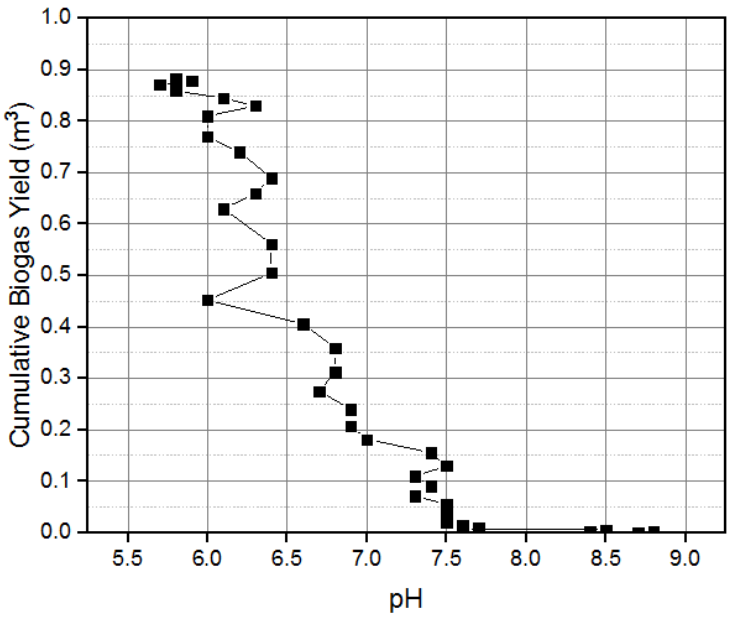

Figure 4.3: Cumulative Biogas Yield versus Daily Recorded pH

4.2.2 Biogas Yield

Total volume of biogas produced after 40 days of digestion was 0.883m^3, an average of approximately 0.022m^3/day. No phase records the highest biogas production than the exponential phase (0.681m^3) followed by the stationary phase (0.176m^3). This is because the phases had live cells that are actively converting the nutrients in the CM slurry to biogas. Hence, the phases mentioned cannot be compared with the lag phase (which is the beginning of microorganism acclimatization to their environment) and the death phase (where population of the microorganism drops quickly). So, volume of biogas generated is almost constant during the lag days, increasing to 0.068m^3 (peak production) at the growth phase and then decreasing over the remaining phases. The CBY plotted against CM retention time is shown in Figure 4.4.

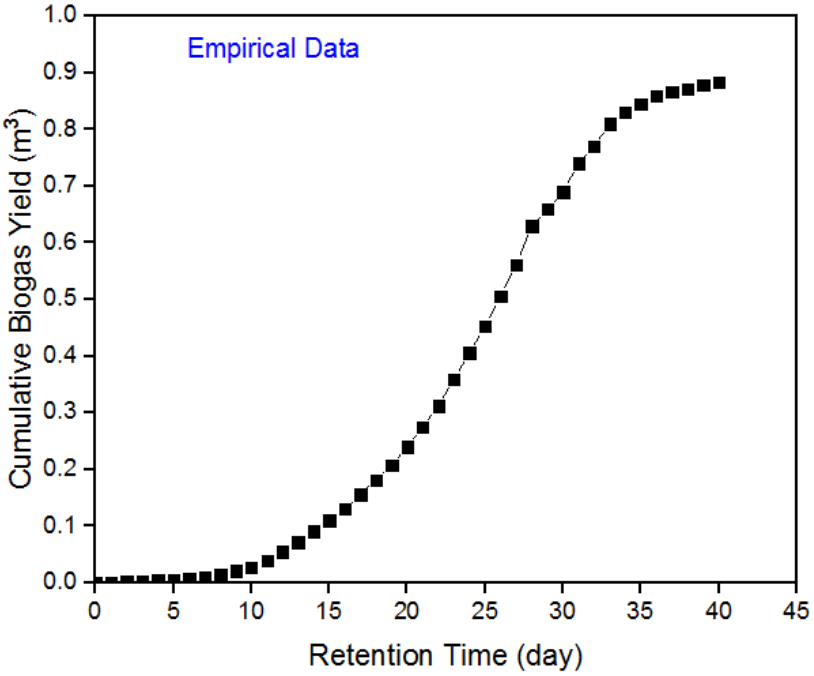

Figure 4.4: Cumulative Biogas Yield with Retention Time for the Chicken Manure Substrate

According to AirFacts (2020), 100kg of chicken litter will generate ≅20m^3 of biogas, corresponding with Bijman (2014)'s 200m^3 of biogas from 1000kg of chicken litter containing 55%DM and 42% OM in 30days. Biogas volume of 0.883m^3 produced here for 40 days digestion of 7.2kg of CM with 53%DM and 88%OM content is less than those obtained by the two authors. Compared to cow dung and domestic waste generating 0.18m^3 and 0.17m^3 of biogas respectively, according to Jyothilakshmi and Prakash (2016), CM produces higher amount of biogas. Since 1m^3 of biogas is equivalent to 2.1kWhe of electricity and 2.5kWth of heat according to Bijman (2014), 0.883 m^3 of biogas generated can produce 1.8543kWhe of electricity and 2.2kWth of heat in a biogas engine. GC analysis result where the component of the gas is displayed at different height versus run time is shown in Figure 4.5.

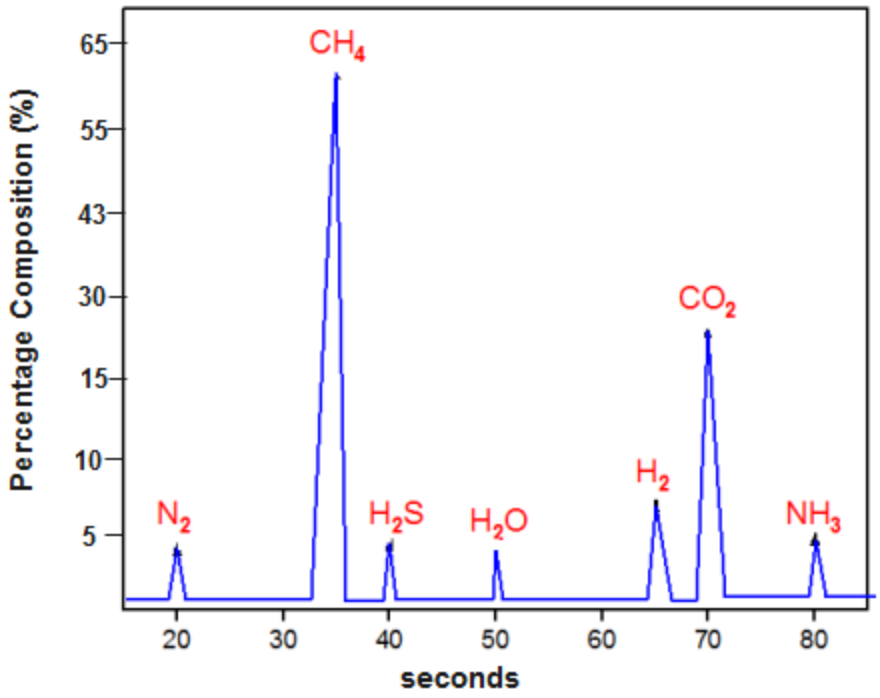

Figure 4.5: GC Biogas Analysis

The compositions of the gas were found based on peak areas occupied by CH_4 (178.87mm^2), CO_2 (82.34mm^2), H_2 (16.47mm^2), H_2S (3.97mm^2), NH_3 (1.70mm^2), N_2 (0.28mm^2) and H_2O (0.28mm^2) in the graph. Dividing the respective areas of the gas by the total area occupied gives the percentage of the component gases, which gives CH_4 (63%), CO_2 (29%), H_2 (5.8%), H_2S (1.4%), NH_3 (0.6%), N_2 (0.1%) and H_2O (0.1%). Results obtained is within Abuabdou *et al.* (2020)'s and Granado *et al.* (2017)'s reported compositions for biogas. The produced biogas is not pure, but further purification makes it biomethane with natural gas qualities. For instance %CH_4 > 40% here gives it a characteristic flammability according to Parsaee *et al.* (2019) even though it is not yet purified and implies a high resulting biomethane. Also, Bijman (2014) state that sulphur levels >2000ppm is corrosive and needs to be removed or reduced.

4.3 Analysis of Growth Kinetics

Microbial concentration (CFU/ml) of the triplicate SDE is shown in Figure 4.6a-c.

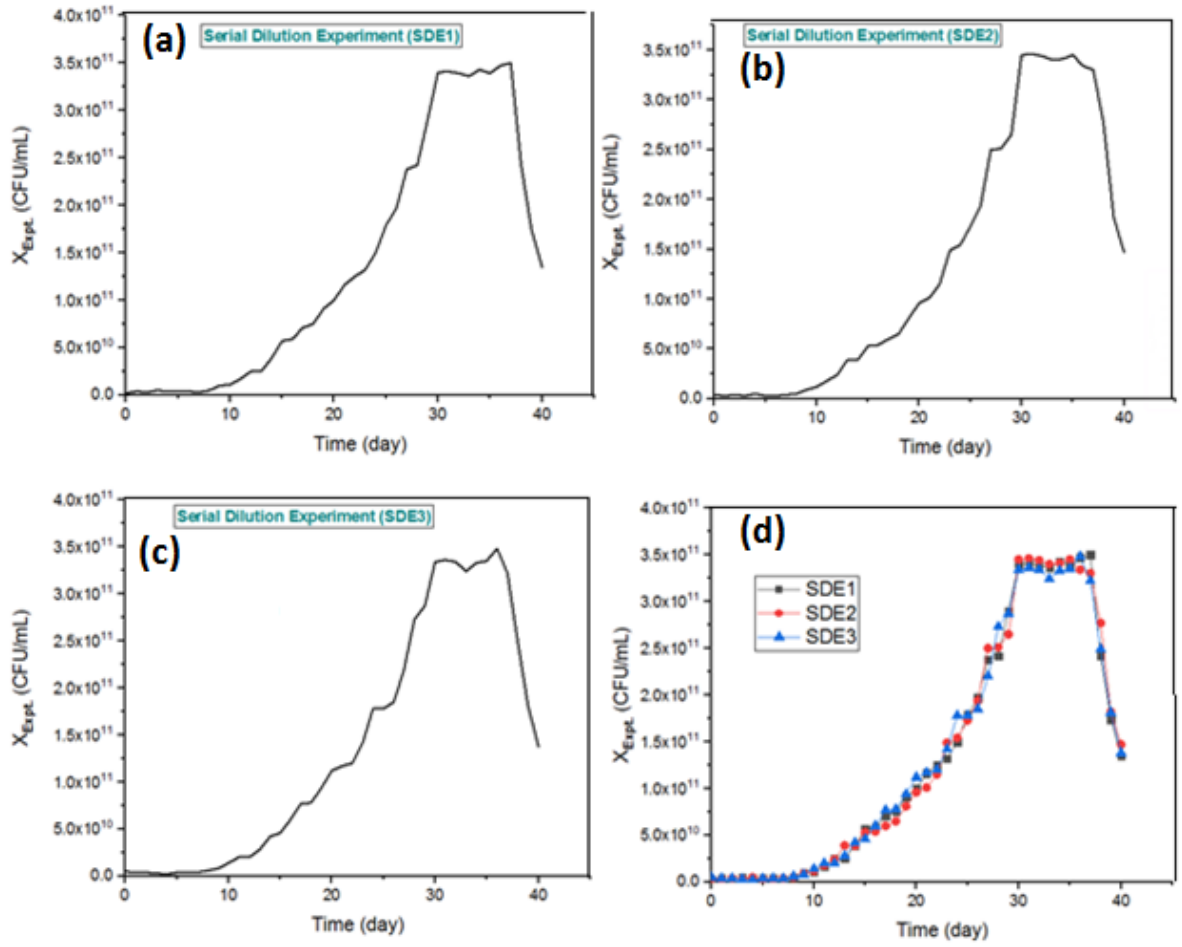

Figure 4.6: Cell Concentration Against Time for the SDEs

The SDEs provides almost identical plot as shown in Figure 4.6d, a further demonstration of accuracy of results. It is further attributed to high TDF which enable microorganism colonies to be seen and counted. If TDF is low, colonies would be too numerous to count (TNTC). Colonies > 300 are considered TNTC and would make generation of data for kinetic study very difficult. Despite the colonies are an average of 48 colonies > 300, as shown in the Appendix, after incubation (maximum number of colonies for SDE1 = 350, SDE2 = 346 and SDE3 = 348, producing an average of 343 colonies beyond the theoretical counting limits when t = 30-37 days), the data poses no observable statistical challenge. O'Toole (2016) in his short write-up on the history and origin of colony number boundaries stated that researchers started by putting the acceptable range at 20-400, then 30-300 while others stood at 20-250.

Even though Microbiologist do not prefer colonies that are < 30 or too few to count (TFTC), it is however, very significant in this study. Few colonies were counted for 13 days as shown in Figure 4.6, which implies a very long LP or the presence of slow-growing microorganism struggling with

the alkaline CM fed at the beginning of the process. But the initial temperature of 31℃ was favorable for the survival of the microorganisms present to move to the next growth phase. Also, Datta (2021) reported few colonies he found in 17, 22 and 15 colonies at different DFs in tap water. Since data accuracy is assured, due to fits of the three X results as shown in Figure 4.6d, an average of the microbial concentration (log-log plot of Figure 4.7) will further be analyzed.

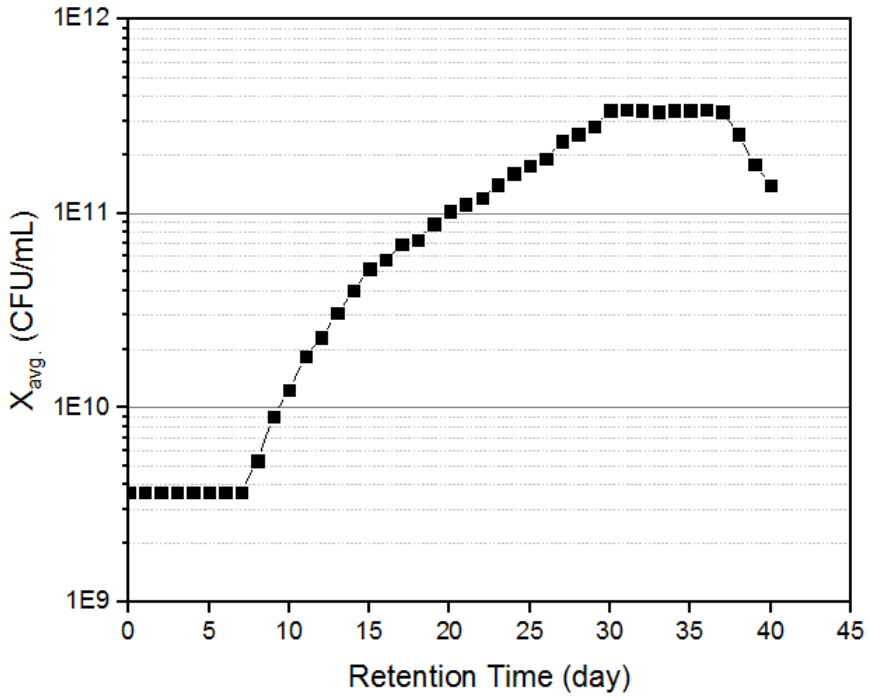

Figure 4.7: Average Cell Concentration Versus Time on a Log-log Scale

From an initial microbes concentration, $X_0 = 3.67 \times 10^9$CFU/ml at t = 0 day maintained for 7 days, concentration increases exponentially to X = 3.40×10^{11}CFU/ml at t = 23 days, maintaining an average value of X = 3.38×10^{11}CFU/ml for 7 days and falling to X = 1.40×10^{11}CFU/ml. These change in X pattern forms what is referred to as growth curve.

4.3.1 Microbial Growth Phases

Logarithm of the average cell concentration plotted against fermentation time as shown in Figure 4.8, illustrates four significant phases of cell growth.

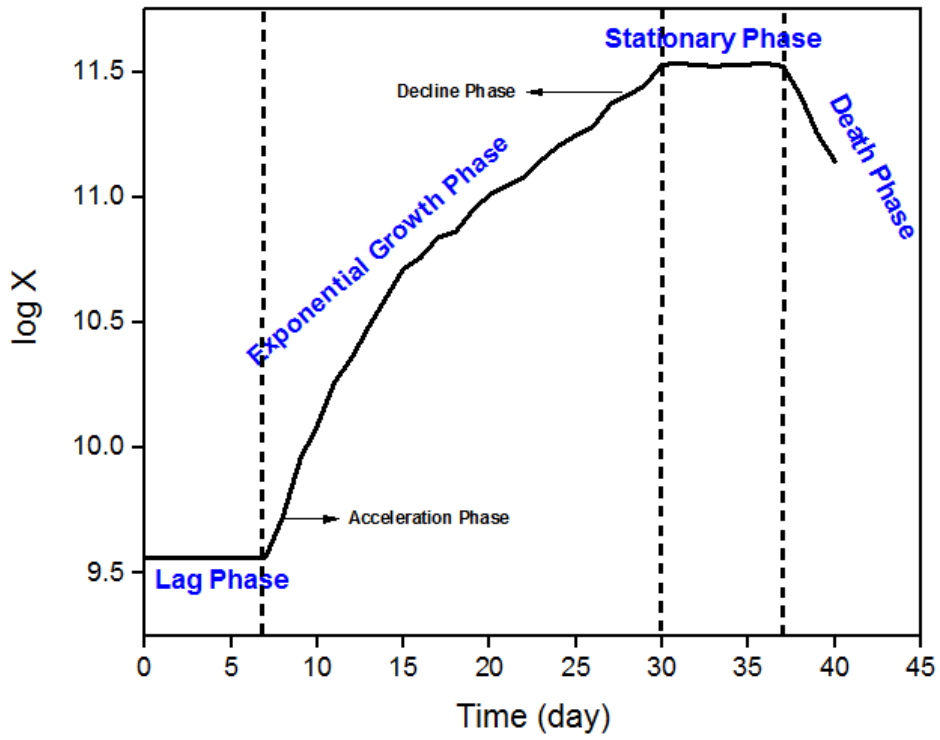

Figure 4.8: Microbial Growth Curve

The plot is identical to Figure 4.7, depicting the lag phase where microorganism acclimatize by synthesizing necessary enzymes to degrade substrate and other biochemicals. That is, rate of cell accumulation, $\frac{dX}{dt} = 0$. The growth phase is where rate of growth > rate of death, which follows the equation for exponential growth given by $\frac{dX}{dt} = \mu X$. At this point, gas production increases rapidly. The population begins to decline to a point where rate of growth is equivalent to the rate of death or $\frac{dX}{dt} = 0$. Death phase is caused by cell destruction and decomposition and is usually a short period of time observed in minimal increase in biogas generation as earlier depicted in Figure 4.4. between t = 37-40 days. At the acceleration phase, available cells $N_0 = 3.67$ with concentrations $X_0 = 3.67 \times 10^6$mg/L, begin to multiply by continuously forming duplicates. From the phase through the growth phase to the final decline phase, generation time can be estimated from Figure 4.9.

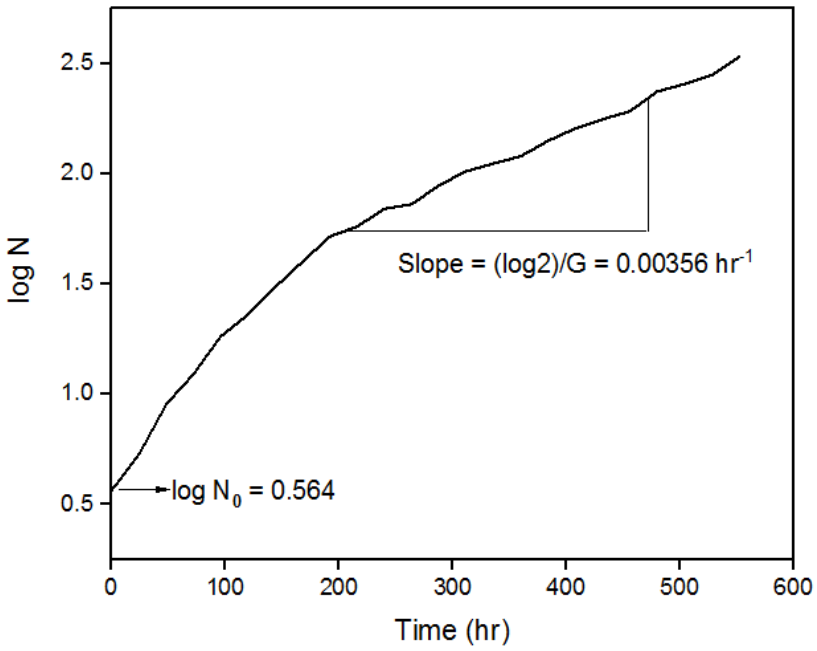

Figure 4.9: Biomass Doubling Time Estimation

It is true that different microorganism have different growth phase, thus, slight curving of the supposed linear plot in Figure 4.9 might be linked to superimposed growth rates of the respective microorganism inside the CM. Percentage increase in the microbial population undergoing exponential growth in this work was computed for the period of 552 hours spent and was found to be 92.55%. Hence, G = 84.56hrs = 3.52 days cannot be compared with literature works that mostly reports G for specific microorganism inside their substrate. At the death phase, where $\frac{dX}{dt} = -bX$, first order decay constant or the kinetic constant of death occurrences 'b' obtained from the slope of the linear plot of Figure 4.10 gave -0.0006 hr^{-1}. The negative sign implies a declining state of the microbial population which lasts only for 3 days (72 hrs) in this study. A very long death phase implies failure of the process, either due to pH, temperature or low nutrient content in the biodigester causing early deaths of useful microorganisms.

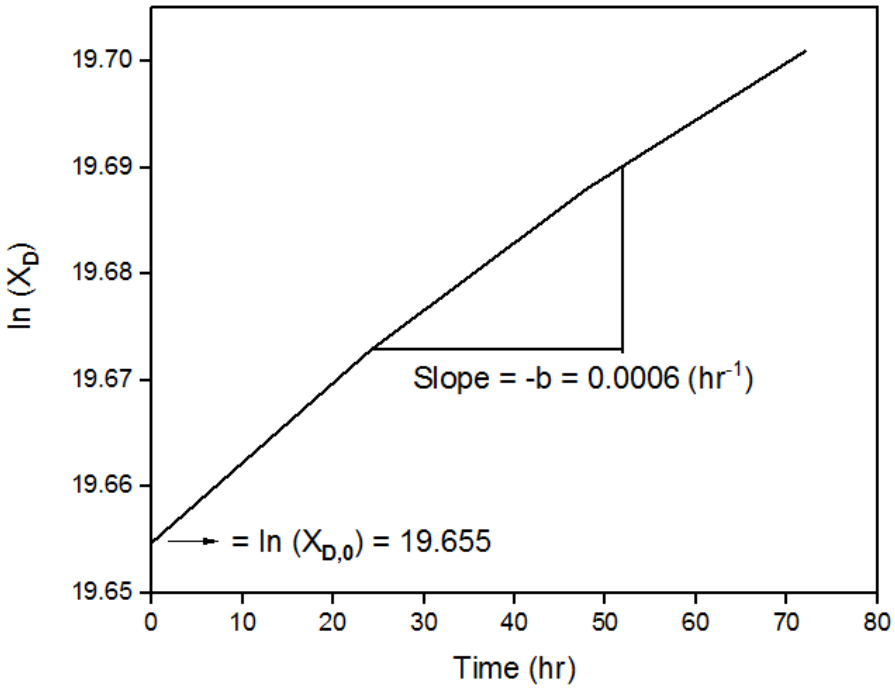

Figure 4.10: Determination of Death Constant

Figure 4.11 and 4.12 shows that as microorganism population increases, substrate concentration decreases as generally agreed.

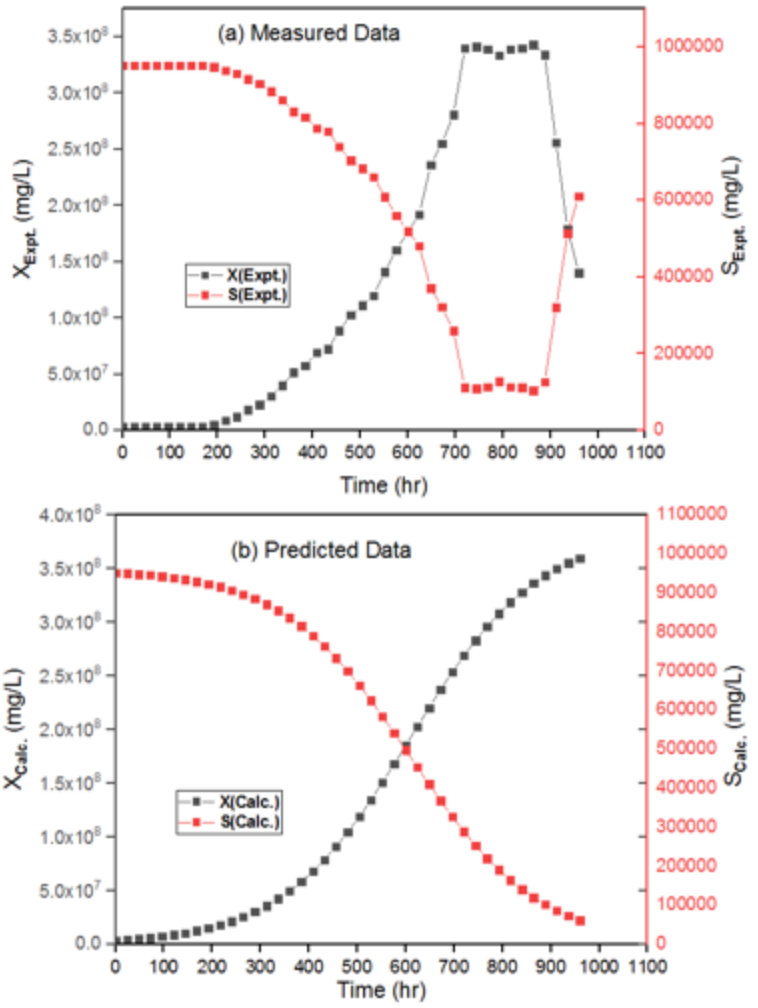

Figure 4.11: Substrate and Biomass Concentration from SDE and Kinetic Equation

Predicted data plot in Figure 4.11b fits properly to the experimental results and hence estimates the parameters k = 0.0076 hr^{-1} and $K_s = 3.838 \times 10^8$mg/L correctly using $X_\infty = 384619046.7$ mg/L. Figure 4.11a also shows the behavior of the CM substrate concentration through the various phases of the growth of microorganism. It is high ($S_0 = 952380.95$ mg/L) initially and decreases to an average constant value (= 115476.1881 mg/L) at the stationary phase. At the end of the stationary phase, only few microorganism are alive to further decompose the feedstock and hence reduce the substrate concentration. Concentration of the substrate at the death phase is the remaining amount in the reactor and might increase slightly due to added weight of the dead microorganism. This increase is shown in Figure 11a at RT = 912-960 hours of the measured data which is insignificant and is basically theoretical as it was calculated using Equation 3.37. The predicted data resulting in S-line of Figure 11b strikes out the shoot in amount of S at the death

phase which is believed to be the ideal situation, because a digester with CM and no microorganism remains the same. So, the concentration of the remaining substrate can only be taken from the predicted data or measured experimentally.

Linear relationship between the substrate concentration and the cell concentration exists. Figure 4.12 better explains this relationship looking at it from the bottom right upwards (where X is high and S is low). Accuracy in microbial population count is very difficult, though this data assumes that single microorganism grow to form a single colony, multiple microorganism forming single colony hides some number of viable cells that were unknowingly counted as one. Values of X therefore doesn't guarantee a 100% precise data because it fails to include gain in concentration due to growth in weight/size of the microorganism. Against the typical mass of microorganism which is 1pg, microorganism inside the slurry are capable of growing to 1ng or their sizes might be even less (e.g. 1fg). Though, assuming a weight of 1ng in this work wouldn't pose much problem to kinetic analysis. Despite this, plot as the one shown in Figure 4.12 must depict ideal conditions of X and S as explained earlier.

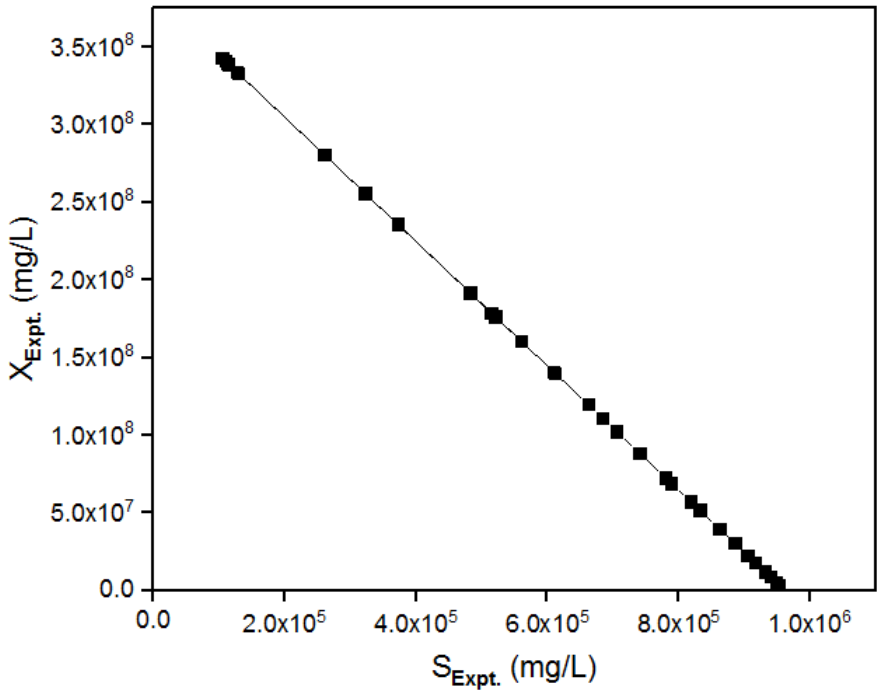

Figure 4.12: Showing the Relationship Between Substrate Concentration and Cell Concentration

4.3.2 Effect of Substrate Concentration on Specific Growth Rate

The rectangular hyperbola in Figure 4.13 is called the Monod plot based on cell growth at the exponential phase.

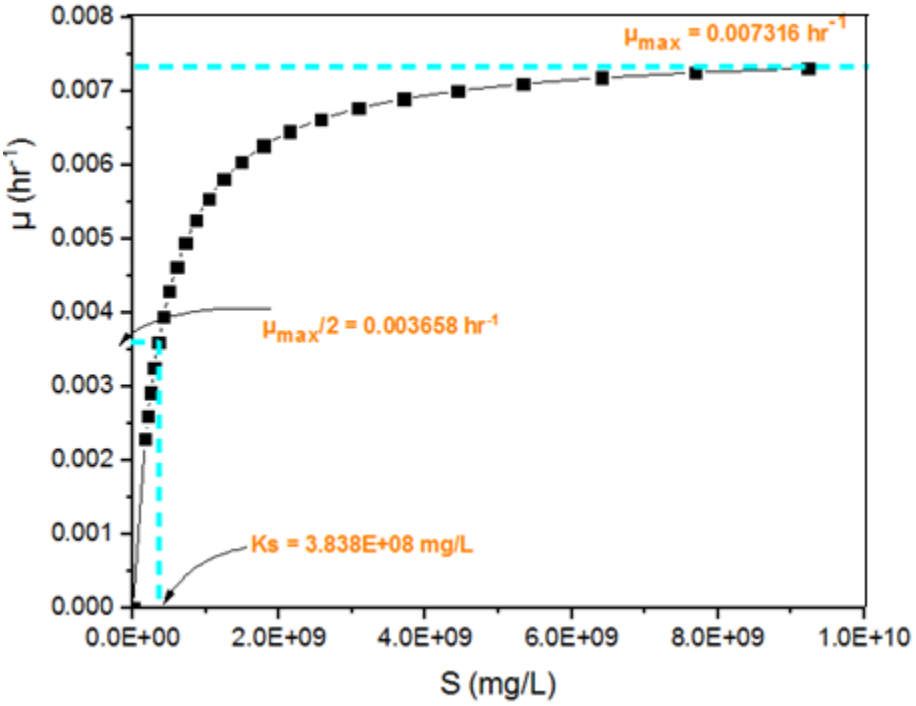

Figure 4.13: Monod Plot Based on μ and S Computed from Experimental Values of Microbial Concentration

The curve starts from S = 0 mg/L corresponding to $\mu = 0\ hr^{-1}$, to a peak value, μ_{max} where S is also high. The plot is divided into 3-sections based on S amount. For low S (i.e. $S \ll K_s$), growth have first order dependence on S (growth is highly sensitive to S) and the Monod equation reduces to $\mu = \frac{\mu_{max} S}{K_s}$. That is, when S (nutrient) is very little, cells had to compete for it. This points to the fact that amount of substrate limits how fast the cells can grow. So, addition of more substrate causes proportional increase in cell growth rate. The center region is called the mixed order section that satisfies the Monod equation proper. When S is high (i.e. $S \gg K_s$), growth is at μ_{max} and kinetics reduces to a zero-order expression $\mu = \mu_{max}$. Here, each cell can have as much nutrient or substrate as they so desire due to its abundance because the specific growth rate is high and constant. Lineweaver-Burke plot, Hanes-Woolf pot and Eadie-Hofstee plot (all linear), as shown in Figure 4.14, emerged as a result of manipulations done to the actual Monod equation and provides a much easier approach of estimating the Monod kinetic parameters (μ_{max} and K_s).

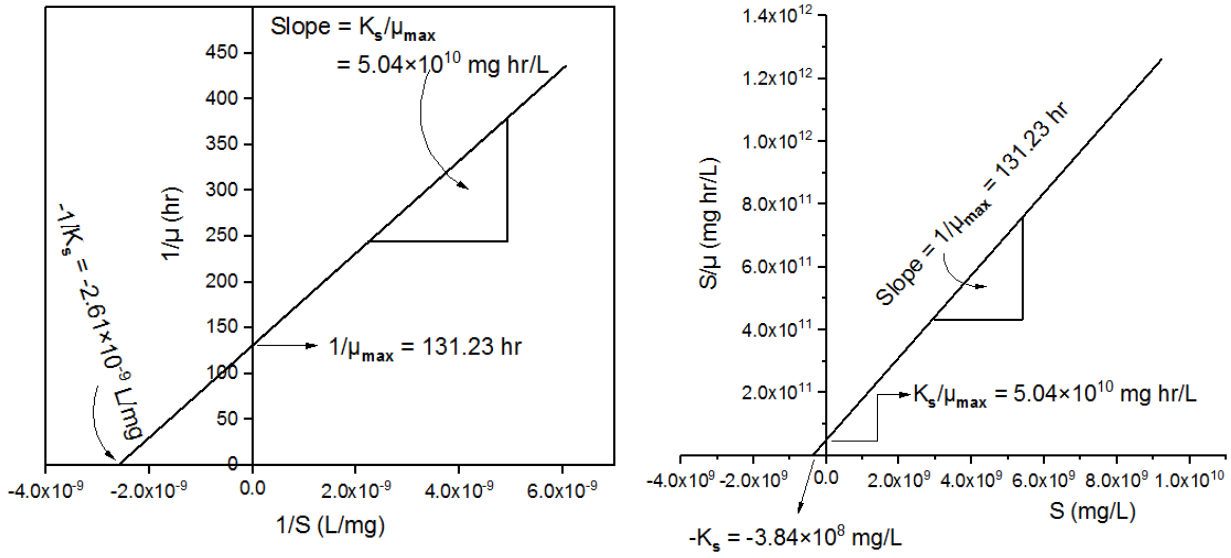

(a) Lineweaver-Burke Plot

(b) Hanes-Woolf Plot

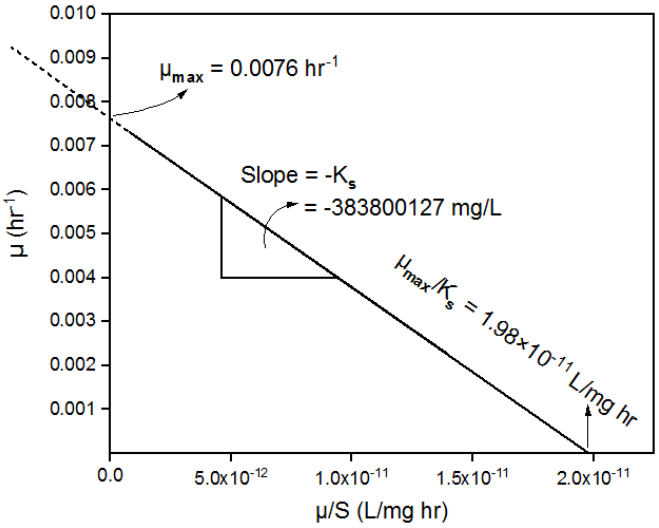

(c) Eadie-Hofstee Plot

Figure 4.14: Alternative Plot for Determining Monod Parameters

The S data used for estimating these parameters excluded toxic S that are capable of inhibiting microbial growth. Effect of toxic S is seen in models proposed by Andrew, Halden, Aiba-Edwards, Haldane, Webb, Alagappan & Cowan and the Double Exponential model. The explanation of the substrate relationship with the K_s was earlier explained by Maier (2009) which is in accordance with this work. Equations of the respective Lineweaver-Burke Plot, Hanes-Woolf Plot and the Eadie-Hofstee Plots for results obtained here are given in Equations 4.1-4.3:

$$\frac{1}{\mu} = \frac{3.838\times10^{8}}{0.007316}\left(\frac{1}{S}\right) + \frac{1}{0.007316} \quad (4.1)$$

$$\frac{S}{\mu} = \frac{3.838\times10^{8}}{0.007316} + \frac{1}{0.007316}S \quad (4.2)$$

$$\mu = 0.007316 - 3.838 \times 10^{8}\frac{\mu}{S} \quad (4.3)$$

The above model equations can hence be used for S and μ estimates spanning the period of the experimental growth phase.

4.4 POLYMATH Kinetic Data Fitting

4.4.1 Growth Model and Comparison of Regression Parameter

In this study, the 23 growth kinetic models identified in the literature were fitted to empirical data so as to estimate their respective kinetic parameters. The fitted plots are shown in Figures 4.15-4.22, where five models including Monod with decay rate, Wayman & Tseng, Han & Levenspiel, Luong and Moser models had $R^2 = 1$, which imply that all the points lie on the regression line (with no errors). RMSE's of these models were closer to 0, also indicating a good fit with same estimates ($\mu_{max} = 0.0076201h^{-1}$ & $K_s = 3.838 \times 10^8\ mg/l$) compared to Monod parameters. Coefficient of determination, $R^2 = 0.999777$ in Webb model was 99.98% fitted to the Monod line, though type of parameters estimated were not the same in all the six models so far mentioned.

If models are to be compared based on unique parameters estimated, then Monod with decay rate (with estimated parameters: μ_{max}, K_s, K_i & b), Wayman and Tseng (with estimated parameters: μ_{max}, K_s, i, K_i & S_θ), Webb (with estimated parameters: μ_{max}, K_s & K_i) and Luong (with estimated parameters: μ_{max}, K_s, n, m & S_m) are models that fits perfectly to Monod plot or experimental data obtained in this work. Models such as Double exponential, Haldane, Aiba-Edwards, Andrew, Halden, Andrew with decay rate and Webb model estimated the same inhibition constant, $K_i = 1.01 \times 10^{12}$ except for Alagappan and Cowan where $K_i = 2.643 \times 10^8$. Alagappan and Cowan model can be said to be the worst model as none of the estimated parameters was positive and it showed a deviating curve in Figure 4.16. Han and Levenspiel and Luong models are the only two models with maximum substrate concentration, S_m, presenting a 100% fit (Figure 4.21.

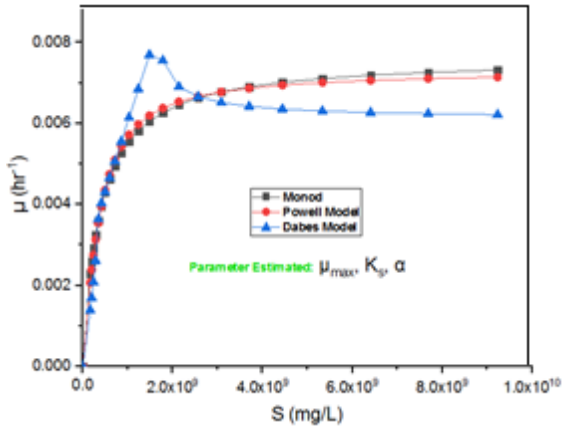

Figure 4.15: Fitting Powel and Dabes Model to Monod Plot

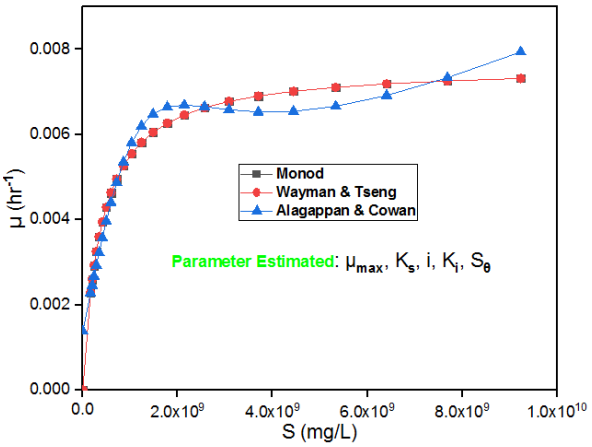

Figure 4.16: Fitting (i) Wayman & Tseng and (ii) Alagappan & Cowan Model to Monod Equation

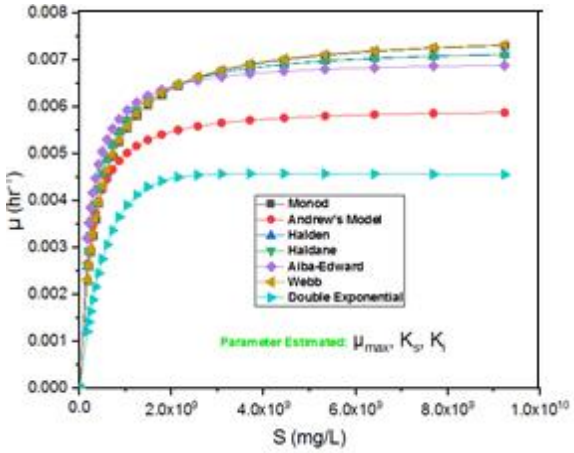

Figure 4.17: Estimating μ_{max}, K_s & K_i by Fitting Six Growth Models to Monod Data

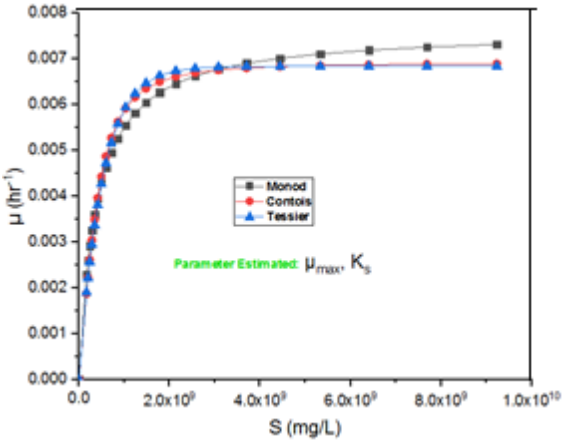

Figure 4.18: Contois and Tessier Model Parameter Estimation by Regression

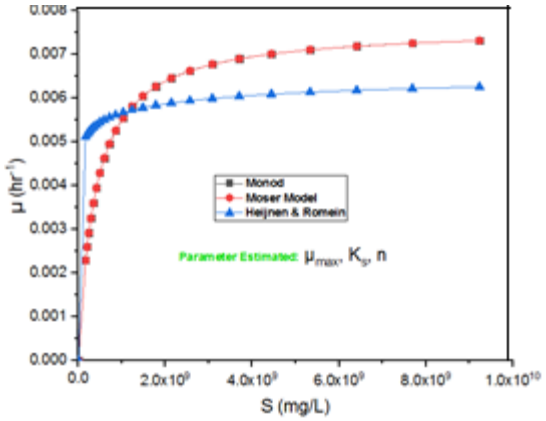

Figure 4.19: Estimating Growth Parameters by Data Fit using Monod

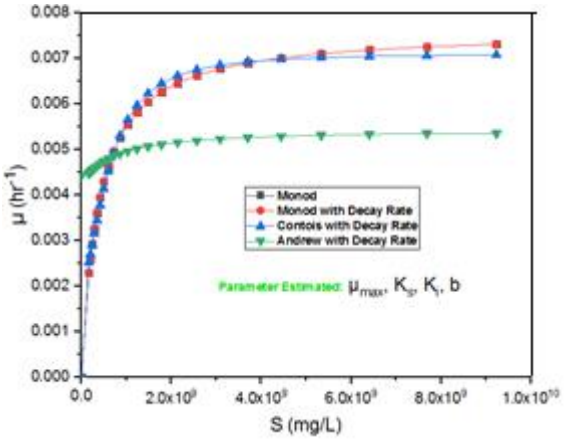

Figure 4.20: Monod Fitted to Models Based on Substrate Decay Rate

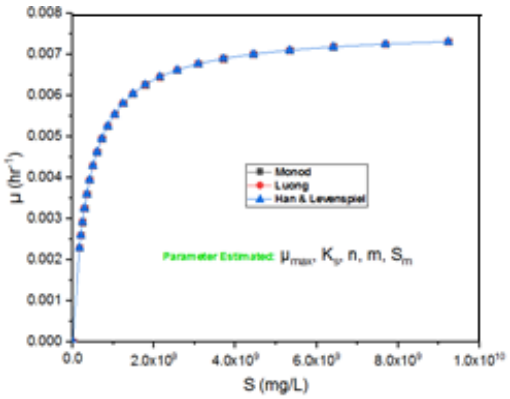

Figure 4.21: Luong and Han & Levenspiel Microbial Growth Parameter Estimate by Regression with Monod Equation

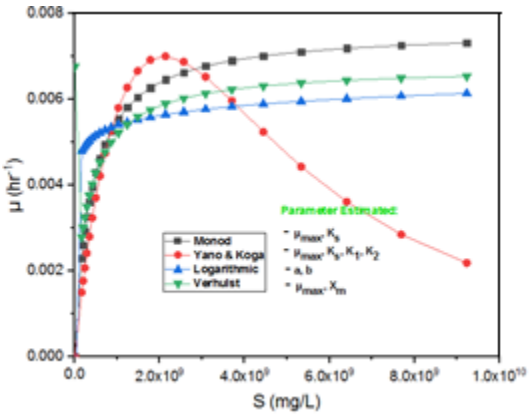

Figure 4.22: Verhulst, Logarithmic and Yano & Koga Estimates of Growth Parameters from Monod Data

Values of μ_{max} and K_s obtained in majority of the growth models in Table 4.2 are approximately same.

Table 4.2. Growth Kinetics and Statistical Parameter Estimates from POLYMATH

Model	Parameter	R^2	Adj. R^2	RMSE
Monod	$\mu_{max} = 0.0076201$	1.0000	1.0000	1.05E-06
	$K_s = 3.838 \times 10^8$			
Monod with Decay rate	$\mu_{max} = 0.0076201$	1.0000	1.0000	1.05E-06
	$K_s = 3.838 \times 10^8$			
	$b = -8.207 \times 10^{-8}$			
Contois	$\mu_{max} = 0.0069123$	0.98033	0.97944	0.0012
	$K_s = 1.649958$			
Contois with Decay rate	$\mu_{max} = 0.0053514$	0.99502	0.99456	0.0006
	$K_s = 3.684928$			
	$b = -0.001763$			
Andrew	$\mu_{max} = 0.0060722$	0.39251	0.33465	0.0033
	$K_s = 2.142 \times 10^8$			
	$K_i = 1.01 \times 10^{12}$			
Verhulst	$\mu_{max} = 0.0067649$	0.41148	0.38474	0.0035
	$X_m = 4.566 \times 10^8$			
Powell	$\mu_{max} = 0.0054542$	0.99557	0.99515	0.0005
	$K_s = 2.301 \times 10^8$			
	$\alpha = 1.158878$			
Aiba-Edwards	$\mu_{max} = 0.007104$	0.91568	0.90766	0.0022
	$K_s = 2.013 \times 10^8$			
	$K_i = 1.01 \times 10^{12}$			
Webb	$\mu_{max} = 0.0076046$	0.99977	0.99976	0.0001
	$K_s = 3.764 \times 10^8$			
	$K_i = 1.01 \times 10^{12}$			
Luong	$\mu_{max} = 0.0076201$	1.0000	1.000	2.44E-08
	$K_s = 3.838 \times 10^8$			
	$S_m = 1.01 \times 10^{12}$			
	$n = -0.0003264$			

Model	Parameter	R^2	Adj. R^2	RMSE
Wayman and Tseng	$\mu_{max} = 0.0076201$ $K_s = 3.838 \times 10^8$ $S_\theta = 8.276 \times 10^8$ $i = -1.67 \times 10^{-20}$	1.0000	1.000	1.356E-09
Logarithmic	$a = -0.0015569$ $b = 0.0003353$	0.58252	0.56355	0.0053
Andrew with Decay rate	$\mu_{max} = 0.0012249$ $K_s = 8.621 \times 10^8$ $K_i = 1.01 \times 10^{12}$ $b = -0.0042405$	0.474	0.39568	0.006745
Moser	$\mu_{max} = 0.0076201$ $K_s = 3.838 \times 10^8$ $n = 0.999999$	1.000	1.0000	1.18E-05
Tessier	$\mu_{max} = 0.0068388$ $K_s = 5.061 \times 10^8$	0.976	0.97458	0.001287
Halden	$\mu_{max} = 0.0074275$ $K_s = 3.063 \times 10^8$ $K_i = 1.01 \times 10^{12}$	0.988	0.98677	0.000868
Haldane	$\mu_{max} = 0.0074154$ $K_s = 3.035 \times 10^8$ $K_i = 1.01 \times 10^{12}$	0.987	0.98589	0.000899
Dabes	$\mu_{max} = 0.0031107$ $K_s = 3.187 \times 10^8$ $\alpha = 1.402752$	0.848	0.83370	0.002885
Heijnen and Romein	$\mu_{max} = 0.0065558$ $K_s = 8.411 \times 10^4$ $n = 0.0587962$	0.553	0.5105374	0.005043
Yano and Koga	$\mu_{max} = 0.0153219$ $K_s = 1.521 \times 10^9$ $K_1 = 1.01 \times 10^{10}$ $K_2 = 4.157 \times 10^9$	0.135	0.0053872	0.005634

Model	Parameter	R^2	Adj. R^2	RMSE
Han and Levenspiel	$\mu_{max} = 0.0076103$	1.000	1.0000	8.53E-08
	$K_s = 3.833 \times 10^8$			
	$S_m = 4.57 \times 10^{11}$			
	$n = -0.0003408$			
	$m = 1.532309$			
Alagappan and Cowan	$\mu_{max} = -0.04822$	0.952	0.9421286	0.001577
	$K_s = -9.9 \times 10^9$			
	$K_i = -2.643 \times 10^8$			
	$i = -5.61 \times 10^{-13}$			
	$S_\theta = -2.452 \times 10^9$			
Double exponential	$\mu_{max} = 0.004602$	0.033	-0.058988	0.008705
	$K_i = 1.01 \times 10^{12}$			
	$K_s = 5.407 \times 10^8$			

Note that, K_s estimated by POLYMATH was negative in Alagappan & Cowan models, deviating from the norms in both value and its plot which appeared curved upward as a result. Those with near 100% R^2 and adjusted R^2 demonstrated a perfect fit. As regards CM, none of this can be compared with literature findings as only cattle manure has its kinetic parameters estimated from Contois model (Alqahtani, 2013). The study satisfied the two cases of the Contois model that points to inverse relationship between μ and X. One, it is first-order kinetics for biomass growth, where $S/X \gg K_s$ leading to $\mu \cong \mu_{max}X$. Two, it is first-order kinetics for substrate consumption, where $S/X \ll K_s$ leading to $\mu = \mu_{max}\left(\frac{S}{K_s}\right)$, which means X population rises and obstruct substrate uptake and growth of microbe. In the Haldane model, two explanations can be given its curve; proportional rate increase with S occurs at low S, making $K_s \gg S + \frac{S^2}{K_i}$ and $\mu \cong \mu_{max}\left(\frac{S}{K_s}\right)$, and inverse relationship between rate and S occurs at high S, making $K_s + S \ll \frac{S^2}{K_i}$ and $\mu \cong \mu_{max}\left(\frac{K_i}{S}\right)$.

4.4.2 Biogas Kinetics Model Fitting

The Cone, Transfert, Modified Gompertz and Logistic models can be fitted to measured CBY versus retention time plot as shown in Figures 4.23 and 4.24. Similar approach in fitting empirical

CBY data has been followed by Abubakar *et al.* (2022) and Chinenyenwa *et al.* (2022) utilizing liquid manure and yam peels for the biogas feedstock using some selected models. The four models properly fit the empirical result. Though, proper fit is not a measure of correctness of the data, some models give close estimates of BP, k, LP and SF values while others deviate.

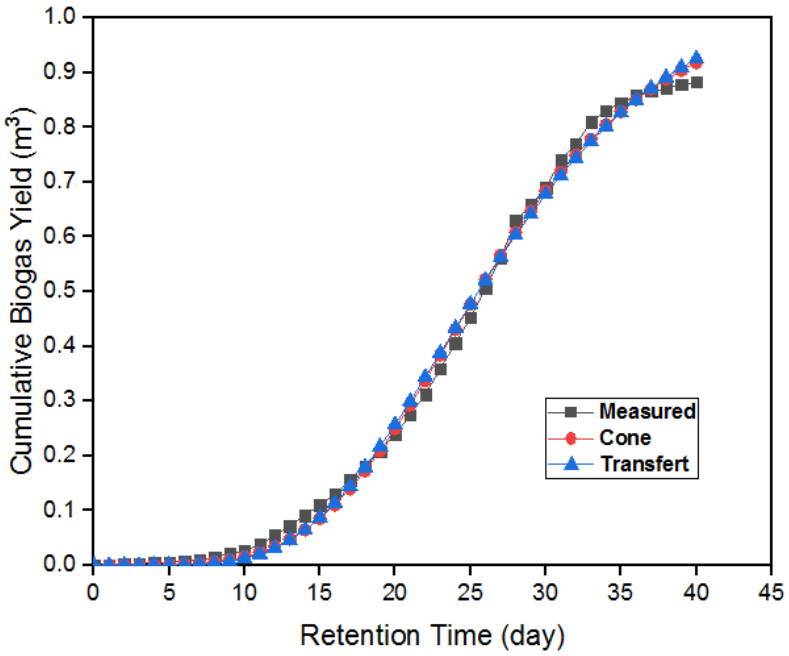

Figure 4.23: Fitted Cone & Transfert Models to CBY versus RT Plot

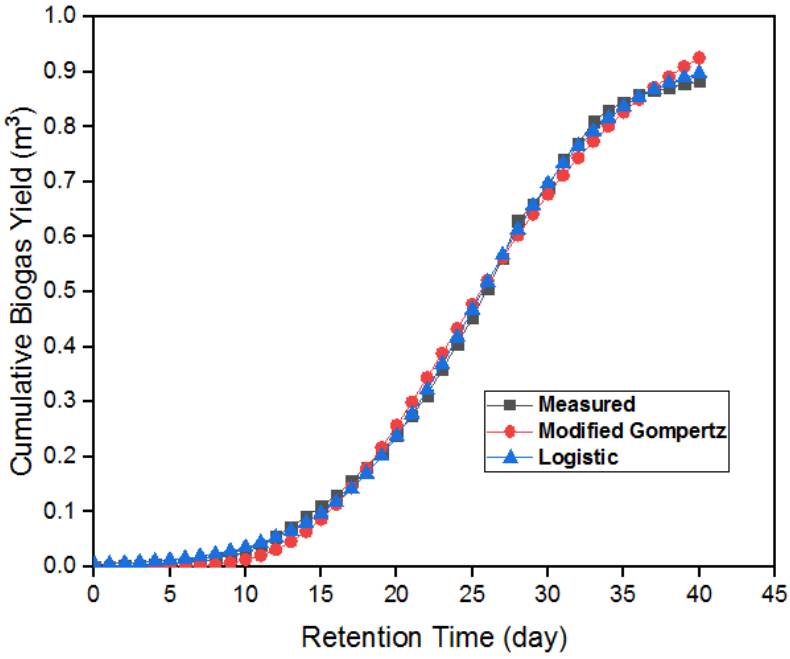

Figure 4.24: Fitted Modified Gompertz & Logistic Models to Measured CBY

From Table 4.3, R^2 of all the biogas models are closer to unity (demonstrating a good fit), k estimated in Transfert model doesn't compare favorably with the rest of the models. Therefore, plots of Modified Gompertz, Logistic and Cone model fits the measured data as they have similar and same number of parameter as well as being non-linear according to Pererva *et al.* (2020). Alternatively, it could be said that, best model is Logistic and Cone model based on the highest value of the adj. R^2 followed by modified Gompertz and Transfert models (two of which cannot be concluded as they have equal adj. $R^2 = 0.99613$. RMSE values ranges from 0.009375-0.137137, as shown in Table 4.3.

Table 4.3: MAPE, RMSE and Bias and Accuracy Factors of the Model

Model	MAPE	RMSE	AF	BF
Modified Gompertz	24.38987	0.020248	1.980345	1.90345
Cone	34.21464	0.137137	3.907264	3.907264
Logistic	−38.5674	0.009375	1.215339	0.8822816
Transfert	24.38968	0.020248	1.980317	1.980317

Venkateshkumar *et al.* (2020) reported that lower RMSE indicate a better fit. This confirms the selected models based on the R^2 criteria and Syaichurrozi *et al.* (2018) who based model selection on MAPE. An MAPE<20% can be taken as a good model, hence Logistic is favored compared to other models. A 100% fit imply a BF=AF=1 according to (Kang *et al.*, 2021), whereas BF>1 in modified Gompertz, Cone and Transfert models are considered a fail-safe model and BF<1 in Logistic model is considered a fail-dangerous model according to Halmi *et al.* (2014). The AF estimates are > 1, where higher values suggest less precise prediction (as in Cone model).

To select the best biogas kinetic model, in this case, AIC, BIC and F-test were compared using values obtained from Origin Pro. Logistic function model has lower AIC value compared to modified Gompertz, Cone and Transfert model and so is more likely to be correct. Cone model has lower AIC compared to modified Gompertz and Transfert model and is therefore more likely to be correct. AIC comparison also favor modified Gompertz model over Transfert model. BIC difference >10 ranks the models, starting from the most correct model as; Logistic, Cone, modified Gompertz and Transfert model, just in a similar fashion as AIC, but a BIC difference < 2 obtained by comparing modified Gompertz and Transfert model renders the result inconclusive. Dinh *et al.* (2018) experiment shows that, modified Gompertz model have lower AIC = 39.41 compared to

AIC = 43.48 of Cone model estimates from CM and corn straw digestion, making it the correct model.

Modified Gompertz, Transfert and Logistic function models has the LP in their respective model equations of which estimates gives 14.328days for modified Gompertz and Transfert model and 14.713days for Logistic model against the 7 days period obtained from measurement. However, this estimates is in the range of values obtained by Duan *et al.* (2018) which were between 11.37-15.73 days for modified Gompertz model and 11.48-15.8days for Logistic model for CM plus algal digestate substrate used. Though, the Duan *et al.* (2018)'s data cannot be used to compare estimates in Table 4.3 as they are gotten from co-digested AD process, Liu *et al.* (2018)'s LP = 14.29 days for CM substrate estimated from modified Gompertz model is approximately identical to LP obtained in this work. But Ma *et al.* (2021)'s LP = 5.20 days for layer CM from modified Gompertz model and Dinh *et al.* (2018)'s LP = 7.0328 days from Cone model for CM plus corn straw AD are around the 7 days experimental LP period in this work. Maximum specific biogas production rate, k = 0.0688day^{-1} according to Dinh *et al.* (2018) from modified Gompertz model for CM versus corn straw processed, almost satisfy 3 models given positive k in Table 4.4 for CM. Negative value of k in Transfert model makes it the worst performing model. According Origin Pro, the data are too small to make conclusions on F-test for the models analyzed. But RSS values used during F-test suggest Logistic model as the preferred model because it has a small RSS value.

Table 4.4: Regression Parameter Estimated from Fitted Biogas Kinetic Model

Model	Parameter	R^2	Adj. R^2	RSS	AIC	BIC
Modified Gompertz	BP = 1.073076 m^3 k = 0.0447788 day^{-1} LP = 14.32809 day	0.99632	0.99613	0.01681	−310.66405	−304.92087
Cone	BP = 1.06351 m^3 k = 0.03814 day^{-1} SF = 4.36841 day	0.99723	0.99708	0.01266	−322.27873	−316.53555
Logistic	BP = 0.9325659 m^3 k = 0.0503514 day^{-1} LP = 15.71288 day	0.99921	0.99917	0.0036	−373.8043	−368.06112
Transfert	BP = 1.073082 m^3 k = −0.0447783 day^{-1} LP = 14.32796 day	0.99632	0.99613	0.01681	−310.66402	−304.92084

CHAPTER FIVE

CONCLUSION AND RECOMMENDATIONS

5.1 Conclusion

The following conclusions can be made:

1. Approximately $1m^3$ of biogas consisting of 63% CH_4 and 29% CO_2 was generated after 40 days from the nutrient-rich CM sample utilized. The temperature, pH and water content of the digesting substance resulted in an efficient biogas production, and where they deviate, sufficient adjustment was done to favour microbial growth.
2. Colony counting reveals the presence of microorganisms inside the CM substrate which undergoes varying growth phases inside the bioreactor, from $X = 3.67 \times 10^9$ to 3.34×10^{11} mg/L. The basic Monod equation helps significantly in explaining the cell demand for nutrients and the nutrient/substrate utility. It could be seen that not all developed models on growth kinetics satisfy the recorded data. Only Monod with decay rate, Wayman and Tseng, Han and Levenspiel, Loung and Moser models fit the Monod plot, which shows that inhibition doesn't significantly affect the process, as they are estimated low by the models (also evident in low $K_i = 1.01 \times 10^{12}$ value obtained).
3. Regression parameters, AIC and BIC was able to rank the models based on the most correct from Logistic (-373.8043 & -368.06112), Cone (-322.27873 & -316.53555), modified Gompertz model (-310.66405 & -304.92087) and lastly Transfert model (-310.66402 & -304.92084). POLYMATH has proven to be an effective analytical software for estimating unknown parameters in user-define nonlinear models as evidenced in the fitted biogas models to empirical data. Also, profiling has resulted in a raw biogas with sufficient CH_4 content that can serve the same purpose as natural gas if upgraded.

5.2 Recommendations

The following recommendations are made:

1) Other sustainable feedstock such as fruit waste, human waste and farm residues should be considered for kinetic study.

2) It is recommended that separate kinetic study be carried out on individual microorganisms categorized into fungi, protozoa, microorganism, and viruses or groups involving soluble substrate degraders, lignin degraders and hemi-cellulose degraders.
3) Importance of pH and temperature has been highlighted in the study. Due to fluctuations, these two parameters are often taking as range of values. To address this challenge, pH and temperature controllers are recommended to be embedded to the biogas feedstock tank or container to record changes to maintain at desired set points.

REFERENCES

Abdelhay, A., Al-Hasanat, L., & Albsoul, A. (2021). Anaerobic co-digestion of cattle manure and raw algae: Kinetic study and optimization of methane potential by RSM. *Pol. Journal of Environmental Studies*, *30*(2), 1029–1037. https://doi.org/10.15244/pjoes/125523

Abid, M., Wu, J., Seyedsalehi, M., Hu, Y., & Tian, G. (2021). Novel insights of impacts of solid content on high solid anaerobic digestion of cow manure: Kinetics and microbial community dynamics. *Bioresource Technology*, *333*(125205), 1–10. https://doi.org/10.1016/j.biortech.2021.125205

Abraham, C. (2018). *Study of biogas production from distillery waste water over immobilized biomass* (K. Kiriamiti & O. Ajoyi (eds.)). Moi University.

Abuabdou, S. M. A., Ahmad, W., Aun, N. C., & Bashir, M. J. K. (2020). A review of anaerobic membrane bioreactors (AnMBR) for the treatment of highly contaminated land fill leachate and biogas production: Effectiveness, limitations and future perspectives. *Journal of Cleaner Production*, *255*(120215), 1–12. https://doi.org/10.1016/j.jclepro.2020.120215

Abubakar, A. M., Umdagas, L. B., Waziri, A. Y., & Itamah, E. I. (2022). Estimation of biogas potential of liquid manure from kinetic models at different temperature. *International Journal of Scientific Research in Computer Science and Engineering (IJSRCSE)*, *10*(2), 46–63. https://doi.org/10.5281/zenodo.6835863

Abubakar, A. M., & Yunus, M. U. (2021). Reporting biogas data from various feedstock. *International Journal of Formal Sciences: Current and Future Research Trends (IJFSCFRT)*, *11*(1), 23–36. https://doi.org/https://doi.org/10.5281/zenodo.6603733

Adeyemo, A. J., Akingbola, O. O., & Ojeniyi, S. O. (2019). Effects of poultry manure on soil infiltration, organic matter contents and maize performance on two contrasting degraded alfisols in southwestern Nigeria. *International Journal of Recycling of Organic Waste in Agriculture*, *8*(1), 73–80. https://doi.org/10.1007/s40093-019-0273-7

AirFacts. (2020). Manure digestion for biogas from cow/pig/chicken manure. *Are Volume of Gas and Solid Equivalent*, 1–2. www.Gazpack.nl/biogas-from-cow-dung-pig-and-chicken-manure

Alfa, M. I., Owamah, H. I., Onokwai, A. O., Gopikumar, S., Kumar, S. S., Bajar, S., Samuel, O. D., & Illabor, S. C. (2020). Evaluation of biogas yield and kinetics from the anaerobic co-digestion of cow dung and horse dung: A strategy for sustainable management of livestock manure. *Energy, Ecology and Environment*, 1–10. https://doi.org/10.1007/s40974-020-00203-0

Ali, M. M., Dia, N., Bilal, B., & Ndongo, M. (2018). Theoretical models for prediction of methane production from anaerobic digestion: A critical review. *International Journal of Physical Sciences*, *13*(13), 206–216. https://doi.org/10.5897/IJPS2018.4740

Ali, S., Tawaf, A. S., Afzal, A., & Tabassum, R. (2017). Evaluating the co-digestion effects on chicken manure and rotten potatoes in batch experiments. *International Journal of Biosciences (IJB)*, *10*(6), 150–159. https://doi.org/10.12692/ijb/10.6.150-159

Almomani, F. (2020). Prediction of biogas production from chemically treated co-digested agricultural waste using artificial neural network. *Fuel*, *280*(118573), 1–13. https://doi.org/10.1016/j.fuel.2020.118573

Alqahtani, R. T. (2013). *Modeling of biological wastewater treatment* [University of Wollongong-Research Online]. http://ro.uow.edu.au/theses/3951

Amirian, M. M., Irwin, A. J., & Finkel, Z. V. (2022). Extending the Monod model of microbial growth with memory. *Quantitative Biology: Populations and Evolution*, 1–13. https://doi.org/10.48550/arXiv.2207.02028

Annuar, M. S. M., Tan, I. K. P., Ibrahim, S., & Ramachandran, K. B. (2008). A kinetic model for growth and biosynthesis of medium-chain-length poly-(3-hydroxyalkanoates) in Pseudomonas pudita. *Brazilian Journal of Chemical Engineering*, *25*(02), 217–228. www.abeq.org.br/bjche

Aragón-noriega, E. A., Alcántara-razo, E., Valenzuela-quiñónez, W., & Rodríguez-quiroz, G. (2015). Multi-model inference for growth parameter estimation of the Bigeye Croaker Micropogonias megalops in the upper gulf of California. *Revista de Biología Marina y Oceanografía*, *50*(1), 25–38. https://doi.org/10.4067/S0718-19572015000100003

Arana, I., Orruno, M., & Barcina, I. (2013). *How to solve practical aspects of microbiology* (pp.

1–10).

Ardestani, F. (2012). Survey of the nutrient utilization and cell growth kinetic wioth Verhulst, Contois and Exponential models for Penicillium brevicompactum ATCC 16024 in batch bioreactor. *World Applied Sciences Journal*, *16*(1), 135–140.

Arifan, F., Abdullah, A., & Sumardiono, S. (2021). Kinetic study of biogas production from animal manure and organic waste in Semarang City by using anaerobic digestion method. *Indonesian Journal of Chemistry*, *21*(5), 1221–1230. https://doi.org/10.22146/ijc.65056

Aziz, M. A., Kassim, K. A., Elsergany, M., Anuar, S., Jorat, M. E., Ahsan, A., & Imteaz, M. A. (2019). Recent advances on palm oil mill effluent (POME) pretreatment and anaerobic reactor for sustainable biogas production. *Renewable and Sustainable Energy Reviews*, *119*(109603), 1–31. https://doi.org/10.1016/j.rser.2019.109603

Bakraoui, M., Karouach, F., Ouhammou, B., Aggour, M., Essamri, A., & El Bari, H. (2020). Biogas production from recycled paper mill wastewater by UASB digester: Optimal and mesophilic conditions. *Biotechnology Reports*, *25*, 1–8. https://doi.org/10.1016/j.btre.2019.e00402

Baltrėnas, P., Kolodynskij, V., & Urbanas, D. (2019). Biogas production from chicken manure at different organic loadings using a special zeolite additive (ZeoVit sorbent). *Journal of Renewable Sustainable Energy*, *11*(063101), 1–11. https://doi.org/10.1063/1.5119840

Barreto, F., Silva, S. D. Q., Aquino, S. F. De, Paranhos, A. G. D. O., Adarme, O. F. H., & Barreto, G. F. (2019). Methane production by co-digestion of poultry manure and lignocellulosic biomass: Kinetic ad energy assessment. *Bioresource Technology*, *1–32*, 122588. https://doi.org/10.1016/j.biortech.2019.122588

Bayen, T., Rapaport, A., & Tani, F. Z. (2018). Optimal periodic control of the chemostat with Contois growth function. *IFAC International Conference on Mathematical Modelling-(MATHMOD 2018)*, 730–734. https://doi.org/10.1016/j.ifacol.2018.03.124

Bharathiraja, B., Sudharsana, T., Jayamuthunagai, J., Praveenkumar, R., & Chozhavendhan, S. (2018). Biogas production – A review on composition, fuel properties, feed stock and principles of anaerobic digestion. *Renewable and Sustainable Energy Reviews*, *90*, 570–582.

https://doi.org/10.1016/j.rser.2018.03.093

Bhatt, A. H., & Tao, L. (2020). Economic perspectives of biogas production via anaerobic digestion. *Bioengineering*, *7*(74), 1–19. https://doi.org/10.3390/bioengineering7030074

Bijman, T. (2014). Biogas from poultry waste – A case. *Nijhuis Water Technology*, *June*, 1–12.

Bodegom, P. Van. (2007). Microbial maintenance: A critical review on its quantification. *Microbial Ecology*, *53*, 513–523. https://doi.org/10.1007/s00248-006-9049-5

Brémond, U., Buyer, R. De, Steyer, J., Bernet, N., & Carrere, H. (2018). Biological pretreatments of biomass for improving biogas production: An overview from lab scale to full-scale. *Renewable and Sustainable Energy Reviews*, *90*, 583–604. https://doi.org/10.1016/j.rser.2018.03.103

Brugger, S. D., Baumberger, C., Jost, M., Jenni, W., Brugger, U., & Muhlemann, K. (2012). Automated counting of bacterial colony forming units on agar plates. *PLOS ONE*, *7*(3), 1–6. https://doi.org/10.1371/journal.pone.0033695

Brunerová, A., Müller, M., Gürdil, A. G. K., Sleger, V., & Brozek, M. (2020). Analysis of the physical-mechanical properties of a pelleted chicken litter organic fertiliser. *Research in Agricultural Engineering*, *66*(4), 131–139. https://doi.org/10.4491/eer.2018.081

Cao, W., Cao, C., Guo, L., Jin, H., Dargusch, M., Bernhardt, D., & Yao, X. (2016). Hydrogen production from supercritical water gasification of chicken manure. *International Journal of Hydrogen Energy*, 1–10. https://doi.org/10.1016/j.ijhydene.2016.09.031

Cayci, G., Temiz, C., & Ok, S. S. (2017). The effects of fresh and composted chicken manures on some soil characteristics. *Communications in Soil Science and Plant Analysis*, *00*(00), 1–11. https://doi.org/10.1080/00103624.2017.1373794

Cheong, D., Kim, J., & Lee, C. (2019). Improving biomethanation of chicken manure by co-digestion with ethanol plant effluent. *International Journal of Environmental Research and Public Health*, *16*(5023), 1–10. https://doi.org/10.3390/ijerph16245023

Chinenyenwa, N. N., Joseph, N. T., Chijioke, O. E., & Nnamdi, E. V. (2022). Biogas production kinetic studies from yam peels. *Journal of Engineering and Applied Sciences (JEAS)*, *20*(1),

753–766.

Choi, N. C., Choi, J., Kim, S. B., & Kim, D. J. (2008). Modeling of growth kinetics for Pseudomonas putida during toluene degradation. *Applied Microbial and Cell Physiology*, *81*, 135–141. https://doi.org/10.1007/s00253-008-1650-8

Chowdhury, T., Chowdhury, H., Hossain, N., Ahmed, A., Hossen, M. S., Chowdhury, P., Saidur, R., & Thirugnanasambandam, M. (2020). Latest advancements on livestock waste management and biogas production: Bangladesh's perspective. *Journal of Cleaner Production*, *272*(122818), 1–20. https://doi.org/10.1016/j.jclepro.2020.122818

Dalk, K., & Ugurlu, A. (2015). Biogas production from chicken manure at different organic loading rates in a mesophilic-thermopilic two stage anaerobic system. *Journal of Bioscience and Bioengineering*, *xx*(xx), 1–8. https://doi.org/10.1016/j.jbiosc.2015.01.021

Datta, A. (2021). Determination of viable microbial count present in tap water. *International Journal of Innovative Science and Research Technology*, *6*(4), 246–247. https://doi.org/10.1520/STP36000S.The

Dede, O. H., & Ozer, H. (2018). Enrichment of poultry manure with biomass ash to produce organomineral fertiliser. *Environmental Engineering Research*, *23*(4), 449–455. https://doi.org/10.4491/eer.2018.081

Deepanraj, B., Sivasubramanian, V., & Jayaraj, S. (2015). Kinetic study on the effect of temperature on biogas production using a lab scale batch reactor. *Ecotoxicology and Environmental Safety*, 1–5. https://doi.org/10.1016/j.ecoenv.2015.04.051

Delgadillo-Mirquez, L., Hernández-sarabia, M., & Machado-Higuera, M. (2018). Mathematical modelling and simulation for biogas production from organic waste. *International Journal of Engineering Systems Modelling and Simulation*, *10*(2), 97–102.

Dinh, P. V, Fujiwara, T., Phu, S. T. P., & Hoang, M. G. (2018). Kinetic of biogas production in co-digestion of vegetable waste, horse dung, and sludge by batch reactors. *IOP Conference Series: Earth and Environmental Science*, 1–9.

Dlangamandla, N., Ntwampe, S. K. O., Angadam, J. O., Chidi, B. S., & Mewa-ngongang, M. (2019). Kinetic parameters of Saccharomyces cerevisiae alcohols production using

Nepenthes mirabilis pod digestive fluids-mixed agro-waste hydrolysates. *Fermentation*, *5*(10), 1–14. https://doi.org/10.3390/fermentation5010010

Duan, N., Ran, X., Li, R., Kougias, P. G., Zhang, Y., Lin, C., & Liu, H. (2018). Performance evaluation of mesophilic anaerobic digestion of chicken manure with algal digestate. *Energies*, *11*(1829), 1–11. https://doi.org/10.3390/en11071829

Elalami, D., Carrere, H., Monlau, F., Abdelouahdi, K., Oukarroum, A., & Barakat, A. (2019). Pretreatment and co-digestion of wastewater sludge for biogas production: Recent research advances and trends. *Renewable and Sustainable Energy Reviews*, *114*(109287), 1–23. https://doi.org/10.1016/j.rser.2019.109287

Eronmosele, P., Thelma, A. E., & Essienubong, A. I. (2020). Comparative study of the kinetics of biogas yield from the codigestion of poultry droppings with waterleaf and poultry droppings with elephant grass. *Engineering Sciences (NWSAENS)*, *15*(3), 139–150. https://doi.org/10.12739/NWSA.2020.15.3.1A0457

Fahriansyah, M. A., & Sriharti. (2019). Design of conventional mixer for biogas digester. *3rd International Symposium on Green Technology for Value Chains 2018*, 1–8. https://doi.org/10.1088/1755-1315/277/1/012017

Fakkaew, K., & Polprasert, C. (2021). Air stripping pre-treatment process to enhance biogas production in anaerobic digestion of chicken manure wastewater. *Bioresource Technology Reports*, *14*(January), 100647. https://doi.org/10.1016/j.biteb.2021.100647

Faraz, R. M. (2020). A preliminary study: Effect of initial pH and Saccharomyces cerevisiae addition on biogas production from acid-pretreated Salvinia molesta and kinetics. *Energy*, 118226. https://doi.org/10.1016/j.energy.2020.118226

Francis, M. I., Liba, J. W., Atsanda, N. N., & Jukunda, R. (2016). Level of awareness of poultry diseases and management practices by poultry farmers in Maiduguri metropolis, Borno State, Nigeria. *Nigerian Veterinary Journal*, *37*(4), 230–235.

Fuchs, W., Wang, X., Gabauer, W., Ortner, M., & Li, Z. (2018). Tackling ammonia inhibition for efficient biogas production from chicken manure: Status and technical trends in Europe and China. *Renewable and Sustainable Energy Reviews*, *97*, 186–199.

https://doi.org/10.1016/j.rser.2018.08.038

Gallipoli, A., Braguglia, C. M., Gianico, A., Montecchio, D., & Pagliaccia, P. (2020). Kitchen waste valorization through a mild-temperature pretreatment to enhance biogas production and fermentability: Kinetics study in mesophilic and thermophilic regime. *Journal of Environmental Sciences*, *89*, 167–179. https://doi.org/10.1016/j.jes.2019.10.016

Ge, J., Huang, G., Sun, X., Yin, H., & Han, L. (2019). New insights into the kinetics of bacterial growth and decay in pig manure–wheat straw aerobic composting based on an optimized PMA–qPCR method. *Microbial Biotechnology*, *12*(3), 502–514. https://doi.org/10.1111/1751-7915.13380

Germec, M., & Turhan, I. (2021). Predicting the experimental data of the substrate specificity of Aspergillus niger inulinase using mathematical models, estimating kinetic constants in the Michaelis-Menten equation, and sensitivity analysis. *Biomass Conversion and Biorefinery*, 1–12. https://doi.org/10.1007/s13399-021-01830-1

Ghatak, M. Das, & Mahanta, P. (2014). Comparison of kinetic models for biogas production rate from saw dust. *International Journal of Research in Engineering and Technology (IJRET)*, 248–254.

González-figueredo, C., Flores-estrella, R. A., & Rojas-rejón, O. A. (2018). Fermentation: Metabolism, kinetic models, and bioprocessing. In *Current Topics in Biochemical Engineering* (pp. 1–17). InTech Open. https://doi.org/10.5772/intechopen.82195 solid

Granado, R. L., Antune, A. M. S., Fonseca, F. V., Sánchez, A., Barrena, R., & Font, X. (2017). Technology overview of biogas production in anaerobic digestion plants: A European evaluation of research and development. *Renewable and Sustainable Energy Reviews*, *80*, 44–53. https://doi.org/10.1016/j.rser.2017.05.079

Gummadi, S. N., & Santhosh, D. (2010). Kinetics of growth and caffeine demethylase production of Pseudomonas sp. in bioreactor. *Journal of Ind Microbiology Biotechnology*, *37*, 901–908. https://doi.org/10.1007/s10295-010-0737-2

Hakimi, M., Shamsudin, M. R., Pendyala, R., Aminah, S., & Gunny, A. A. N. (2021). Co-anaerobic digestion of chicken manure and selected additives for biogas production. *IOP*

Conference Series: Earth and Environmental Science, 1–8. https://doi.org/10.1088/1755-1315/765/1/012055

Haleem, A. M., Al-bakri, S. A., & Al-Hiyaly, S. A. K. (2013). Determination of microbial content in poultry meat in local Iraqi markets. *Journal of Microbiology Research*, *3*(6), 205–207. https://doi.org/10.5923/j.microbiology.20130306.02

Halmi, M. I. E., Shukor, M. S., Johari, W. L. W., & Shukor, M. Y. (2014). Mathematical modeling of the growth kinetics of Bacillus spp. on tannery effluent containing chromate. *Journal of Environmental Bioremediation & Toxicology (JEBAT)*, *2*(1), 6–10. http://journal.hibiscuspublisher.com

Hamitouche, A., Bendjama, Z., Amrane, A., Kaouah, F., & Hamane, D. (2012). Relevance of the Luong model to describe the biodegradation of phenol by mixed culture in a batch reactor. *Ann Microbiology*, *62*, 581–586. https://doi.org/10.1007/s13213-011-0294-6

Haryanto, A., Triyono, S., & Wicaksono, N. H. (2018). Effect of hydraulic retention time on biogas production from cow dung in a semi continuous anaerobic digester. *International Journal of Renewable Energy Development (IJRED)*, *7*(2), 93–100. https://doi.org/https://doi.org/10.14710/ijred.7.2.93-100

Hassan, M., Umar, M., Ding, W., & Mehryar, E. (2017). Methane enhancement through co-digestion of chicken manure and oxidative cleaved wheat straw: Stability performance and kinetic modeling perspectives. *Energy*, *141*, 2314–2320. https://doi.org/10.1016/j.energy.2017.11.110

Hawkins, J. L., Uknalis, J., Oscar, T. P., Schwarz, J. G., Vimini, B., & Parveen, S. (2019). The effect of previous life cycle phase on the growth kinetics, morphology, and antibiotic resistance of Salmonella Typhimurium DT104 in brain heart infusion and ground chicken extract. *Frontiers in Microbiology*, *10*(1043), 1–11. https://doi.org/10.3389/fmicb.2019.01043

HomeBioGas. (2021). *What is Biogas? A Beginner's Guide*. Homebiogas.Com. www.homebiogas.com/what-is-biogas-a-beginners-guide-

Hongguang, Z., Jing, Y., & Xiaowei, C. (2019). *Application of Modified Gompertz Model to Study*

on Biogas production from middle temperature co-digestion of pig manure and dead pigs. *03022*.

Horf, M., Gebbers, R., Vogel, S., Markus, O., Piepel, M.-F., & Olfs, H.-W. (2021). Determination of nutrients in liquid manures and biogas digestates by portable Energy-Dispersive X-ray Fluorescence Spectrometry. *Sensors*, *21*(11), 1–12. https://doi.org/10.3390/s21113892

Hossain, M. F., Rahman, M. T., & Kabir, S. M. L. (2017). Microbial assessment of milk collected from different markets of Mymensingh, Gazipur and Sherpur districts of Bangladesh and determination of antimicrobial resistance patterns of the isolated bacteria. *Asian-Australasian Journal of Food Safety and Security*, *1*(1), 7–16. www.ebupress.com/journal/aajfss

IRENA. (2016). *Measuring small-scale biogas capacity and production*. www.irena.org/publications

Jaffar, M. M., & Rehman, A. M. (2020). Wheat straw optimization via its efficient pretreatment for improved biogas production. *Civil Engineering Journal*, *6*(6), 1056–1063. https://doi.org/10.28991/cej-2020-03091528

Jiang, H., Shen, Y., Ma, C., Zhao, J., Wang, Y., Li, Y., & Zhou, H. (2021). Solid-state anaerobic digestion of chicken manure and corn straw with different loading amounts. *Polish Journal of Environmental Studies*, *30*(3), 2117–2125. https://doi.org/10.15244/pjoes/124180

Jijai, S., & Siripatana, C. (2017). Kinetic model of biogas production from of Thai rice noodle wastewater (Khanomjeen) with chicken manure. *Energy Procedia*, *138*, 386–392. https://doi.org/10.1016/j.egypro.2017.10.177

Jyothilakshmi, R., & Prakash, S. V. (2016). Design, fabrication and experimentation of a small scale anaerobic biodigester for domestic biodegradable solid waste with energy recovery and sizing calculations. *Procedia Environmental Sciences*, *35*, 749–755. https://doi.org/10.1016/j.proenv.2016.07.085

Kainthola, J., Kalamdhad, A. S., & Goud, V. V. (2019). A review on enhanced biogas production from anaerobic digestion of lignocellulosic biomass by different enhancement techniques. *Process Biochemistry*, *84*, 81–90. https://doi.org/10.1016/j.procbio.2019.05.023

Kandasamy, S., Palanichamy, M., & Mani, S. R. (2020). Mass culture of Cladocerans,

Diaphanasoma sarsi and Ceriodaphnia cornuta using chicken manure. *Asian Journal of Experimental Science*, *34*(2), 7–11. www.ajesjournal.com

Kang, M. S., Park, J. H., & Kim, H. J. (2021). Predictive modeling for the growth of Salmonella spp. in liquid egg white and application of scenario-based risk estimation. *Microorganisms*, *9*(486), 1–12. https://doi.org/10.3390/microorganisms9030486

Keskin, T., Arslan, K., Karaalp, D., & Azbar, N. (2018). The determination of the trace element effects on basal medium by using the statistical optimization approach for biogas production from chicken manure. *Waste and Biomass Valorization*, *0*(0), 1–10. https://doi.org/10.1007/s12649-018-0273-2

Khayal, O. (2019). Main types and applications of biogas plants. *Nile Valley University*, 1–11. https://doi.org/10.13140/RG.2.2.32559.69287

Ksheem, A. M. A. (2015). *Optimising nutrient extraction from chicken manure and compost* [University of Southern Queensland]. https://doi.org/10.13140/RG.2.1.1973.3842

Kyurkchiev, N., Markov, S., & Iliev, A. (2016). A note on the Schnute growth model. *International Journal of Engineering Research and Development*, *12*(6), 47–54.

Lasagna, E., Ceccobelli, S., Cardinali, I., Perini, F., Bhadra, U., Thangaraj, K., Dababani, R. C., Rai, N., Sarti, F. M., Lancioni, H., & Ige, A. O. (2017). Mitochondrial diversity of Yoruba and Fulani chickens: A biodiversity reservoir in Nigeria. *Poultry Science*, *99*(6), 2852–2860. https://doi.org/10.1016/j.psj.2019.12.066

Latinwo, G. K., & Agarry, S. E. (2015). Modelling the kinetics of biogas production from mesophilic anaerobic co-digestion of cow dung with plantain peels. *International Journal of Renewab;e Energy Development*, *4*(1), 55–63. https://doi.org/10.14710/ijred.4.1.55-63

Lenkiewicz, Z., & Webster, M. (2017). *How to convert organic waste into biogas: A step-by-step guide*. CIWM (Chartered Institution of Wastes Management). wasteaid.org.uk/toolkit

Li, C., Strömberg, S., Liub, G., Nges, I. A., & Liu, J. (2016). Assessment of regional biomass as co-substrate in the anaerobic digestion of chicken manure: Impact of co-digestion with chicken processing waste, seagrass and Miscanthus. *Biochemical Engineering Journal*, 1–38. https://doi.org/10.1016/j.bej.2016.11.008

Li, P., Li, W., Sun, M., Xu, X., Zhang, B., & Sun, Y. (2019). Evaluation of biochemical methane potential and kinetics on the anaerobic digestion of vegetable crop residues. *Energies*, *12*(26), 1–14. https://doi.org/10.3390/en12010026

Li, Y. K., Hu, X. M., & Feng, L. (2020). Characteristics of biogas production via high-temperature dry fermentation of chicken manure. *Applied Ecology and Environmental Research*, *18*(4), 4883–4895. https://doi.org/10.15666/aeer/1804_48834895

Li, Y., Zhang, R., Chen, C., Liu, G., He, Y., & Liu, X. (2013). Biogas production from co-digestion of corn stover and chicken manure under anaerobic wet, hemi-solid, and solid state conditions. *Bioresource Technology*, *149*, 406–412. https://doi.org/10.1016/j.biortech.2013.09.091

Lim, Y. F., Chan, Y. J., Abakr, Y. A., Sethu, V., Singh, A., Lee, J., & Gareth, M. (2021). Evaluation of potential feedstock for biogas production via anaerobic digestion in Malaysia: Kinetic studies and economics analysis. *Environmental Technology*, *0*(0), 1–18. https://doi.org/10.1080/09593330.2021.1882587

Lin, Y. P., Huang, G. H., Lu, H. W., & He, L. (2008). Modeling of substrate degradation and oxygen consumption in waste composting processes. *Waste Management*, *28*(8), 1375–1385. https://doi.org/10.1016/j.wasman.2007.09.016

Liu, S. (2017). How cells grow. In *Bioprocess Engineering: Kinetics, Sustainability, and Reactor Design* (2nd ed., pp. 629–697). Elsevier B. V. https://doi.org/10.1016/B978-0-444-63783-3.00011-3

Liu, X. Y., Wang, J. J., Nie, J. M., Wu, N., Yang, F., & Yang, R. J. (2018). Biogas production of chicken manure by two-stage fermentation process. *E3S Web of Conferences (ICEMEE 2018)*, *38*(01048), 5–8. https://doi.org/10.1051/e3sconf/20183801048

Lohani, S. P., Acharya, A., Koirala, R., Koirala, A., Lamsal, B., & Khanal, S. N. (2020). Anaerobic co-digestion of food waste, goat and chicken manure for sustainable biogas production. *International Journal of Energy Applications and Technologies*, *7*(4), 120–125. https://doi.org/10.31593/ijeat.748982

Lv, Y., Wang, L., Xingyu, L., Chen, B., & Zhang, M. (2022). Degradation kinetics of aromatic

VOCs polluted wastewater by functional bacteria at laboratory scale. *Scientific Reports*, *12*(19053). https://doi.org/10.1038/s41598-022-21356-4

Ma, J., Chen, F., Xue, S., Pan, J., Khoshnevisan, B., Yang, Y., Liu, H., & Qiu, L. (2021). Improving anaerobic digestion of chicken manure under optimized biochar supplementation strategies. *Bioresource Technology*, *325*(124697), 124697. https://doi.org/10.1016/j.biortech.2021.124697

Maier, R. M. (2009). Bacterial growth. In *Review of Basic Microbiological Concepts* (pp. 37–54). Academic Press Inc.

Mancini, G., Papirio, S., Lens, P. N. L., & Esposito, G. (2018). Increased biogas production from wheat straw by chemical pretreatments. *Renewable Energy*, *119*, 608–614. https://doi.org/10.1016/j.renene.2017.12.045

Marwan, M. I., Dahlia, H., Chee, W. K., Zarrahimah, Z., Harnita, E., & Liyana, N. M. R. (2018). Comparison of growth rate of Salmonella for antigen production. *Malaysian Journal of Veterinary Research*, *9*(2), 122–129.

Matheri, A. N., Ndiweni, S. N., Belaid, M., Muzenda, E., & Hubert, R. (2017). Optimising biogas production from anaerobic co-digestion of chicken manure and organic fraction of municipal solid waste. *Renewable and Sustainable Energy Reviews*, *80*, 756–764. https://doi.org/10.1016/j.rser.2017.05.068

Matsumura, Y., Suganuma, Y., Ichikawa, T., Kim, W., Nakashimada, Y., & Nishida, K. (2021). Reaction rate of hydrothermal ammonia production from chicken manure. *ACS Omega*, 1–5. https://doi.org/10.1021/acsomega.1c03418

Mazaheri, D., & Shojaosadati, S. A. (2013). Mathematical models for microbial kinetics in solid-state fermentation: A review. *Iranian Journal of Biotechnology*, *11*(3), 156–167.

Momodu, A. S., & Adepoju, T. D. (2021). System dynamics kinetic model for predicting biogas production in anaerobic condition: Preliminary assessment. *Science Progress*, *104*(4), 1–25. https://doi.org/10.1177/00368504211042479

Muloiwa, M., Nyende-byakika, S., & Dinka, M. (2020). Comparison of unstructured kinetic bacterial growth models. *South African Journal of Chemical Engineering*, *33*, 141–150.

https://doi.org/10.1016/j.sajce.2020.07.006

Najafi, B., Ardabili, S. F., Shamshirband, S., & Chau, K. (2019). Development of a modified kinetic method for modelling of biogas produced from biomass. *Energies*, 1–16.

Neshat, S. A., Mohammadi, M., Najafpour, G. D., & Lahijani, P. (2017). Anaerobic co-digestion of animal manures and lignocellulosic residues as a potent approach for sustainable biogas production. *Renewable and Sustainable Energy Reviews*, *79*, 308–322. https://doi.org/10.1016/j.rser.2017.05.137

Nong, H. T. T., Whangchai, K., Unpaprom, Y., Thararux, C., & Ramaraj, R. (2020). Development of sustainable approaches for converting the agro-weeds Ludwigia hyssopifolia to biogas production. *Biomass Conversion and Biorefinery*, 1–9. https://doi.org/10.1007/s13399-020-01083-4

Noori, N. A., & Ismail, Z. Z. (2019). Process optimization of biogas recovery from giant reed (Arundo donax) alternatively pretreated with acid and oxidant agent: Experimental and kinetic study. *Biomass Conversion and Biorefinery*, 1–15. https://doi.org/10.1007/s13399-019-00481-7

Nsair, A., Onen Cinar, S., Alassali, A., Abu Qdais, H., & Kuchta, K. (2020). Operational parameters of biogas plants: A review and evaluation study. *Energies*, *13*(15), 1–27. https://doi.org/10.3390/en13153761

O'Toole, G. A. (2016). Classic spotlight: Plate counting you can count on. *Journal of Bacteriology*, *198*(23), 3127. https://doi.org/10.1128/JB.00711-16.Address

Okpokwasili, G. C., & Nweke, C. O. (2005). Microbial growth and substrate utilization kinetics. *African Journal of Biotechnology*, *5*(4), 305–317. http://www.academicjournals.org/AJB%0D

Onay, M. A. K. B. D. T. T. (2020). Enhanced biogas production from chicken manure via enzymatic pretreatment. *Journal of Material Cycles and Waste Management*, *0123456789*. https://doi.org/10.1007/s10163-020-01039-w

Oosterkamp, W. J., & Oosterbeek, O. (2018). Chicken manure digestion. *Current Biochemical Engineering*, *3*(April), 1–2. https://doi.org/10.2174/2212711903666160831141935

Opurum, C. C. (2021). Kinetic study on biogas production from cabbage (Brassica oleracea) waste and its blend with animal manure using Logistic Function Model. *Journal of Advances in Microbiology*, *21*(1), 34–43. https://doi.org/10.9734/JAMB/2021/v21i130317

Opurum, C. C., Nweke, C. O., Nwanyanwu, C. E., & Nwogu, N. A. (2021). Modelling of biphasic biogas production process from mixtures of livestock manure using Bi-logistic Function and Modified Gompertz Equation. *Annual Research & Review in Biology*, *36*(3), 116–129. https://doi.org/10.9734/ARRB/2021/v36i330358

Paar, M., Schrabmair, W., Mairold, M., Oettl, K., & Reibnegger, G. (2019). Global regression using the explicit solution of Michaelis-Menten kinetics employing Lambert's W Function: High robustness of parameter estimates. *Biological Chemistry and Chemical Biology*, *4*, 1903–1908. https://doi.org/10.1002/slct.201803610

Paritosh, K., Mathur, S., Pareek, N., & Vivekanand, V. (2017). Feasibility study of waste (d) potential: co-digestion of organic wastes, synergistic effect and kinetics of biogas production. *International Journal of Environmental Science and Technology*, 1–10. https://doi.org/10.1007/s13762-017-1453-5

Parralejo, A. I., Royano, L., González, J., & González, J. F. (2019). Industrial Crops & Products Small scale biogas production with animal excrement and agricultural residues. *Industrial Crops & Products*, *131*, 307–314. https://doi.org/10.1016/j.indcrop.2019.01.059

Parsaee, M., Kiani, M., Kiani, D., & Karimi, K. (2019). A review of biogas production from sugarcane vinasse. *Biomass and Bioenergy*, *122*, 117–125. https://doi.org/10.1016/j.biombioe.2019.01.034

Pecar, D., Pohleven, F., & Goršek, A. (2020). Kinetics of methane production during anaerobic fermentation of chicken manure with sawdust and fungi pre-treated wheat straw. *Waste Management*, *102*, 170–178. https://doi.org/10.1016/j.wasman.2019.10.046

Pererva, Y., Miller, C. D., & Sims, R. C. (2020). Existing empirical kinetic models in biochemical methane potential (BMP) testing, their selection and numerical solution. *Water*, *12*(1831), 1–16. https://doi.org/10.3390/w12061831

Perni, S., Andrew, P. W., & Shama, G. (2005). Estimating the maximum growth rate from

microbial growth curves: Definition is everything. *Food Microbiology*, *22*(6), 491–495. https://doi.org/10.1016/j.fm.2004.11.014

Piekutin, J., Puchlik, M., Haczykowski, M., & Dyczewska, K. (2021). The efficiency of the biogas plant operation depending on the substrate used. *Energies*, *14*(3157), 1–12. https://doi.org/10.3390/ en14113157

Raja, I. A., & Wazir, S. (2017). Biogas production: The fundamental processes. *Universal Journal of Engineering Science*, *5*(2), 29–37. https://doi.org/10.13189/ujes.2017.050202

Rajput, A. A., & Visvanathan, C. (2018). Effect of thermal pretreatment on chemical composition, physical structure and biogas production kinetics of wheat straw. *Journal of Environmental Management*, *221*, 45–52. https://doi.org/10.1016/j.jenvman.2018.05.011

Ram, Y., Dellus-Gur, E., Bibi, M., & Hadany, L. (2019). *Predicting microbial growth in a mixed culture from growth curve data*. *116*(29), 14698–14707. https://doi.org/10.1073/pnas.1902217116

Rea, J. (2014). *Kinetic modeling and experimentation of anaerobic digestion* (A. Slocum & A. Hosoi (eds.)) [Massachusetts Institute of Technology]. http://hdl.handle.net/1721.1/92070

Reynolds, J. (2016). Serial dilution protocols. *American Society for Microbiology*, 1–7.

Rubežius, M., Venslauskas, K., Navickas, K., & Bleizgys, R. (2020). Influence of aerobic pretreatment of poultry manure on the biogas production process. *Processes*, *8*(1109), 1–12. https://doi.org/10.3390/pr8091109

Sakthiselvan, P., Meenambiga, S. S., & Madhumathi, R. (2019). *Kinetic studies of on cell growth*. IntechOPen. https://doi.org/http://dx.doi.org/10.5772/intechopen.84353 References

Salvesen, I., & Vadstein, O. (2000). Evaluation of plate count methods for determination of maximum specific growth rate in mixed microbial communities, and its possible application for diversity assessment. *Journal of Applied Microbiology*, *88*, 442–448.

Sarker, S., Lamb, J. J., Hjelme, D. R., & Lien, K. M. (2019). A review of the role of critical parameters in the design and operation of biogas production plants. *Applied Sciences*, *9*(9), 1–38. https://doi.org/10.3390/app9091915

Sawyerr, N., Trois, C., Workneh, T. S., & Okudoh, V. (2019). An overview of biogas production: Fundamentals, applications and future research. *International Journal of Energy Economics and Policy*, *9*(2), 105–116. https://doi.org/10.32479/ijeep.7375

Selvaraj, B., Krishnasamy, S., Munirajan, S., Alagirisamy, S., Dhanushkodi, M., & Gopalsamy, S. (2018). Kinetic modelling of augmenting biomethane yield from poultry litter by mitigating ammonia. *International Journal of Green Energy*, *00*(00), 1–7. https://doi.org/10.1080/15435075.2018.1529580

Shapovalov, Y., Salyuk, A., Kotynsky, A., & Tarasenko, R. (2019). The research of dry chicken manure methanogenesis stability. *Environmental Problems*, *4*(1), 15–18.

Shariful Islam, M., Kabir, K. M. A., Tanimoto, J., & Saha, B. B. (2021). Study on Spirulina platensis growth employing non-linear analysis of biomass kinetic models. *Heliyon*, *7*, 1–9. https://doi.org/10.1016/j.heliyon.2021.e08185

Shen, J., Zhao, C., Liu, Y., Zhang, R., Liu, G., & Chen, C. (2018). Biogas production from anaerobic co-digestion of durian shell with chicken, dairy, and pig manures. *Energy Conversion and Management*, 1–10. https://doi.org/10.1016/j.enconman.2018.06.099

Silva, T. H. L., dos Santos, L. A., de Melo Oliveira, C. R., Porto, T. S., Juca, J. F. T., & Santos, A. Fe. de S. (2021). Determination of methane generation potential and evaluation of kinetic models in poultry wastes. *Biocatalysis and Agricultural Biotechnology*, *32*(101936), 1–8. https://doi.org/10.1016/j.bcab.2021.101936

Singh, G., Shamsuddin, M. R., & Lim, S. W. (2018). Characterization of chicken manure from Manjung Region. *OP Conf. Series: Materials Science and Engineering*, 1–7. https://doi.org/10.1088/1757-899X/458/1/012084

Sukhesh, M. J., & Rao, P. V. (2018). Synergistic effect in anaerobic co-digestion of rice straw and dairy manure- a batch kinetic study. *Energy Sources, Part A: Recovery, Utilization, and Environmental Effects*, *0*(0), 1–12. https://doi.org/10.1080/15567036.2018.1550536

Syaichurrozi, I., & Rusdi, R. (2020). Development of simple kinetic model on biogas production from co-digestion of vinasse waste and tofu residue at variation of C/N Ratio. *World Chemical Engineering Journal*, *4*(1), 18–28. http://jurnal.untirta.ac.id/index.php/WCEJ

Syaichurrozi, I., Suhirman, S., & Hidayat, T. (2018). Effect of initial pH on anaerobic co-digestion of Salvinia molesta and rice straw for biogas production and kinetics. *Biocatalysis and Agricultural Biotechnology*, 1–33. https://doi.org/10.1016/j.bcab.2018.10.007

Szlachta, J., Prask, H., Fugol, M., & Luberanski, A. (2018). Effect of mechanical pre-treatment of the agricultural substrates on yield of biogas and kinetics of anaerobic digestion. *Sustainability*, *10*(3669), 1–16. https://doi.org/10.3390/su10103669

Talaiekhozani, A., Jafarzadeh, N., Fulazzaky, M. A., Talaie, M. R., & Beheshti, M. (2015). Kinetics of substrate utilization and bacterial growth of crude oil degraded by Pseudomonas aeruginosa. *Journal of Environmental Health Science and Engineering*, *13*(64), 1–8. https://doi.org/10.1186/s40201-015-0221-z

Tanczuk, M., Junga, R., Kolasa-Wiecek, A., & Niemiec, P. (2019). Assessment of the energy potential of chicken manure in Poland. *Energies*, *12*(1244), 1–18. https://doi.org/10.3390/en12071244

Tazdait, D., Abdi, N., Grib, H., Lounici, H., Pauss, A., & Mameri, N. (2013). Comparison of different models of substrate inhibition in aerobic batch biodegradation of malathion. *Turkish Journal of Engineering & Environmental Sciences*, *37*, 221–230. https://doi.org/10.3906/muh-1211-7

Teferra, D. M., & Wubu, W. (2018). *Biogas for clean energy*. InTech Open. https://doi.org/10.5772/intechopen.79534

Tena, M., Perez, M., & Solera, R. (2021). Effect of hydraulic retention time on the methanogenic step of a two-stage anaerobic digestion system from sewage sludge and wine vinasse: Microbial and kinetic evaluation. *Fuel*, *296*(120674), 1–10. https://doi.org/10.1016/j.fuel.2021.120674

Tetteh, E. K., & Rathilal, S. (2020). Kinetics and nanoparticle catalytic enhancement of biogas production from wastewater using a magnetized biochemical methane potential (MBMP) system. *Catalysts, 10*(1200), 1–19. https://doi.org/10.3390/catal10101200

Uche, A. M., Emmanuel, O. T., Paul, O. U., Olawale, A., Frank, K. B., Rita, O. O., & Martin, O. S. (2020). Design and construction of fixed dome digester for biogas production using cow

dung and water hyacinth. *African Journal of Environmental Science and Technology*, *14*(1), 15–25. https://doi.org/10.5897/AJEST2019.2739

Ulukardesler, A. H. (2021). Anaerobic co-digestion of grass and cow manure: Kinetic modeling comparison and GHG emission reduction. *Research Square*, 1–15.

UlukardeŞler, A. H., & Atalay, F. S. (2018). Kinetic studies of biogas generation using chicken manure as feedstock. *Journal of Polytechnic*, *0900*(4), 913–917. https://doi.org/10.2339/politeknik.389622

Ulusoy, Y., Ulukardesler, A. H., Arslan, R., & Tekin, Y. (2018). Energy and emission benefits of chicken manure biogas production: A case study. *Environmental Science and Pollution Research*, 1–7. https://doi.org/10.1007/s11356-018-3466-0

Um-e-Habiba, Khan, M. S., Raza, W., Gul, H., Hussain, M., Malik, B., Azam, M., & Winter, F. (2021). A study on the reaction kinetics of anaerobic microbes using batch anaerobic sludge technique for beverage industrial wastewater. *Separations*, *8*(43), 1–16. https://doi.org/10.3390/ separations8040043 Academic

Van, D. P., Minh, G. H., Phu, S. T. P., & Fujiwara, T. (2018). A new kinetic model for biogas production from co-digestion by batch mode. *Global Journal of Environmental Science and Management*, *4*(3), 251–262. https://doi.org/10.22034/gjesm.2018.03.001

Velazquez-Marti, B., Meneses-Quelal, O. W., Gaibor-Chavez, J., & Nino-Ruiz, Z. (2018). Review of mathematical models for the anaerobic digestion process. In R. B. Jeyakumar & Y. K. Ravi (Eds.), *Anaerobic Digestion* (p. 246). IntechOpen. https://doi.org/10.5772/intechopen.80815

Venkateshkumar, R., Shanmugam, S., & Veerappan, A. R. (2020). Anaerobic co-digestion of cow dung and cotton seed hull with different blend ratio: Experimental and kinetic study. *Biomass Conversion and Biorefinery*, 1–111. https://doi.org/10.1007/s13399-020-01006-3

Wang, F., Pei, M., Qiu, L., Yao, Y., Zhang, C., & Qiang, H. (2019). Performance of anaerobic digestion of chicken manure under gradually elevated organic loading rates. *International Journal of Environmental Research and Public Health*, *16*(2239), 1–17. https://doi.org/10.3390/ijerph16122239

Wang, J., Matsushita, T., Yuminaga, J., & Jia, H. (2021). Study on the preparation method and

combustion characteristics of biomass char fuel made from chicken manure synergistic plastic waste. *IOP Conference Series: Earth and Environmental Science PAPER*, 1–9. https://doi.org/10.1088/1755-1315/696/1/012027

Wang, Y., & Witarsa, F. (2016). Application of Contois, Tessier, and First-order kinetics for modeling and simulation of a composting decomposition process. *Bioresource Technology*, *220*, 384–393. https://doi.org/10.1016/j.biortech.2016.08.099

Wang, Z.-W., & Li, Y. (2014). A theoretical derivation of the Contois equation for kinetic modeling of the microbial degradation of insoluble substrates. *Biochemical Engineering Journal*, *82*, 134–138. https://doi.org/10.1016/j.bej.2013.11.002

Wu, A., Lovett, D., Mcewan, M., Cecelja, F., & Chen, T. (2016). A spreadsheet calculator for estimating biogas production and economic measures for UK-based farm-fed anaerobic digesters. *Bioresource Technology*, *220*, 479–489. https://doi.org/10.1016/j.biortech.2016.08.103

Xu, J., Tang, J., Jin, Y., Song, J., Yang, R., Sablani, S. S., & Zhu, M.-J. (2018). *High temperature water activity as a key factor influencing survival of Salmonella Enteritidis PT30 in thermal processing*. *509*, 1–43. https://www.sciencedirect.com/science/article/pii/S0956713518305991

Yang, H., Deng, R., Jin, J., Wu, Y., Jiang, X., & Shi, J. (2021). Hydrolytic performances of different organic compounds in different lignocellulosic biomass during anaerobic digestion. *Environmental Engineering Resources*, *27*(4), 1–10. https://doi.org/10.4491/eer.2021.013

Yilmaz, S., & Sahan, T. (2020). Utilization of pumice for improving biogas production from poultry manure by anaerobic digestion: A modeling and process optimization study using response surface methodology. *Biomass and Bioenergy*, *138*(105601), 1–10. https://doi.org/10.1016/j.biombioe.2020.105601

Yunardi, H., Rinaldi, W., & Fathanah, U. (2015). *Development and validation of a modified Contois kinetics model for microalgae Chlorella kessleri* (pp. 1–6). Chemical Engineering Department, Universitas Syiah Kuala.

Yusof, T. R. T., Abdul Rahman, N., Ariff, A. B., & Man, H. C. (2019). Evaluation of hydrogen

and methane production from co-digestion of chicken manure and food waste. *Polish Journal of Environmental Studies*, *28*(4), 1–11. https://doi.org/10.15244/pjoes/86222

Zahedi, S., Mart, C., Solera, R., & Perez, M. (2020). Evaluating the effectiveness of adding chicken manure in the anaerobic mesophilic codigestion of sewage sludge and wine distillery wastewater: Kinetic modeling and economic approach. *Energy & Fuels*, 1–8. https://doi.org/10.1021/acs.energyfuels.0c01852

Zeb, I., Ma, J., Mehboob, F., Kafle, G. K., Amin, B. A. Z., Nazir, R., Ndegwa, P., & Frear, C. (2019). *Kinetic and microbial analysis of methane production from dairy wastewater anaerobic digester under ammonia and salinity stresses*. 1–36. https://www.sciencedirect.com/science/article/pii/S0959652619303221

Zhang, F., Li, Y., Yang, M., & Li, W. (2012). Content of heavy metals in animal feeds and manures from farms of different scales in Northeast China. *International Journal of Environmental Research and Public Health*, *9*, 2658–2668. https://doi.org/10.3390/ijerph9082658

Zhang, L., Loh, K., & Zhang, J. (2019). Enhanced biogas production from anaerobic digestion of solid organic wastes: Current status and prospects. *Bioresource Technology Reports*, *5*, 280–296. https://doi.org/10.1016/j.biteb.2018.07.005

Zhao, C., Mu, H., Zhao, Y., Wang, L., & Zuo, B. (2017). Microbial characteristics analysis and kinetic studies on substrate composition to methane after microbial and nutritional regulation of fruit and vegetable wastes anaerobic digestion. *Bioresource Technology*, 1–30. https://doi.org/10.1016/j.biortech.2017.10.041

Zhao, C., Yan, H., Liu, Y., Huang, Y., Zhang, R., Chen, C., & Liu, G. (2016). Bio-energy conversion performance, biodegradability, and kinetic analysis of different fruit residues during discontinuous anaerobic digestion. *Waste Management*, *52*, 295–297. https://doi.org/10.1016/j.wasman.2016.03.028

Zhenlin, Y., Weiqiang, Z., Deshuang, Y., Yuntai, B., & Li, J. (2019). Enhanced carbon and nitrogen removal performance of simultaneous anammox and denitrification (SAD) with with mannitol addition treating saline wastewater. *Journal of Chemical Technology and Biotechnology*, *94*(2), 377–388. https://doi.org/https://doi.org/10.1002/JCTB.5781

APPENDICES

A. Colony forming unit of SDE1, 2 and 3

		SDE1			SDE2			SDE3		
Date	Time (days)	No. of colonies	CFU/mL	log X	No. of colonies	CFU/mL	log X	No. of colonies	CFU/mL	log X
18/10/2021	0	2	2.00E+09	9.30103	4	4.00E+09	9.60205999	5	5.00E+09	9.698970004
19/10/2021	1	4	4.00E+09	9.60205999	3	3.00E+09	9.47712125	4	4.00E+09	9.602059991
20/10/2021	2	3	3.00E+09	9.47712125	4	4.00E+09	9.60205999	4	4.00E+09	9.602059991
21/10/2021	3	5	5.00E+09	9.69897	3	3.00E+09	9.47712125	3	3.00E+09	9.477121255
22/10/2021	4	4	4.00E+09	9.60205999	5	5.00E+09	9.69897	2	2.00E+09	9.301029996
23/10/2021	5	4	4.00E+09	9.60205999	3	3.00E+09	9.47712125	4	4.00E+09	9.602059991
25/10/2021	6	4	4.00E+09	9.60205999	3	3.00E+09	9.47712125	4	4.00E+09	9.602059991
26/10/2021	7	3	3.00E+09	9.47712125	4	4.00E+09	9.60205999	4	4.00E+09	9.602059991
27/10/2021	8	5	5.00E+09	9.69897	5	5.00E+09	9.69897	6	6.00E+09	9.77815125
28/10/2021	9	10	1.00E+10	10	9	9.00E+09	9.95424251	8	8.00E+09	9.903089987
29/10/2021	10	11	1.10E+10	10.0413927	12	1.20E+10	10.0791812	14	1.40E+10	10.14612804
30/10/2021	11	17	1.70E+10	10.2304489	18	1.80E+10	10.2552725	20	2.00E+10	10.30103
1/11/2021	12	25	2.50E+10	10.39794	24	2.40E+10	10.3802112	20	2.00E+10	10.30103
2/11/2021	13	25	2.50E+10	10.39794	39	3.90E+10	10.5910646	28	2.80E+10	10.44715803
3/11/2021	14	39	3.90E+10	10.5910646	39	3.90E+10	10.5910646	42	4.20E+10	10.62324929
4/11/2021	15	57	5.70E+10	10.7558749	53	5.30E+10	10.7242759	46	4.60E+10	10.66275783
5/11/2021	16	59	5.90E+10	10.770852	54	5.40E+10	10.7323938	60	6.00E+10	10.77815125
6/11/2021	17	71	7.10E+10	10.8512583	60	6.00E+10	10.7781513	77	7.70E+10	10.88649073
8/11/2021	18	75	7.50E+10	10.8750613	65	6.50E+10	10.8129134	78	7.80E+10	10.8920946
9/11/2021	19	91	9.10E+10	10.9590414	81	8.10E+10	10.908485	94	9.40E+10	10.97312785
10/11/2021	20	100	1.00E+11	11	96	9.60E+10	10.9822712	112	1.12E+11	11.04921802
11/11/2021	21	116	1.16E+11	11.064458	101	1.01E+11	11.0043214	117	1.17E+11	11.06818586
12/11/2021	22	125	1.25E+11	11.09691	115	1.15E+11	11.0606978	120	1.20E+11	11.07918125
13/11/2021	23	132	1.32E+11	11.1205739	149	1.49E+11	11.1731863	142	1.42E+11	11.15228834

15/11/2021	24	150	1.50E+11	11.1760913	154	1.54E+11	11.1875207	178	1.78E+11	11.25042
16/11/2021	25	179	1.79E+11	11.252853	173	1.73E+11	11.2380461	178	1.78E+11	11.25042
17/11/2021	26	197	1.97E+11	11.2944662	194	1.94E+11	11.2878017	185	1.85E+11	11.26717173
18/11/2021	27	238	2.38E+11	11.376577	250	2.50E+11	11.39794	220	2.20E+11	11.34242268
19/11/2021	28	242	2.42E+11	11.3838154	251	2.51E+11	11.3996737	273	2.73E+11	11.43616265
20/11/2021	29	290	2.90E+11	11.462398	265	2.65E+11	11.4232459	287	2.87E+11	11.4578819
22/11/2021	30	340	3.40E+11	11.5314789	345	3.45E+11	11.5378191	334	3.34E+11	11.52374647
23/11/2021	31	341	3.41E+11	11.5327544	346	3.46E+11	11.5390761	336	3.36E+11	11.52633928
24/11/2021	32	339	3.39E+11	11.5301997	344	3.44E+11	11.5365584	334	3.34E+11	11.52374647
25/11/2021	33	336	3.36E+11	11.5263393	340	3.40E+11	11.5314789	324	3.24E+11	11.51054501
26/11/2021	34	343	3.43E+11	11.5352941	341	3.41E+11	11.5327544	333	3.33E+11	11.52244423
27/11/2021	35	339	3.39E+11	11.5301997	345	3.45E+11	11.5378191	335	3.35E+11	11.52504481
29/11/2021	36	347	3.47E+11	11.5403295	334	3.34E+11	11.5237465	348	3.48E+11	11.54157924
30/11/2021	37	350	3.50E+11	11.544068	330	3.30E+11	11.5185139	322	3.22E+11	11.50785587
1/12/2021	38	242	2.42E+11	11.3838154	277	2.77E+11	11.4424798	249	2.49E+11	11.39619935
2/12/2021	39	174	1.74E+11	11.2405492	182	1.82E+11	11.2600714	181	1.81E+11	11.25767857
3/12/2021	40	135	1.35E+11	11.1303338	147	1.47E+11	11.1673173	138	1.38E+11	11.13987909

B. Substrate Concentration, pH, Temperature and Cumulative Biogas Yield

Time (hr)	No. of Microorganism (N)	X (Expt.) (mg/L)	S (Expt.) (mg/L)	Temp. (℃)	pH	μ (hr^{-1})	S (Monod) (mg/L)	Volume of gas (m^3)	CBY (m^3)
0	3.67	3.67E+09	952380.95	31	8.7	0.007547	39875324542.53	0	0
24	3.67	3.67E+09	952380.95	31	8.7	0.007533	33210805839.82	0.000833333	0.000833333
48	3.67	3.67E+09	952380.95	30	8.8	0.007516	27660154172.64	0.000833333	0.001666667
72	3.67	3.67E+09	952380.95	32	8.4	0.007495	23037204593.72	0.000833333	0.0025
96	3.67	3.67E+09	952380.95	35	8.5	0.007471	19186906630.40	0.001666667	0.004166667
120	3.67	3.67E+09	952380.95	31	8.5	0.007441	15980124000.99	0.001666667	0.005833333
144	3.67	3.67E+09	952380.95	34	7.6	0.007407	13309303474.81	0.001666667	0.0075

168	3.67	3.67E+09	952380.95	31	7.7	0.007365	11084867612.65	0.001666667	0.009166667
192	5.33	5.33E+09	948214.2833	31	7.6	0.007316	9232210402.48	0.005833333	0.015
216	9.00	9.00E+09	939047.6167	29	7.5	0.007258	7689195026.42	0.005833333	0.020833333
240	12.33	1.23E+10	930714.2833	30	7.5	0.007189	6404069835.58	0.005833333	0.026666667
264	18.33	1.83E+10	915714.2833	30	7.5	0.007109	5333732636.27	0.011666667	0.038333333
288	23.00	2.30E+10	904047.6167	32	7.5	0.007014	4442285072.71	0.016666667	0.055
312	30.67	3.07E+10	884880.95	35	7.3	0.006904	3699828621.52	0.016666667	0.071666667
336	40.00	4.00E+10	861547.6167	34	7.4	0.006776	3081461816.29	0.019166667	0.090833333
360	52.00	5.20E+10	831547.6167	30	7.3	0.006629	2566445069.92	0.019166667	0.11
384	57.67	5.77E+10	817380.95	31	7.5	0.00646	2137505083.50	0.02	0.13
408	69.33	6.93E+10	788214.2833	32	7.4	0.006269	1780255512.00	0.025833333	0.155833333
432	72.67	7.27E+10	779880.95	31	7	0.006053	1482714456.44	0.025833333	0.181666667
456	88.67	8.87E+10	739880.95	29	6.9	0.005813	1234902599.38	0.025833333	0.2075
480	102.67	1.03E+11	704880.1167	30	6.9	0.005549	1028508505.69	0.0325	0.24
504	111.33	1.11E+11	683215.1167	30	6.7	0.005262	856609862.84	0.035	0.275
528	120.00	1.20E+11	661547.6167	31	6.8	0.004955	713441311.43	0.0375	0.3125
552	141.00	1.41E+11	609047.6167	29	6.8	0.00463	594201079.08	0.046666667	0.359166667
576	160.67	1.61E+11	559880.1167	32	6.6	0.004292	494889932.40	0.046666667	0.405833333
600	176.67	1.77E+11	519880.1167	31	6	0.003946	412177045.47	0.046666667	0.4525
624	192.00	1.92E+11	481547.6167	31	6.4	0.003598	343288286.32	0.0525	0.505
648	236.00	2.36E+11	371547.6167	32	6.4	0.003253	285913174.50	0.056666667	0.561666667
672	255.33	2.55E+11	323215.1167	29	6.1	0.002918	238127389.16	0.068333333	0.63
696	280.67	2.81E+11	259880.1167	32	6.3	0.002596	198328228.73	0.03	0.66
720	339.67	3.40E+11	112380.1167	28	6.4	0.002293	165180857.40	0.03	0.69
744	341.00	3.41E+11	109047.6167	30	6.2	0.002011	137573535.67	0.05	0.74
768	339.00	3.39E+11	114047.6167	29	6	0.001752	114580333.44	0.03	0.77
792	333.33	3.33E+11	128215.1167	27	6	0.001517	95430074.88	0.04	0.81
816	339.00	3.39E+11	114047.6167	28	6.3	0.001307	79480473.81	0.02	0.83
840	339.67	3.40E+11	112380.1167	29	6.1	0.001121	66196591.85	0.015	0.845
864	343.00	3.43E+11	104047.6167	29	5.8	0.000957	55132896.96	0.014	0.859
888	334.00	3.34E+11	126547.6167	30	5.8	0.000814	45918320.60	0.007	0.866

912	256.00	2.56E+11	321547.6167	31	5.7	0.000691	38243812.37	0.005	0.871
936	179.00	1.79E+11	514047.6167	29	5.9	0.000584	31851974.67	0.007	0.878
960	140.00	1.40E+11	611547.6167	28	5.8	0.000493	26528429.76	0.005	0.883

C. Rate of Cell Growth and Rate of Substrate Consumption